FTA RESEARCH

FEDERAL TRANSIT ADMINISTRATION

Resilient Concrete Crosstie and Fastening System Designs for Light, Heavy, and Commuter Rail Transit

Final Report

FEBRUARY 2020

FTA Report No. 0158
Federal Transit Administration

PREPARED BY

J. Riley Edwards, Ph.D., P.E.
Arthur de Oliveira Lima
Marcus S. Dersch, P.E.
Rail Transportation and Engineering Center (RailTEC)
University of Illinois at Urbana-Champaign (UIUC)

U.S. Department of Transportation
Federal Transit Administration

COVER PHOTO

Courtesy of the Rail Transportation and Engineering Center (RailTEC) at the University of Illinois at Urbana-Champaign.

DISCLAIMER

Resilient Concrete Crosstie and Fastening System Designs for Light, Heavy, and Commuter Rail Transit

Final Report

FEBRUARY 2020

FTA Report No. 0158

PREPARED BY

J. Riley Edwards, Ph.D., P.E.
Arthur de Oliveira Lima
Marcus S. Dersch, P.E.
Rail Transportation and Engineering Center (RailTEC)
University of Illinois at Urbana-Champaign (UIUC)
1243 Newmark Civil Engineering Lab, MC-250
205 N. Mathews Avenue, Urbana, IL 61801

SPONSORED BY

Federal Transit Administration
Office of Research, Demonstration and Innovation
U.S. Department of Transportation
1200 New Jersey Avenue, SE
Washington, DC 20590

AVAILABLE ONLINE

https://www.transit.dot.gov/about/research-innovation

Metric Conversion Table

SYMBOL	WHEN YOU KNOW	MULTIPLY BY	TO FIND	SYMBOL
LENGTH				
in	inches	25.4	millimeters	mm
ft	feet	0.305	meters	m
yd	yards	0.914	meters	m
mi	miles	1.61	kilometers	km
VOLUME				
fl oz	fluid ounces	29.57	milliliters	mL
gal	gallons	3.785	liter	L
ft^3	cubic feet	0.028	cubic meters	m^3
yd^3	cubic yards	0.765	cubic meters	m^3
NOTE: volumes greater than 1000 L shall be shown in m^3				
MASS				
oz	ounces	28.35	grams	g
lb	pounds	0.454	kilograms	kg
T	short tons (2000 lb)	0.907	megagrams (or "metric ton")	Mg (or "t")
TEMPERATURE (exact degrees)				
°F	Fahrenheit	5 (F-32)/9 or (F-32)/1.8	Celsius	°C

REPORT DOCUMENTATION PAGE	*Form Approved* *OMB No. 0704-0188*

1. AGENCY USE ONLY	2. REPORT DATE February 2020	3. REPORT TYPE AND DATES COVERED

4. TITLE AND SUBTITLE Resilient Concrete Crosstie and Fastening System Designs for Light, Heavy, and Commuter Rail Transit	5. FUNDING NUMBERS IL-26-07010-00

6. AUTHOR(S)

J. Riley Edwards, Ph.D., P.E.; Arthur de Oliveira Lima; Marcus S. Dersch, P.E.

7. PERFORMING ORGANIZATION NAME(S) AND ADDRESSE(ES)	8. PERFORMING ORGANIZATION REPORT NUMBER
Rail Transportation and Engineering Center - RailTEC Department of Civil and Environmental Engineering Grainger College of Engineering University of Illinois at Urbana-Champaign 1243 Newmark Civil Engineering Lab, MC-250 205 N. Mathews Avenue, Urbana, IL 61801	FTA Report No. 0158
9. SPONSORING/MONITORING AGENCY NAME(S) AND ADDRESS(ES) U.S. Department of Transportation Federal Transit Administration Office of Research, Demonstration and Innovation East Building 1200 New Jersey Avenue, SE Washington, DC 20590	10. SPONSORING/MONITORING AGENCY REPORT NUMBER FTA Report No. 0158

11. SUPPLEMENTARY NOTES [https://www.transit.dot.gov/about/research-innovation]

12A. DISTRIBUTION/AVAILABILITY STATEMENT Available from: National Technical Information Service (NTIS), Springfield, VA 22161. Phone 703.605.6000, Fax 703.605.6900, email [orders@ntis.gov]	12B. DISTRIBUTION CODE TRI-30

13. ABSTRACT

Rail transit track infrastructure and its components are expected to function as a system, and the performance and correct design of each component is critical to overall system behavior. A critical component in the transfer of load through the track system is the crosstie. Concrete is the dominant crosstie material choice for rail transit applications where safety and reliability of infrastructure are at a premium and maintenance time is often limited. Development and implementation of a structural design method that enables optimization of crosstie design for rail transit applications and loading environments will reduce initial capital cost and recurring maintenance expense; it is also important to characterize the loading environment at the wheel-rail interface. In this project, data collected at field installations throughout the US were used to quantify wheel-rail interface loads, concrete crosstie bending moments, and rail deflections under revenue service train passes. Field results indicated the need for development and application of a probabilistic design method for the flexural capacity of concrete crossties. A prototype crosstie for light rail transit infrastructure was designed, and a design process based on structural reliability analysis concepts was developed. New (proposed) designs are more economical, having a center negative moment capacity reduction of 50% for heavy rail transit. Further field instrumentation was installed on a heavy rail transit agency, in which wheel-rail interface loads were monitored to quantify rolling stock dynamic loading magnitudes and identify bad actor wheels.

14. SUBJECT TERMS Rail Transit, Concrete Crossties, Bending Moments, Input Loads, Design Optimization, Structural Reliability Analysis (SRA), Track Displacements, Fastening Systems	15. NUMBER OF PAGES 124

16. PRICE CODE

17. SECURITY CLASSIFICATION OF REPORT	18. SECURITY CLASSIFICATION OF THIS PAGE	19. SECURITY CLASSIFICATION OF ABSTRACT	20. LIMITATION OF ABSTRACT
Unclassified	Unclassified	Unclassified	

TABLE OF CONTENTS

LIST OF FIGURES

LIST OF TABLES

ABSTRACT

Rail transit track infrastructure and its components are expected to function as a system, and the performance and correct design of each component is critical to the overall system behavior. One of the most critical components in the transfer of load through the track system is the crosstie. Concrete is the dominant crosstie material choice for rail transit applications where safety and reliability of infrastructure are at a premium and maintenance time is often limited. As such, development and implementation of a structural design method that enables optimization of crosstie design for rail transit applications and loading environments will reduce initial capital cost and recurring maintenance expense. Additionally, it is important to characterize the loading environment at the wheel-rail interface, as it is the primary input into the design of rail transit track systems.

Data collected at field installations throughout the United States were used to quantify wheel-rail interface loads, concrete crosstie bending moments, and rail deflections under revenue service train passes. These data allowed researchers to investigate the effects of wheel condition, thermal gradient, axle load, axle location, support condition, and rail transit rolling stock and mode on crosstie bending moments. Field results indicated the need for development and application of a probabilistic design method for the flexural capacity of concrete crossties. A variety of analytical methods were employed to design a prototype crosstie for light rail transit infrastructure. This crosstie was manufactured, installed, and monitored as a part of the project scope. Performance has been encouraging to date, and monitoring will continue beyond this project duration.

Additionally, a design process based on structural reliability analysis concepts was developed whereby target values for reliability indices (β) for new designs are obtained and compared with existing designs for further design optimization. New (proposed) designs are more economical, having a center negative moment capacity reduction of 50% for heavy rail transit. In most cases the proposed designs for both rail modes have fewer prestressing wires and a higher centroid of prestressing steel. In all cases, the flexural capacities at the crosstie center and rail seat are better balanced from a structural reliability standpoint. The probabilistic method using structural reliability analysis fundamentals that is proposed and demonstrated in this work constitutes a critical step in the development of mechanistic-empirical practices for the design of concrete crossties. Additionally, this framework for probabilistic design provides a foundation for the future application of mechanistic-empirical design practices to other rail transit track components. Finally, due to an extension of this project, further field instrumentation was installed on a heavy rail transit agency, in which wheel-rail interface loads were monitored to quantify rolling stock

dynamic loading magnitudes and identify bad actor wheels for addressing by the mechanical department. Future research needs that were identified with respect to rail transit track infrastructure components include the need to further investigate fastening systems with a specific focus on the design and performance of direct fixation (DF) fastening systems.

EXECUTIVE SUMMARY

Rail transit track infrastructure and its components are expected to function as a system, and the performance and correct design of each component is critical to the overall system behavior. One of the most critical components in the transfer of load through the track system is the crosstie. Concrete is the dominant crosstie material choice for rail transit applications, where safety and reliability of infrastructure are at a premium and maintenance time often is limited. As such, development and implementation of a structural design method that enables optimization of crosstie design for rail transit applications and loading environments will reduce initial capital cost and recurring maintenance expense. Additionally, it is important to characterize the loading environment at the wheel-rail interface, as it is the primary input into the design of rail transit track systems.

A comprehensive static load quantification was conducted for light, heavy, and commuter rail transit systems in the US. Additionally, an improved understanding of rail transit loading environments was developed using industry databases and current design recommendations. The applicability of several dynamic factors to the rail transit loading environment was evaluated by comparing the predicted results with field data. Most dynamic factors can predict peak wheel loads for commuter rail systems with high-level accuracy and precision. The effectiveness of the impact factor of 3 recommended by the American Railway Engineering and Maintenance-of-Way Association (AREMA) manual was also studied with respect to the rail transit loading environment in the US. As shown, the impact factor of 3 is adequate for quantifying the effect of track and wheel irregularities on commuter rail transit systems and provides a conservative estimate of wheel loads. Future work (described in Section 2) will include collection and analysis wheel-rail interface data from light, heavy, and commuter rail transit systems to evaluate the effectiveness of the dynamic and impact factors.

To further the aforementioned static load survey, data were collected at field installations throughout the US to quantify wheel-rail interface loads, concrete crosstie bending moments, and rail deflections under revenue service train passes. These data allowed researchers to investigate the effects of wheel condition, thermal gradient, axle load, axle location, support condition, and rail transit rolling stock and mode on crosstie bending moments. Total load factor distributions for the three rail transit systems studied showed significant deviations, demonstrating that unique, specific load factors are needed to adequately represent the existing wheel loads on rail transit infrastructure and improve design of the critical components that make up the track structure. All distributions indicate that the current AREMA impact factor of 3 should be reduced, possibly by as much as half. Existing dynamic load factors also were analyzed, and the Talbot approach to estimating dynamic loading due to speed and wheel diameter was found to be quite conservative, with the light rail transit loading environment over-estimated by a factor of 3. Conversely,

heavy rail transit factors were underestimated by approximately 50%. Finally, it was concluded that commuter rail transit factors closely matched the Talbot prediction.

For a given rail transit mode, in the absence of field data related to the track loading environment, the selection of an appropriate load factor should be based on knowledge of a particular rail transit system's track and rolling stock maintenance practices. It was found that focused load-related field instrumentation can be deployed to answer system-specific loading questions within a given rail transit mode. The relatively modest effort required to install instrumentation and process data from such an installation could provide significant returns on investment with respect to mechanistically designing track components. Taken as a whole, field results indicated the need for development and application of a probabilistic design method for the flexural capacity of concrete crossties.

A variety of analytical methods were employed to design a prototype concrete crosstie for light rail transit infrastructure. Three critical design elements were studied in the initial design phase of this project: 1) reducing prestressing levels, 2) introducing flexural reinforcements, and 3) introducing shear reinforcements. Accordingly, test specimens were designed based on FEM results and the aforementioned design elements. In the center negative tests, two design options were studied to reinforce the crosstie—shear reinforcement and synthetic fiber, both of which changed the mode of failure of the crosstie from pure shear to flexure and flexural-shear. In the rail seat positive test, reducing prestressing levels by eliminating wires led to the reduction in capacity about 30%. Reducing the jacking force of the wire led to the delay of strand rupture and made the tie more flexible. Introducing flexural reinforcement alleviated the risk of strand rupture but led to shear failure. Introducing shear reinforcement led the ties to have more ductile behavior, and there was significant residual strength after the peak. Introducing flexural confinement improved the ductility of the crosstie and also strengthened the ultimate capacity. The prototype crosstie was manufactured, installed, and monitored as a part of the project scope. Performance has been encouraging to date, and monitoring will continue beyond this project duration.

Additionally, a design process based on structural reliability analysis concepts was developed whereby target values for reliability indices (β) for new designs are obtained and compared with existing designs for further design optimization. New (proposed) designs are more economical, having a center negative moment capacity reduction of 50% for heavy rail transit. In most cases the proposed designs for both rail modes have fewer prestressing wires and a higher centroid of prestressing steel. In all cases, the flexural capacities at the crosstie center and rail seat are better balanced from a structural reliability standpoint. The probabilistic method using structural reliability analysis fundamentals proposed

and demonstrated in this work constitutes a critical step in the development of mechanistic-empirical practices for the design of concrete crossties. Additionally, this framework for probabilistic design provides a foundation for the future application of mechanistic-empirical design practices to other rail transit track components.

Finally, and as the result of an extension of this project, further field instrumentation was installed at a heavy rail transit agency, in which wheel-rail interface loads were monitored to quantify rollingstock dynamic loading magnitudes and identify bad actor wheels for addressing by the mechanical department. Further monitoring of the prototype crossties installed in light rail infrastructure also was conducted; they have continued to perform well in their second year of revenue field service.

The results from this project benefit the transit industry in a variety of ways. Products produced include the following:

- **Prototype crosstie designs** developed with applicability to multiple rail transit modes
- **Prototype crossties** manufactured and installed
- **Field sites established** for monitoring over long (multi-year) time durations
- **Improved communication and cohesiveness** through transit agency infrastructure management meeting at the UIUC-organized international crosstie and fastening system symposia and other conference interactions
- **Workforce development** gains (students trained in rail transit and pursuing careers in the rail transit sector)

Future research needs identified with respect to rail transit track infrastructure components include the need to further investigate fastening systems with a specific focus on the design and performance of direct fixation (DF) fastening systems.

SECTION

1

Introduction, Background, Survey, and Loading Quantification

Introduction and Background

Light, heavy, and commuter rail transit agencies face a myriad of loading and operating conditions that must be considered in the design and maintenance of their track infrastructure and its components. It is not uncommon for a single rail corridor to experience a wide variety of passenger train loads (due to different speeds, axle loads, etc.), track geometry characteristics, and environmental conditions (including extreme weather events). These factors are both internal (e.g., railcar loading) and external (e.g., climatic, extreme weather events, etc.) to the crosstie and fastening system, and they must all be considered to design "optimized" components that can perform under a wide range of service conditions.

For a variety of reasons, concrete crossties are a dominant material choice for light, heavy, and commuter rail transit operators. The methods of designing concrete crossties and fastening systems for transit systems are not developed based on mechanistic design practices considering actual field loadings and service demands but are largely based on empirical results and practical experience. As such, some systems have not fulfilled their intended design life, and the need for mechanistic design practices and more resilient component designs is recognized by the manufacturers of track components, researchers, and rail transit operators.

Additionally, deficiencies in concrete crosstie performance have been noted on passenger and transit corridors in the US (e.g., Amtrak's Northeast Corridor, Metro-North Railroad, MBTA, etc.) that include premature deterioration of concrete due to chemical attack, premature deterioration of the rail pad, and some structural failures [1, 2]. Other examples, such as Hurricane Sandy in 2012, from which New York City-area transit systems are still recovering, relay the need for more resilient infrastructure components with increased robustness, adaptiveness, and readiness [3–5]. As a result of Hurricane Sandy, the elastic fastening systems that were underwater were replaced, an issue that corrosion-proof fastening systems would likely mitigate.

To address the need for an optimized, resilient railway crossties for rail transit and commuter rail properties in the US, this project is a multi-faceted

applied research, development, and revenue-service demonstration project that consists of field instrumentation, analytical modeling, and design software development for light, heavy, and commuter rail transit agencies, culminating in prototype crosstie development, installation, and evaluation.

Project Objective

The objective of this project is to use innovative technologies and methods to characterize the desired performance and resiliency requirements for concrete crossties and fastening systems, quantify their behavior under load, and develop resilient infrastructure component design solutions for concrete crossties and fastening systems for light, heavy, and commuter rail operators. This project includes the development of prototype crossties with the overall objective of keeping public transportation safe and in a state of good repair, especially during natural disasters and other externally-caused extreme events.

The parallel objectives of this project are as follows:

1. Develop and execute a survey of rail transit industry experts to benchmark the current state of rail transit industry track component research needs.
2. Conduct a comprehensive field investigation of the performance demands on concrete crossties and fastening systems on light, heavy, and commuter rail transit.
3. Develop an analytical finite element model (using field loading data) for concrete crosstie and fastening systems on light, heavy, and commuter rail transit systems.
4. Conduct focused laboratory instrumentation to validate analytical modeling and further the knowledge gained during field experimentation.
5. Develop mechanistic design recommendations for resilient transit applications of concrete crossties on light, heavy, and commuter rail transit systems.
6. Manufacture and install resilient prototype crossties and fastening systems in revenue service on two of the following modes—light, heavy, or commuter rail transit.

The aforementioned objectives result in the design and deployment of concrete crossties with increased robustness, adaptiveness, and readiness that is achieved through 1) new recommended design practices for optimized and resilient systems based on field data, analytical modeling, and mechanistic design principles, 2) improved safety and performance, 3) lower maintenance costs, and 4) lower life-cycle costs (LCC).

Most importantly, this project addresses one of the primary strategic goals of the US Department of Transportation: State of Good Repair [6]. Lower life-cycle costs will result in lengthened maintenance intervals, increasing capital and operating costs available for other infrastructure improvements, and

increasing the track capacity available to operate during extreme events and under normal operating conditions.

Definitions of Light, Heavy, and Commuter Rail Transit

For the purposes of this project, the definitions of light, heavy, and commuter rail transit were taken from the National Transit Database (NTD) Glossary, published by the Federal Transit Administration (FTA) [7]:

- *Light Rail* – a transit mode that is typically an electric railway with a light volume of traffic compared to heavy rail. It is characterized by:
  - Passenger cars operating singly (or in short, usually two-car, trains) on fixed rails in shared or exclusive right-of-way (ROW)
  - Vehicle power drawn from an overhead electric line via a trolley or a pantograph
- *Heavy Rail* – a transit mode that is an electric railway with the capacity for a heavy volume of traffic. It is characterized by:
  - High speed and rapid acceleration passenger cars operating singly or in multi-car trains on fixed rails
  - Separate ROW from which all other vehicular and foot traffic are excluded
- *Commuter Rail* – a transit mode that is an electric- or diesel-propelled railway for urban passenger train service consisting of local short-distance travel operating between a central city and adjacent suburbs. Such rail service, using either locomotive hauled or self-propelled railroad passenger cars, is generally characterized by:
  - Specific station-to-station fares
  - Usually only one or two stations in the Central Business District (CBD)

Project Work Packages (Tasks)

Work Package 1 – Field Load Environment Characterization

Prior to initiating research and experimentation activities described in this project, a comprehensive literature, design, and specifications review and comparison were conducted by the University of Illinois at Urbana-Champaign (UIUC) to document the current state of the art in transit crosstie and fastener design. This was conducted through the use of many resources, including the William W. Hay Railroad Engineering Collection at UIUC, which contains portions of the Federal Railroad Administration (FRA) and Association of American Railroads (AAR) libraries and is the largest rail-focused collection in the western hemisphere. Industry partnerships and other rail transit industry experts were also used to direct and guide this project through the involvement of the American Public Transportation Association (APTA).

Additionally, a survey of transit properties was conducted to determine the most critical aspects of crossties and fastening systems that should be made resilient in the face of natural disasters or other events that place increased stress on infrastructure and its components. These inputs were used to guide the field and laboratory experimental efforts as well as the analytical modeling components of this project.

This phase focused on gaining a quantitative understanding of the loads that are experienced at varying interfaces in the crosstie and fastener system and modeling of the crosstie/fastening system to provide greater understanding of how the properties of crossties and fasteners affect their performance and transmittal of loads. Loads were considered that pertain to everyday operation as well as discrete extreme events that may impose additional loading on the infrastructure.

Prior to this project, the exact loads that each fastening system and crosstie component is expected to withstand, attenuate, and/or transfer were not sufficiently understood. Additionally, premature failures have been identified by US transit and commuter railroads as one of the primary problems with concrete crossties on their networks. With proper understanding of the loads that each component in the crosstie/fastening system is expected to carry, correct materials and design recommendations can be made to increase the life-cycle and performance of fastening systems (reduce life-cycles costs) through effective design solutions to the current problems. Optimization is especially valuable for transit agencies, where safety and ride quality are at a premium.

Work Package 2 – Full-Scale Laboratory Experimentation for FE Model Validation

This phase included laboratory testing using state-of-the-art testing equipment at the Research and Innovation Laboratory (RAIL) at UIUC. RAIL has a wide array of adaptable servo-hydraulic testing equipment with highly-precise strain, deformation, load measurement, and control and has the unique ability to apply accurate wheel rail loads using a fully-instrumented wheel set (IWS). The performance of commercially-available crossties and fasteners or custom-built specimens was evaluated using the testing facilities and equipment at UIUC to evaluate an expansive matrix of loading configurations. Along with the physical testing, computer-based finite element (FE) modeling was performed to describe the load path through the system under all anticipated scenarios (part of Work Package 3).

Work Package 3 – Analytical Modeling and Development of Simplified Design Tool

This phase included the development of a detailed FE model of a typical rail transit concrete crosstie design. The objective of FE modeling was to characterize the load path and stress distribution of the crosstie and fastener system numerically. The FE model was capable of quantifying the stress distribution, deformation, and slip between components. The software facilitated simulation of the loading events as a function of time to gain insight into friction, slip, and abrasion that affects long-term performance of the fastener system. The FE model was calibrated using the experimental results from the field (Work Package 1) and laboratory (Work Package 2) and used to replicate different system properties and loading conditions. The FE software used possessed important features such as the ability to capture the nonlinear plastic behavior of concrete under load and the ability to describe the contact properties (e.g., penetration and friction) at critical interfaces in the system.

FE model inputs include rail pad stiffness, clamping force, rail seat bearing area, etc., and provide a measure of the loads at each interface and other outputs that are useful in the analysis and design of crossties and fastening systems (FE model to be further developed and verified under future sources of funding). The load inputs were derived from literature, field tests, and industry sponsor expert opinions. It is intended to approach the load definition problem using a probabilistic approach that accounts for load variability. These functions represent the foundation for the stochastic analysis that will lead to a better understanding of not only the peak load, average load, or "design load" of interest, but also of the variability of loading over the entire service life of the crossties. This approach provided greater insight and a more accurate understanding of load history, the effect of geometry and materials selection, and the effect of small displacements that may occur over the life of the system.

Work Package 4 – Prototype Crosstie Design, Manufacture, and Installation

This phase began with the identification and characterization of the critical qualities that are known to control the performance of crossties based on the findings from field and laboratory experimentation and analytical modeling data. The objective of this phase was to incorporate mechanistic design principles and key inputs for resilient fastening systems into the design and manufacture of prototype components to be placed in a revenue service test installation. With this knowledge, UIUC partnered with concrete crosstie and fastening system manufacturers to design and manufacture prototype systems, install them, and monitor them for the remainder of the period of performance of this contract. Future funding and projects would extend the field monitoring phase of this research.

Work Package 5 – External Review, Planning, Management, Reporting, and Communications

This work package included the third-party external review of this project, as well as project planning, management, reporting, and communications. Deliverables, presentations, demonstrations, and reports were produced throughout the period of performance per the schedule of deliverables. This phase will aid in the appropriate transfer of technology (technology transfer) to the necessary parties within the US transit industry. Each Fall throughout the duration of this project, an industry partners meeting was organized by UIUC to disseminate project results to transit agencies, crosstie and fastener manufacturers, and other rail engineering researchers.

Rail Transit Infrastructure Performance Survey – Summary of Results

Survey of Rail Transit Track Superstructure Design and Performance Objectives

The primary objective of the Survey of Rail Transit Track Superstructure Design and Performance (hereafter referred to as the "Transit Survey") was to poll the rail transit community on the use and performance of concrete crossties and elastic fastening systems and develop an understanding of the current state-of-practice regarding the design and performance of concrete crosstie and fastening system in rail transit systems. The Transit Survey characterized the critical factors affecting the performance of concrete crossties and fastening systems in transit environment. It assessed the resilience of rail transit infrastructure to natural disasters, identified the most vulnerable components, and provided information needed to guide many aspects of the FTA project, including FE modeling, laboratory experimentation, and field testing. Finally, it enabled UIUC to continue establishing relationships and encourage collaboration with rail transit agencies, researchers, and manufacturers around the world.

The Transit Survey provided insight to guide many aspects of the FTA project at UIUC, including modeling, laboratory instrumentation and experimentation, and field instrumentation and experimentation. In terms of modeling, results from this survey helped determine typical loading scenarios using modeling and loading methodologies from previous research. The survey results related to modeling also provided references for literature related to previous analysis, allowing UIUC's team to incorporate past research efforts and findings into its current work. The responses from the survey also included criteria from laboratory testing performed on concrete crossties and fastening systems around the world, offering the capability to compare North American test

criteria and methodologies with multiple international standards. Finally, the survey results helped to steer the field experimentation efforts by identifying conditions where failure most commonly occurs and developing a greater understanding of probabilistic loading conditions and failure modes.

Audience

The Transit Survey was distributed to professionals in many different positions and organizations within the rail transit industry, including infrastructure owners, operators, or maintainers. This breadth of coverage provided varied perspectives on the usage and performance of concrete crossties and fastening systems. Additionally, the survey's audience was geographically diverse, with responses from various transit agencies across the US.

Development

The Transit Survey was developed with extensive input from many experts in concrete crosstie and fastening system design, production, maintenance, and research. First, a list of questions was developed internally at UIUC regarding the design, usage, performance, and failure of concrete crossties and fastening systems. After researching various online survey tools and creating an initial test survey, the questions were distributed to the UIUC FTA project industry partners for review and subsequent revision. The industry partners, who include experts in concrete crosstie and elastic fastening system design and performance improvement in North America, provided feedback based on the US rail transit experience and what the rail transit industry would like to gain from such a survey. After a modification and revision period, the survey was distributed to the rail transit community using the online survey tool Surveygizmo and Google Forms.

Detailed Responses

The content of the Transit Survey, which includes many aspects of the usage, design, production, performance, failure, recommended practices, testing, and research of the concrete crosstie and fastening system, can be explored by seeing the comprehensive question and response lists found in Appendices A, B, and C:

- Appendix A – Transit Agency Survey
- Appendix B – Concrete Crosstie Manufacturer Survey
- Appendix C – Fastening System Manufacturer Survey

Results

A prevailing comment related to the development of revised design recommendations was the need to consider failure mechanisms and field performance of components and systems. Causes of failure provide insight

into ways in which concrete crosstie and fastening systems can be improved. The most common failures identified in the survey were rail seat deterioration (RSD) and other forms of rail cant deficiency, broken or worn shoulder, and cracking from environmental or chemical degradation.

Figure 1-1 depicts the criticality of concrete crosstie and fastening system problems from most to least critical, as expressed by the North American respondents.

Figure 1-1

Five most important track structure conditions in terms of contributing to occurrence of rail transit accidents (ranked 1 to 5, with 5 most critical)

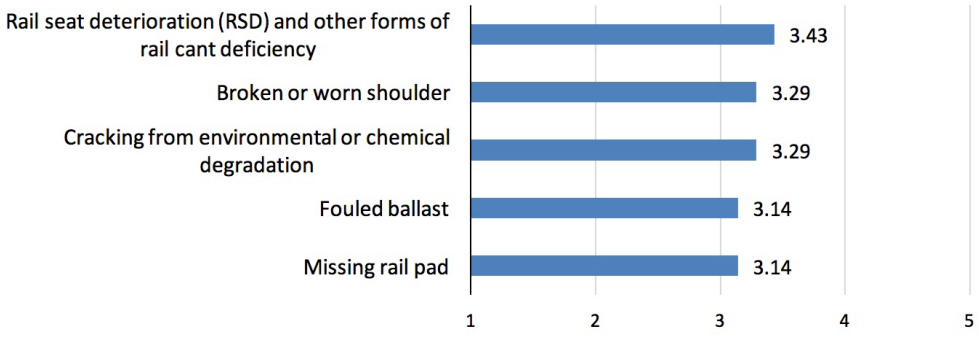

In the US, the most critical problem with rail transit infrastructure was determined to be RSD and other forms of rail cant deficiency. It should be noted, however, that as of the writing of this report, the authors are not aware of any significant instances of RSD on rail transit properties. Other problems, according to rail transit respondents, include wear and fatigue in the shoulder and other components of the fastening system, cracking from environmental or chemical degradation, fouled ballast, and missing rail pads.

Figure 1-2 communicates the most important deficiencies of concrete crosstie and fastening system from most to least critical, as expressed by the rail transit responses. The results from the rail transit agencies suggest that alkali-silica reaction (ASR) is the most critical deficiency of concrete crosstie on rail transit track.

Figure 1-2

Most important deficiencies of concrete crosstie and fastening systems in terms of contributing to occurrence of rail transit accidents (ranked 1–5, with 5 most critical)

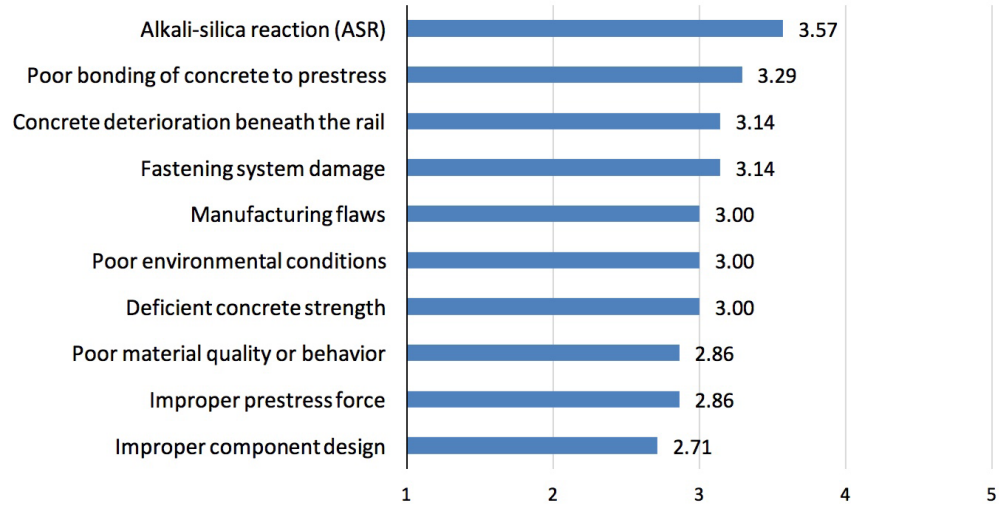

Figure 1-3 communicates the most important research areas for rail transit infrastructure. As most transit agencies indicated, track system design: determining the track service environment and required crosstie characteristics—is the most critical research area, which also aligns with the scope of this project. Other important research areas include fastener design (clips, insulators, inserts, rail pads, and under tie pads), optimization of crosstie design (spacing, cross-section, body shape, specific uses), material design (concrete mix, pre-stress strand arrangement), and prevention of RSD or repair of abraded crossties.

Figure 1-3

Most important rail transit crosstie and fastening system research areas (ranked 1–5, with 5 most critical)

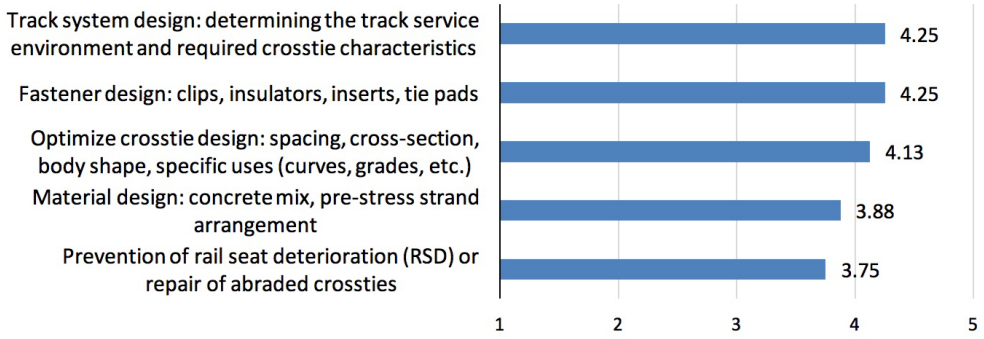

Table 1-1 provides a summary of rail transit infrastructure design practices obtained from the survey responses. The most common concrete crosstie spacing is 30 in., whereas most freight railroad track has a concrete crosstie spacing of 24 in. The most predominant fastening systems are Pandrol's Fastclip and e-Clip. CXT, KSA, and Rocla are the most common suppliers of concrete crossties for rail transit track. As of the development of this final report, KSA has been acquired by Rocla, which was purchased by Vossloh Fastening Systems. Rail transit has multiple common rail sections, including 90 AS, 100 ARA-A, 100-8, 115 RE, and 136 RE, most of which are smaller than what are commonly used on freight railroad track.

Transit vehicles operate at much higher speeds compared to freight trains, with maximum operating speeds ranging from 55 mph to 125 mph depending on the type of vehicle and infrastructure.

Table 1-1

Summary of Responses for Crosstie and Fastening System Survey

	North American Responses
Participant Demographics	
Total number of responses	8
Infrastructure Overview	
Track miles	258 track-miles
Track miles of ballasted concrete crosstie track	56 track-miles
Typical concrete crosstie spacing	24 in., 30 in.
Common fastening systems	Pandrol Fast Clip, e-clip
Common concrete crossties	CXT, KSA, Rocla
Common rail sections	90 AS, 100 ARA-A, 100-8, 115RE, 136RE
Maximum operating speed	55, 65, 70, 80 mph

Concrete Crosstie Census and Practices

In addition to the Transit Survey, a census was undertaken to understand the usage of concrete crossties and fastening system types throughout the US. The primary objective of the Concrete Crosstie Census and Practices (hereafter referred to as the "Tie Census") was to quantify the usage of concrete crossties and various fastening system types on rail transit systems throughout the US, as well as design loads and other characteristics of these systems. Data were collected via discussion with industry contacts at many transit systems in the US, which were reflective of the current state of the industry in 2013 when the Tie Census was undertaken.

Pertinent information collected via the Tie Census was broken down and tabulated for ease of comparison between systems, transit modes, etc. Streetcar and cable car systems have been omitted from these tables.

Concrete Crosstie and Fastening System Usage

Tables 1-2, 1-3, and 1-4 quantify the number of concrete crossties on surveyed rail transit properties, broken down by transit mode. These charts also note what fastening systems are used on concrete crossties at each system.

Table 1-2

Concrete Crosstie Usage on Light Rail Transit Systems

Agency/Transit System	City/Geographical Area	Number of Concrete Crossties	Fastening System(s)
Capital Metro	Austin, TX		
CATS*	Charlotte, NC		
DART*	Dallas, TX	460,000	e-clip, Fastclip
GCRTA*	Cleveland, OH	962	e-clip
Hampton Roads Transit	Norfolk, VA	22,000	e-clip
Houston METRO	Houston, TX	45,000	e-clip
Maryland MTA	Baltimore, MD	116,000	Pandrol
MBT*	Boston, MA	10,600	e-clip
Metro	Minneapolis, MN		
MetroLink	St. Louis, MO		
Metro Rail	Los Angeles, CA	312,300	
Muni Metro	San Francisco, CA		
Niagara Frontier T.A.	Buffalo, NY		
NJ Transit	Camden, NJ	42,200	Pandrol
NJ Transit	Jersey City, NJ	46,400	e-clip
NJ Transit	Newark, NJ	3,000	e-clip
PA Transit	Pittsburgh, PA	0	N/A
RTD*	Denver, CO	236,500	e-clip
SEPTA*	Philadelphia, PA		
Sound Transit	Seattle, WA	25,400	e-clip, Fastclip
Sun Link	Tucson, AZ		
TRAX*	Salt Lake City, UT	220,000	
TriMet	Portland, OR		
Valley Metro Rail	Phoenix, AZ		
Total		*1,540,362*	–

* CATS = Charlotte Area Transit System, DART = Dallas Area Rapid Transit, GCRTA = Greater Cleveland Regional Transit Authority, MBTA = Massachusetts Bay Transportation Authority, RTD = Regional Transportation District, SEPTA = Southeastern Pennsylvania Transportation Authority, TRAX = Transit Express.

Table 1-3

Concrete Crosstie Usage on Heavy Rail Transit Systems

Agency/Transit System	City/Geographical Area	Number of Concrete Crossties	Fastening System(s)
Baltimore Metro Subway	Baltimore, MD	22,459	Pandrol
BART*	San Francisco, CA		
CTA*	Chicago, IL	400	
GCRTA*	Cleveland, OH	2,850	Pandrol e-clip
MARTA*	Atlanta, GA	77,000	e-clip
MBTA*	Boston, MA	0	N/A
Metrorail	Miami, FL		
Metrorail	Washington, DC	64,500	e-clip
Metro Rail	Los Angeles, CA	26,200	
NYCTA*	New York, NY	35,640	e-clip
PATCO* Speedline	Philadelphia, PA		
PATH*	New York, NY	12,700	e-clip
SEPTA*	Philadelphia, PA	20,000	
Total		*261,749*	–

*BART = Bay Area Rapid Transit, CTA = Chicago Transit Authority, GCRTA = Greater Cleveland Regional Transit Authority , MARTA = Metropolitan Atlanta Rapid Transit Authority, MBTA = Massachusetts Bay Transportation Authority, NYCTA = New York City Transit Authority, PATCO = Port Authority Transit Corporation, PATH = Port Authority Trans-Hudson, SEPTA = Southeastern Pennsylvania Transportation Authority

Table 1-4

Concrete Crosstie Usage on Commuter Rail Transit Systems

Agency/Transit System	Metropolitan Area	Number of Concrete Crossties	Fastening System(s)
Caltrain	San Francisco, CA		
Coaster	San Diego, CA		
FrontRunner	Salt Lake City, UT	235,000	
LIRR*	New York, NY	206,000	e-clip, Fastclip
MARC*	Baltimore, MD	N/A**	N/A
MBCC*	Boston, MA		
Metra	Chicago, IL		
Metro-North Railroad	New York, NY	468,948	e-clip
Metrolink	Los Angeles, CA		
New Jersey Transit	New York, NY		
New Mexico Rail Runner Express	Albuquerque, NM		
NICTD*	Chicago, IL		
Northstar Line	Minneapolis, MN		
RTD*	Denver, CO	88,700	e-clip
SEPTA*	Philadelphia, PA	20,000	
Trinity Railway Express	Dallas-Fort Worth, TX		
Tri-Rail	Miami, FL		
Total		*1,018,648*	–

*LIRR = Long Island Rail Road, MARC = Maryland Area Regional Commuter, MBCC = Massachusetts Bay Commuter Railroad, NICTD = Northern Indiana Commuter Transportation District, RTD = Regional Transportation District, SEPTA = Southeastern Pennsylvania Transportation Authority

**Operates solely on track owned by other railroads

Design Axle Loads and Track Speeds

Tables 1-5, 1-6, and 1-7 contain information on the various axle loads and track speeds used for design purposes by light, heavy, and commuter rail transit systems throughout the US. In most cases, these axle loads correspond to railcars or maintenance vehicles, and the track speeds are the maximum allowable speed on the system.

Table 1-5

Design Axle Loads and Track Speeds for Light Rail Transit Systems

Agency/Transit System	City/Geographical Area	Maximum Design Axle Load (kips)	Maximum Track Speed (mph)
Capital Metro	Austin, TX		
CATS*	Charlotte, NC		
DART*	Dallas, TX	34	65
GCRTA*	Cleveland, OH	23.3	45
Hampton Roads Transit	Norfolk, VA	34	55
Houston METRO	Houston, TX	34	
Maryland MTA	Baltimore, MD	27.8	55
MBTA*	Boston, MA		55
Metro	Minneapolis, MN		55
MetroLink	St. Louis, MO		
Metro Rail	Los Angeles, CA	34	65
Muni Metro	San Francisco, CA		
Niagara Frontier T.A.	Buffalo, NY		
NJ Transit	Camden, NJ	35 (78 frt)**	65
NJ Transit	Jersey City, NJ	34	65
NJ Transit	Newark, NJ		45
PA Transit	Pittsburgh, PA		60
RTD*	Denver, CO	34	57
SEPTA*	Philadelphia, PA	20	50
Sound Transit	Seattle, WA	34	
Sun Link	Tucson, AZ		
TRAX*	Salt Lake City, UT	34	65
TriMet	Portland, OR		
Valley Metro Rail	Phoenix, AZ		60

*CATS = Charlotte Area Transit System, DART = Dallas Area Rapid Transit, GCRTA = Greater Cleveland Regional Transit Authority, MBTA = Massachusetts Bay Transportation Authority, RTD = Regional Transportation District, SEPTA = Southeastern Pennsylvania Transportation Authority, TRAX = Transit Express

Table 1-6

Design Axle Loads and Track Speeds for Heavy Rail Transit Systems

Agency/Transit System	City/Geographical Area	Maximum Design Axle Load (kips)	Maximum Track Speed (mph)
Baltimore Metro Subway	Baltimore, MD	35	60
BART*	San Francisco, CA		
CTA*	Chicago, IL		55
GCRTA*	Cleveland, OH	29.2	60
MARTA*	Atlanta, GA	35	70
MBTA8	Boston, MA		60
Metrorail	Miami, FL		70
Metrorail	Washington, DC		70
Metro Rail	Los Angeles, CA	34	70
NYCTA*	New York, NY		
PATCO* Speedline	Philadelphia, PA		
PATH*	New York, NY	33.4	50
SEPTA*	Philadelphia, PA		50

*BART = Bay Area Rapid Transit, CTA = Chicago Transit Authority, GCRTA = Greater Cleveland Regional Transit Authority, MARTA = Metropolitan Atlanta Rapid Transit Authority, MBTA = Massachusetts Bay Transportation Authority, NYCTA = New York City Transit Authority, PATCO = Port Authority Transit Corporation, PATH = Port Authority Trans-Hudson, SEPTA = Southeastern Pennsylvania Transportation Authority

Table 1-7

Design Axle Loads and Track Speeds for Commuter Rail Transit Systems

Agency/Transit System	Metropolitan Area	Maximum Design Axle Load (kips)	Maximum Track Speed (mph)
Caltrain	San Francisco, CA		
Coaster	San Diego, CA		
FrontRunner	Salt Lake City, UT	78	
LIRR*	New York, NY		75
MARC*	Baltimore, MD		
MBCR*	Boston, MA		
Metra	Chicago, IL		
Metro-North Railroad	New York, NY	Cooper E80	85 (50 frt)
Metrolink	Los Angeles, CA		
New Jersey Transit	New York, NY		
New Mexico Rail Runner Express	Albuquerque, NM		
NICTD*	Chicago, IL		
Northstar Line	Minneapolis, MN		
RTD*	Denver, CO	36	79
SEPTA*	Philadelphia, PA	78	100
Trinity Railway Express	Dallas-Fort Worth, TX		
Tri-Rail	Miami, FL		

*LIRR = Long Island Rail Road, MARC = Maryland Area Regional Commuter, MBCR = Massachusetts Bay Commuter Railroad, NICTD = Northern Indiana Commuter Transportation District, RTD = Regional Transportation District, SEPTA = Southeastern Pennsylvania Transportation Authority

Rail Transit System Characteristics

This section quantifies other pertinent characteristics of the light, heavy, and commuter rail transit systems in the US. Tables 1-8, 1-9, and 1-10 show the number of track miles for each system, and in total for each rail transit mode in the US.

Table 1-8
Light Rail Transit System Characteristics

Agency/Transit System	City/Geographical Area	Track Miles
Capital Metro	Austin, TX	32.3
CATS*	Charlotte, NC	20.7
DART*	Dallas, TX	173.5
GCRTA*	Cleveland, OH	15.4
Hampton Roads Transit	Norfolk, VA	14.8
Houston METRO	Houston, TX	18.5
Maryland MTA	Baltimore, MD	57.4
MBTA*	Boston, MA	54.1
Metro	Minneapolis, MN	35.6
MetroLink	St. Louis, MO	103.4
Metro Rail	Los Angeles, CA	120.9
Muni Metro	San Francisco, CA	79.8
Niagara Frontier T.A.	Buffalo, NY	12.8
NJ Transit	Camden, NJ	57.7
NJ Transit	Jersey City, NJ	48.2
NJ Transit	Newark, NJ	12.6
PA Transit	Pittsburgh, PA	53.5
RTD*	Denver, CO	100
Sacramento RT	Sacramento, CA	80
SEPTA*	Philadelphia, PA	102
Sound Transit	Seattle, WA	53.2
TRAX*	Salt Lake City, UT	100
TriMet	Portland, OR	118
Valley Metro Rail	Phoenix, AZ	48.2
Valley Transit	San Jose, CA	80.1
Total		*1,592.7*

*CATS = Charlotte Area Transit System, DART = Dallas Area Rapid Transit, GCRTA = Greater Cleveland Regional Transit Authority, MBTA = Massachusetts Bay Transportation Authority, RTD = Regional Transportation District, SEPTA = Southeastern Pennsylvania Transportation Authority, TRAX = Transit Express

Table 1-9

Heavy Rail Transit System Characteristics

Agency/Transit System	City/Geographical Area	Track Miles
Baltimore Metro Subway	Baltimore, MD	34.4
BART*	San Francisco, CA	263.8
CTA*	Chicago, IL	303.3
GCRTA*	Cleveland, OH	41.9
MARTA*	Atlanta, GA	119.9
MBTA*	Boston, MA	107.3
Metrorail	Miami, FL	58.8
Metrorail	Washington, DC	228.5
Metro Rail	Los Angeles, CA	43.2
NYCTA8	New York, NY	818
PATCO* Speedline	Philadelphia, PA	33.7
PATH*	New York, NY	43.1
SEPTA*	Philadelphia, PA	64.8
Total		*2,160.7*

*BART = Bay Area Rapid Transit, CTA = Chicago Transit Authority, GCRTA = Greater Cleveland Regional Transit Authority, MARTA = Metropolitan Atlanta Rapid Transit Authority, MBTA = Massachusetts Bay Transportation Authority, NYCTA = New York City Transit Authority, PATCO = Port Authority Transit Corporation, PATH = Port Authority Trans-Hudson, SEPTA = Southeastern Pennsylvania Transportation Authority

Table 1-10

Commuter Rail Transit System Characteristics

Agency/Transit System	Metropolitan Area	Track Miles
Caltrain	San Francisco, CA	
Coaster	San Diego, CA	45.2
FrontRunner	Salt Lake City, UT	100
LIRR*	New York, NY	658
MARC*	Baltimore, MD	
MBCR*	Boston, MA	755.7
Metra	Chicago, IL	
Metro-North Railroad	New York, NY	813
Metrolink	Los Angeles, CA	714.9
New Jersey Transit	New York, NY	544.9
New Mexico Rail Runner Express	Albuquerque, NM	
NICTD*	Chicago, IL	
Northstar Line	Minneapolis, MN	
RTD*	Denver, CO	54
SEPTA*	Philadelphia, PA	222
Trinity Railway Express	Dallas-Fort Worth, TX	
Tri-Rail	Miami, FL	
Total		*3,907.7*

*LIRR = Long Island Rail Road, MARC = Maryland Area Regional Commuter, MBCR = Massachusetts Bay Commuter Railroad, NICTD = Northern Indiana Commuter Transportation District, RTD = Regional Transportation District, SEPTA = Southeastern Pennsylvania Transportation Authority

Conclusions

Based on the data provided in the Tie Census, the following conclusions can be drawn:

- There are at least 2,820,759 concrete crossties on rail transit properties, including:
  - 1,540,362 on light rail transit systems (Table 1-2)
  - 261,749 on heavy rail transit systems (Table 1-3)
  - 1,018,648 on commuter rail transit systems (Table 1-4) (excluding tracks not owned by the transit authority)
- The highest design axle loads for rail transit are:
  - Light rail: 35 kips – NJ Transit (Table 1-5)
  - Heavy rail: 35 kips – MARTA and Baltimore (Table 1-6)
  - Commuter rail: 80 kips – Metro-North Railroad (Table 1-7)

Concrete Crosstie and Fastening System Load Quantification

Understanding of the type and magnitude of loads entering the track system at the wheel-rail interface is critical to developing a holistic understanding of the structural performance of the track superstructure. Quantification of loading conditions is also the first step in further improving the design of the rail transit infrastructure and its components. In the context of experimentation and modeling, these input loading data provide the basis to guide field and laboratory experimental efforts as well as analytical FE modeling of the track's structural performance. A quantitative understanding of the loading environment can lead to optimized components and system designs for the unique loading conditions encountered in various rail transit systems.Unlike freight railroads, the rail transit industry does not have any common set of design standards specifying the loading and capacity of rail transit vehicles. Hence, there is a great variety of transit vehicles that are currently in operation in the US due because transit agencies have the flexibility to modify their vehicle design to accommodate their infrastructure conditions and operational demands.

Prior research at UIUC on load quantification has been focused on understanding the heavy-haul freight railroad environment. However, the results and recommendations from these studies may not be completely applicable to the transit industry due to the fundamental differences between the infrastructure and operational characteristics of rail transit and heavy-haul freight railroads.

Presently, there is no widely-accepted research on quantification of the loading environment for rail transit infrastructure and its components. There are, however, some focused reports and studies that can guide this research effort. The Transit Cooperative Research Program (TCRP) D-5 research report used data captured by a wheel impact load detector (WILD) on VIA Rail in Canada [8]. The report shows that the typical static wheel loads of the VIA Rail vehicles are 16–18 kips with a maximum value of 38 kips [8]. Vuchic documented the vehicle characteristics of several rail transit systems in the US, Europe, and South America [9]; he also studied the relationship between average gross axle load and gross floor area and between power and tare weight. The *Track Design Handbook for Light Rail Transit* summarized the vehicle characteristics from 26 light rail systems in the US and Canada [10]. Other examples of rail transit infrastructure track loading research are case studies that were commissioned by transit agencies, albeit limited in number and scope [11, 12]. However, there is no comprehensive study of rail transit vehicle characteristics in the US across light, heavy, and commuter rail systems. In addition, some transit vehicle and track design standards were established decades ago and have not been updated with respect to the current loading environment. These standards are in need of updating to reflect the changes in current infrastructure and vehicle conditions.

Rail Transit Static Load Quantification

To develop an understanding of the current state of practice regarding the loading environment of rail transit vehicles, researchers at UIUC collected information pertaining to rail transit vehicles using several sources. The 2013 Revenue Vehicle Inventory published by FTA in the National Transit Database (NTD) is used as the primary reference for rail transit vehicles in the US. It is a comprehensive database that contains up-to-date information of rail transit rolling stock from more than 40 of the nation's transit agencies and provides rail transit vehicle fleet size and characteristics, including owner, transit mode, manufacturer, year of manufacture, model number, and seating and standing capacity. However, it fails to document other critical vehicle characteristics that relate to track design, such as tare weight, number of axles, and wheel diameter [13].

Extensive efforts were made to ensure the quality of the information used in this analysis and to obtain as much data as possible. However, it was not possible to obtain information for every railcar. In addition, rail transit systems are frequently purchasing new vehicles, selling vehicles to other systems, and retiring or rehabilitating old vehicles. As such, it is difficult to keep rolling stock information up to date, and the authors of this report understand that as of the writing of this report some data may be stale. The results stemming from this research are valid for understanding general differences in rail transit loading

environment in the US for the three rail transit modes; however, those seeking research on track structural design for transit systems should consult the transit agencies for the most up-to-date information.

Passenger Vehicle Weights

The rail transit industry is currently using the AW0 to AW4 design criteria to design vehicles that are used to transport passengers. AW0 is the empty car weight without any passenger loading. AW1 is the seated load, defined as the empty car weight plus the weight of seated passenger loads at maximum seating capacity. AW2 is the design load of the railcar, defined as the sum of the AW1 load and the weight of standing passengers at the density of 4 passengers per square meter (3.3 passengers per yd^2). AW3 is the crush load, defined as the sum of the AW1 load and the weight of standing passengers at the density of 6 passengers per square meters (5.0 passengers per yd^2). AW4 is the structural design load, defined as the AW1 load and the weight of standing passengers at the density of 8 passengers per square meters (6.7 passengers per yd^2). AW4 is not typically considered in track superstructure design since it is a theoretical loading only for bridge design and virtually certain to never be experienced in service. The rail transit industry is currently using the AW3 load—the crush load—as the maximum load that track components can withstand [10]. As commuter locomotives do not carry revenue passengers, only the AW0 load is used for calculating the load of commuter locomotives.

Given that data on standing space are not generally available for most rail transit vehicles in the US, an alternative expression of the AW3 load is used in this research effort, which equals the empty car weight plus the product of average passenger weight and the maximum passenger capacity for the vehicle [14].

Average Passenger Weight

The *Light Rail Design Handbook* and design specifications from at least a subset of rail transit agencies specifies the average passenger weight to be 155 pounds [10]. However, APTA research shows that 155 pounds was the median weight of the population in the 1970s, and the median weight of the population in the US in 2015 is 182 pounds [15]. Most transit agencies and track component manufacturers current use 175 pounds as average passenger weight. There are also examples of rail transit vehicle design using an average passenger weight of 165 pounds and 180 pounds [14]. None of these values of average passenger weight fully address the increase in average weight since the 1970s. APTA's research suggests the use of 199 pounds for seated passenger weight and 106 lbs/ft^2 for standing passenger weight, taking into account 10 pounds of personal items and 7 pounds for year-round clothing [15]. As data for standing area are generally unavailable for most railcars, it is impractical to calculate total weight using the standing area. Additionally, much prior research fails to consider the

weight of children, which might lower the average passenger weight. Therefore, we propose to use 195 pounds as the average passenger weight. This value is specified by the Flight Standards Service, a subsidiary of the Federal Aviation Administration (FAA), as the average adult passenger winter weight and takes into account weight increases over the past four decades as well as seasonal clothing and personal baggage items [16].

Railcar Passenger Capacity and Number of Active Revenue Vehicles

The 2013 Revenue Vehicle Inventory provides the passenger capacity, both seated and standing capacity and the number of active revenue vehicles for each transit vehicle model in the US [13]. With passenger capacity and empty weight obtained for most transit rail vehicles in the US, AW0 and AW3 loads could be calculated and the near-total transit vehicle weight distribution could be analyzed.

Results and Discussion Regarding Rail Vehicle Weights

The most common type of vehicle used on light rail transit consists of an articulated unit with two sections and three trucks, known as a Light Rail Vehicle (LRV); these are considered as one vehicle in this research. Diesel multiple units (DMUs) and electric multiple units (EMUs) are two common units for heavy rail and commuter rail vehicles; these are self- propelled railcars that can operate either as single cars or in consists of two or more units. DMUs and EMUs are often semi-permanently coupled into married pairs or sets, with a control-equipped vehicle at either end of the set. For the purposes of this research, one heavy rail or commuter rail vehicle is defined as one single car, half of a married pair, or one part of a multi- car set.

The individual axle loads of the majority of light and heavy rail transit vehicles are not typically uniformly distributed for a given vehicle. Due to unbalanced weight distribution in the car body, the axle loads may vary. Since the difference in axle loads on a given vehicle is relatively small, the weight of the car is assumed to be uniformly distributed on all axles. Therefore, the axle load is calculated by dividing the gross weight of the car by the number of axles. The axle load distribution for three modes is shown in Figure 1-4. Additional statistical information of axle load distribution is provided in Table 1-11.

Figure 1-4

Light, heavy, and commuter rail transit axle load distributions

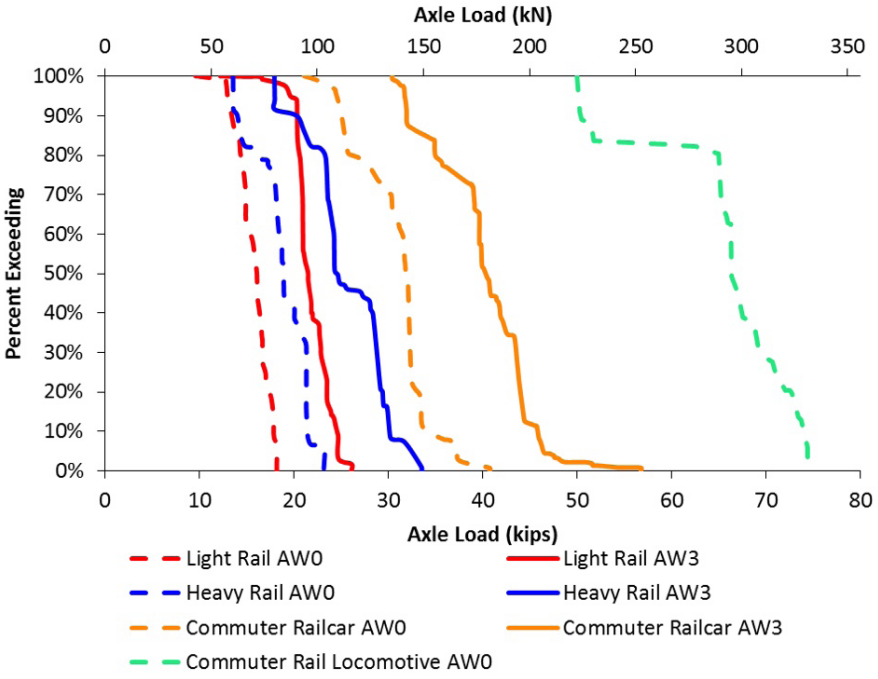

Table 1-11

AW0 (Empty) and AW3 (Crush) Axle Loads for Light, Heavy, and Commuter Rail Transit Vehicles

Transit Mode	AW0 Axle Load (kips)			AW3 Axle Load (kips)		
	Min	Max	Avg	Min	Max	Avg
Light rail	9.6	18.2	15.7	12.2	26.1	21.8
Heavy rail	11.9	23.2	18.7	16.2	33.5	25.5
Commuter railcar	21.1	40.8	30.6	30.4	56.7	40.0
Commuter locomotive	50.0	74.4	65.4	N/A	N/A	N/A
Transit Mode	**AW0 Axle Load (kN)**			**AW3 Axle Load (kN)**		
	Min	Max	Avg	Min	Max	Avg
Light rail	42.7	81.0	69.9	54.3	116.1	97.0
Heavy rail	53.0	103.2	83.2	72.1	149.1	113.5
Commuter railcar	93.9	181.6	136.2	135.3	252.3	178.0
Commuter locomotive	222.5	331.1	291.0	N/A	N/A	N/A

It is important to note that rail transit vehicles do not always govern the design load of rail transit infrastructure. Many commuter rail systems share their infrastructure with freight railroad rolling stock, which typically generate significantly higher axle loads. Work equipment, such as ballast cars and cranes, usually have a higher axle load than the rail transit vehicles. For instance, the largest AW3 axle load of passenger railcars on the Massachusetts Bay Transportation Authority (MBTA) heavy rail system is 33.5 kips, and the static axle load of work equipment on MBTA heavy rail system could be as high as 38 kips [17].

Dynamic Wheel Load Factors

Van Dyk studied the effectiveness of several methods of calculating dynamic wheel load factors for heavy-haul freight railcars by comparing theoretical

results with field data [18]. This study adopted a similar methodology to analyze the effectiveness of these design factors with respect to rail transit loading conditions. Table 1-12 contains the general equations for dynamic factor with the input parameters for each equation.

Table 1-12

Dynamic Factor Equations and Variable Definitions

		Vehicle Parameters Included						Track Parameters Included					
Dynamic Factor	Expression for ϕ	Train Speed	Wheel Diameter	Static Wheel Load	Unsprung Mass	Vehicle Center of Gravity	Locomotive Maintenance Condition	Track Modulus	Track Stiffness at Rail Joint	Track Joint Dip Angle	Cant Deficiency in Curves	Curve Radius	Track Maintenance Condition
Talbot	$1+\frac{33V}{100D}$	•	•										
Indian Railways	$1+\frac{V}{3\sqrt{U}}$	•						•					
Eisenmann	$1+\delta\eta t$	•											•
ORE/ Birmann	$1+\alpha+\beta+\gamma$	•				•	•				•	•	•
German Railways	$1+\frac{11.655V^2}{10^5}-\frac{6.252V^3}{10^7}$	•											
British Railways	$1+14.136(\alpha_1+\alpha_2)V\sqrt{\frac{D_J P_u}{g}}$	•		•	•				•	•			
South African Railways	$1+0.312\frac{V}{D}$	•	•										
Clarke	$1+\frac{15V}{D\sqrt{U}}$	•	•					•					

Variable	Definition
V	Train speed (mph)
D	Wheel diameter (in)
U	Track modulus (psi)
δ	0.1, 0.2, 0.3, depending on track conditions
η	1 for vehicle speeds up to 37 mph $1+\frac{V-37}{87}$ for vehicle speeds between 37 and 125 mph
t	0, 1, 2, 3, depending on chosen upper confidence limits defining probability of exceedance
α	Coefficient dependent on level of track, vehicle suspension, and vehicle speed, estimated to be $0.167\left(\frac{V}{100}\right)^3$ in most unfavorable case
β	Coefficient dependent on wheel load shift in curves (0 in tangent track)
γ	Coefficient dependent on vehicle speed, track age, possibility of hanging crossties, vehicle design, and locomotive maintenance conditions, estimated to be $0.10+0.071\left(\frac{V}{100}\right)^3$ in most unfavorable case
$\alpha_1+\alpha_2$	Total rail joint dip angle (radians)
D_j	Track stiffness at the joints (kN/mm)
P_u	Unsprung weight at one wheel (kN)
g	Acceleration due to gravity (m/s^2)

Source: Adapted from Van Dyk et al.2015

Among the equations used by Van Dyk [18], the South African Railways equation is a variant of Talbot's equation modified for narrow gauge tracks. The majority of rail transit systems in the US are constructed with standard gauge, with the exception of Bay Area Rapid Transit (BART), the Southeastern Pennsylvania Transportation Authority (SEPTA) Market-Frankford Line, Washington Metro, and Pittsburg Light Rail. Therefore, the South African Railways equation is not included in this research. As the British Railways equation is designed specifically for rail joint dips and the American Railway Engineering and Maintenance-of-Way Association (AREMA) *Manual on Railway Engineering* (MRE) Chapter 30 (Ties) equation is to be applied as an upper bound at rail seat in combination with an impact factor, it is not appropriate to compare them with other factors [18, 19].

As the majority of the dynamic factors have vehicle speed, wheel diameter, and track modulus as parameters, measurements or assumptions must be made for the specific rail transit system under investigation. According to Urban Transit System and Technology, the maximum speed for light rail systems is 43 mph, 75 mph for heavy rail transit systems, and 80 mph for commuter rail transit systems [9]. Maryland Area Regional Commuter (MARC) operates the Penn Line, the fastest commuter rail line in the US, at speeds of up to 125 mph [20]. The upper bound of the operating speed used in this analysis is 160 mph so the results could also be applicable to Amtrak trains with higher speeds in the future. The majority of light rail vehicles have a wheel diameter of 26–28⅜ in., the wheel diameter of heavy rail vehicles is 26–34½ in., and the wheel diameter of commuter railcars is 32–36 in., whereas most commuter locomotives have a wheel diameter of 40 in. Therefore, the lower and upper bounds of the new wheel diameter of transit railcars in the US are 26 in. and 36 in., respectively. A track modulus of 3,200 psi is used for the lower bound of track modulus, representing well-maintained timber crosstie track [21]; a track modulus of 10,000 psi is used for the upper bound of track modulus [10]. Since the Talbot, Indian Railways, and Clarke dynamic factors incorporate either or both track modulus and wheel diameter as the parameters in the formula, these three dynamic factors are calculated using both upper and lower bound of track modulus and wheel diameter. Figure 1-5 displays the dynamic factors increasing due to speed for rail transit infrastructure.

Figure 1-5

Summary of design dynamic factors as a function of speed

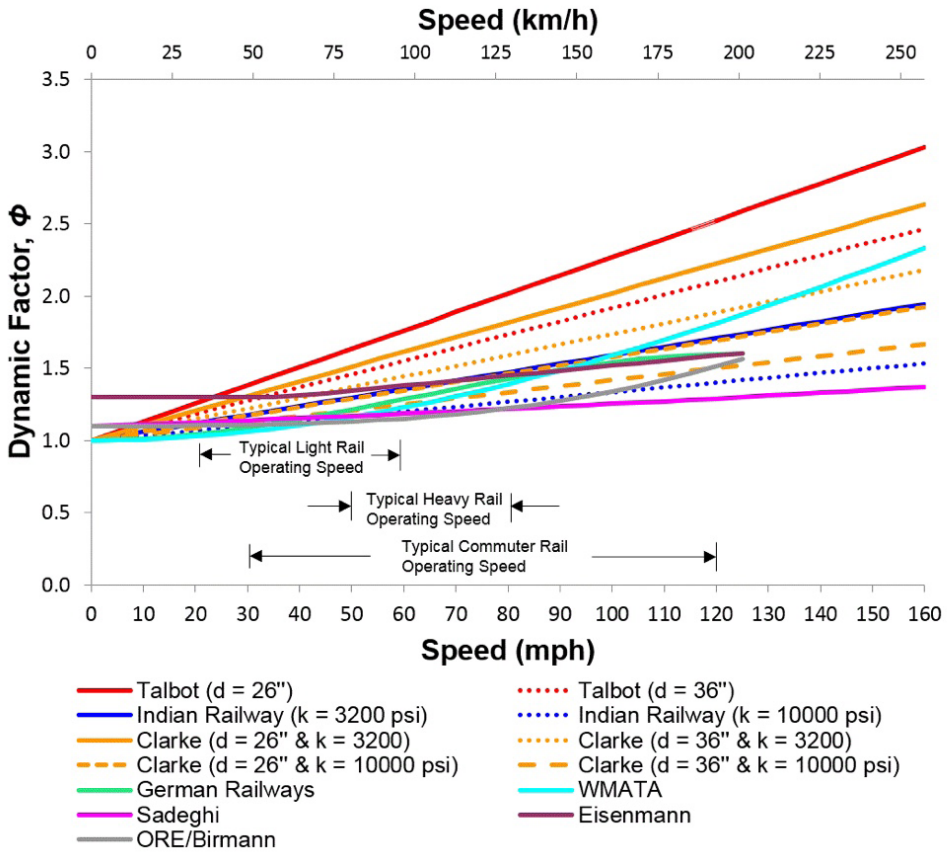

Evaluation of Dynamic Factors

The dynamic factors discussed in the previous sections were developed using different assumptions to adjust for infrastructure and operational conditions. Some of these dynamic factors are also developed specifically for freight railroads, and their applicability to rail transit systems has not been studied. To evaluate the effectiveness of the dynamic factors, actual field-collected WILD data were used to compare the field measured real-time data with the theoretical results generated from the formulas.

Because light rail and heavy rail transit systems rarely have WILD sites installed on their infrastructure, the evaluation of dynamic factors using WILD data will be applicable only to commuter rail systems. The WILD data used in this research were measured on the tangent tracks in Edgewood, Maryland, Marcus Hook, Pennsylvania, and Mansfield, Massachusetts, where MARC, MBTA, and SEPTA commuter rail operate their commuter rail trains on Amtrak's Northeast Corridor (NEC). (No WILD data of SEPTA commuter rail trains were used in this analysis. The MARC trains at the Marcus Hook WILD site were operated under Amtrak during the Thanksgiving weekend for special

operation.) Several parameters in the dynamic factor formulas were modified to accommodate the track and vehicle conditions at these WILD sites. A track modulus of 6,000 psi was used to represent well-maintained concrete crosstie track at these WILD sites [21]. The wheel diameters of MARC and MBTA commuter railcars are typically 36 in. Track quality was assumed to be 0.1 to represent track in very good condition. A confidence factor of 3 was used to generate the upper confidence limit of 99.7%, applicable for rail stresses, fastenings, and crossties. The predicted dynamic factor values are plotted as the ratio of peak vertical wheel load to nominal wheel load. Figure 1-6 shows commuter railcar wheel load data relative to dynamic factors. The metrics in Table 1-13 are used to further evaluate the effectiveness of dynamic factors, and the metrics are explained in detail by Van Dyk [18].

Figure 1-6

Peak/nominal wheel load ratios of commuter rail rolling stock at Edgewood MD, Marcus Hook PA, and Mansfield MA (WILD data from 2010 and 2011)

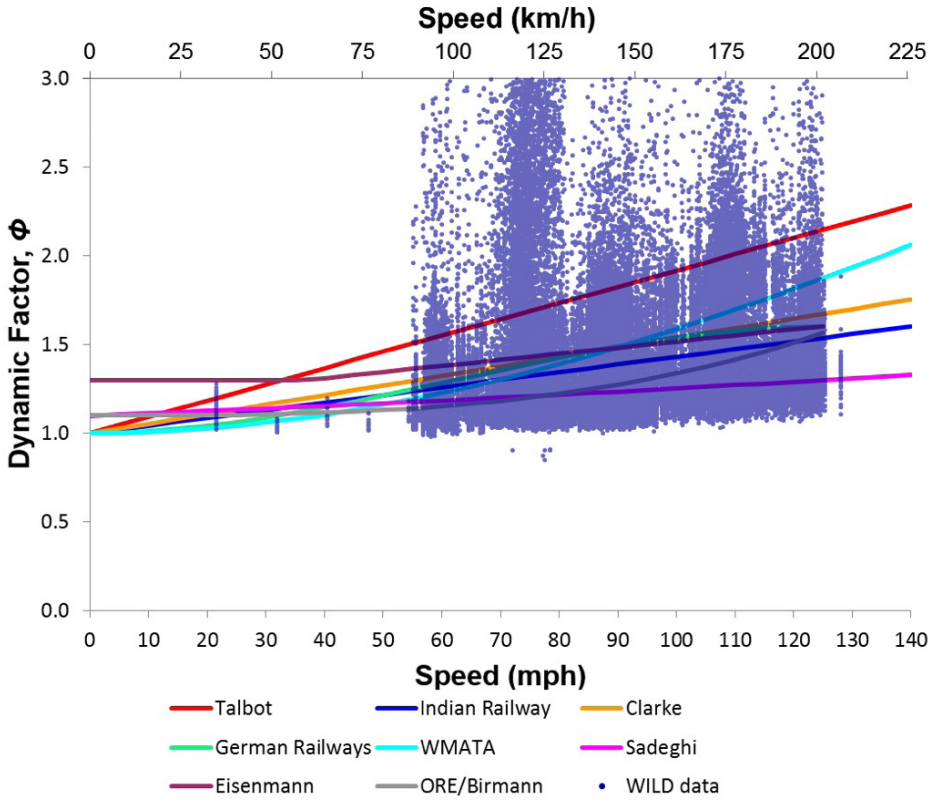

Table 1-13

Evaluation of Dynamic Wheel Load Factors Using Various Metrics

Evaluation Metric	Dynamic Factors							
	Talbot	Indian Railways	Eisenmann	ORE/Birmann	German Railways	Clarke	WMATA	Sadeghi
Percent Exceeding	7%	35%	26%	68%	27%	26%	24%	79%
Mean Signed Difference $\sum \frac{(f(x_i)-y_i)}{n}$	0.47	-0.02	0.07	-0.15	0.08	0.09	0.14	-0.19
Mean Percentage Error $\frac{100\%}{n}\sum(f(x_i)-y_i)/y_i$	35.6	1.5	7.8	-7.9	8.1	9.1	12.7	-10.8
Root Mean Square Deviation $\sqrt{\sum(f(x_i)-y_i)^2/n}$	0.30	0.07	0.08	0.10	0.08	0.08	0.10	0.11
Speed-Weighted Signed Difference $\sum(x_i f(x_i)-x_i y_i)/\sum x_i$	0.48	-0.01	0.07	-0.16	0.08	0.10	0.16	-0.19
Load-Weighted Signed Difference $\sum(Q_i f(x_i)-Q_i y_i)/\sum Q_i$	0.48	0.00	0.09	-0.13	0.10	0.11	0.16	-0.17

More than 60% of wheel loads measured exceed the predicted values generated by ORE/Birmann and Sadeghi dynamic factors. Both of these equations largely underestimate the dynamic factors with a negative signed difference and negative percentage error; therefore, they are not appropriate to calculate dynamic factors for rail transit vehicles. Other than ORE/Birmann and Sadeghi formulas, all the other dynamic factors produce accurate results, with small mean signed differences, small mean percentage error, and small root mean square. Among all dynamic factors, Talbot's has the lowest percentage exceedance and the largest mean signed difference, indicating that it is the most conservative method to calculate dynamic loads.

Evaluation of Impact Factor

The concept of impact factor has been adopted by the rail industry to calculate the increase in wheel load due to track and wheel irregularities, and speed. The AREMA manual defines the impact factor as a percentage increase over static vertical loads intended to estimate the dynamic effect of wheel and rail irregularities [19]. It specifies an impact factor of 200%, which indicates the design load is three times the static load, equivalent to an impact load factor of three [19]. Since the use of impact factors in the AREMA manual is the same

for both freight railroads and rail transit systems, the WILD data show that the current impact factor may not be suitable for the commuter rail transit loading environment. The applicability of the impact factor requires further studies with respect to today's rail transit loading environment. Due to the difference between commuter railcars and locomotives in terms of loading characteristics, these two types of commuter rail equipment were analyzed separately. Using the WILD data at Edgewood, Marcus Hook, and Mansfield, the peak load is plotted against the nominal load in Figures 1-7 and 1-8 for commuter railcars and locomotives, respectively, with lines representing impact factors of 1, 2, 3, and 4.

Figure 1-7

Relationship between peak and nominal wheel loads of commuter railcars on Amtrak Infrastructure at Edgewood MD, Marcus Hook PA, and Mansfield MA (WILD data from 2010 and 2011) and design impact factors

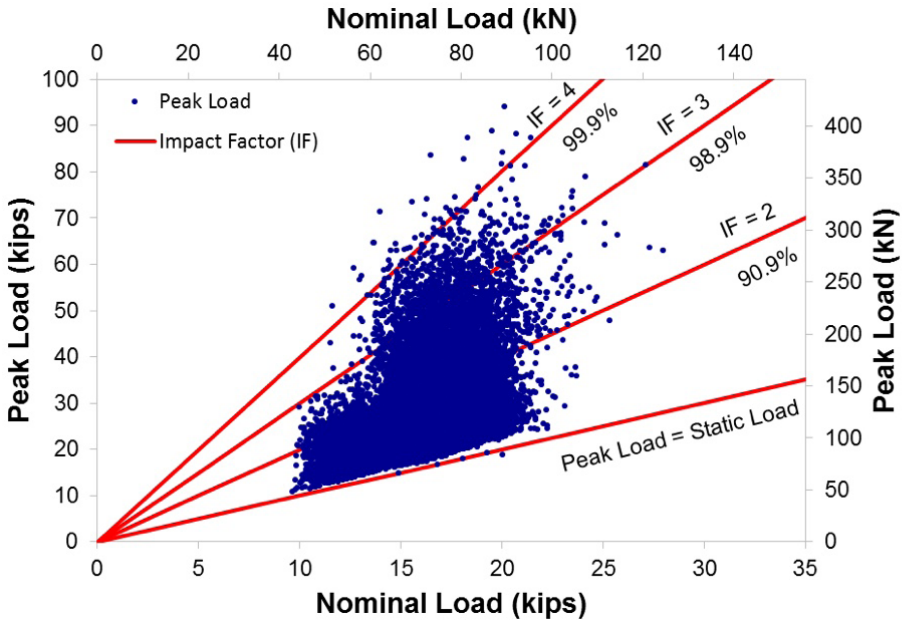

Figure 1-8

Relationship between peak and nominal wheel loads of commuter locomotives on Amtrak Infrastructure at Edgewood MD, Marcus Hook PA, and Mansfield MA (WILD data from 2010 and 2011) and design impact factors

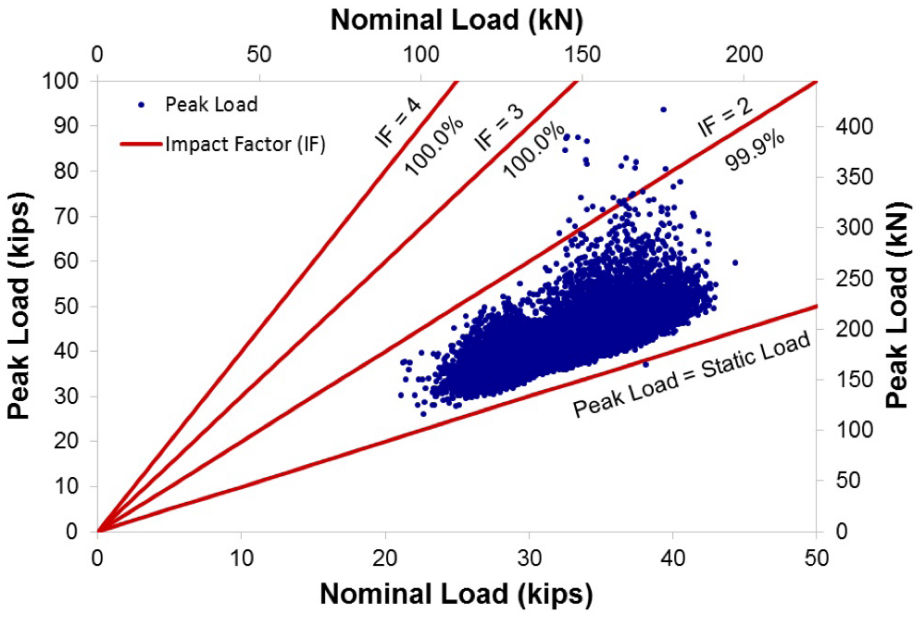

Figures 1-7 and 1-8 show that the impact factor of 3 exceeds 98.9% and 100% of the commuter railcar and locomotives wheel loads, respectively. This indicates that the impact factor of 3 specified by the AREMA manual is adequate for calculating the design load for commuter rail vehicles. However, Figure 1-8 shows that the impact factor of 2 exceeds 99.9% of the commuter locomotives wheel loads, which indicates that an impact factor of 2 is sufficient for calculating the peak wheel load for commuter locomotives. As the nominal wheels of commuter locomotives are significantly higher than those of commuter railcars, an impact factor of 2 for commuter locomotives could reduce the design load for passenger-only track. WILD sites are typically constructed on tangent track using premium track components so that track irregularities are minimized in order to better understand the health of the rolling stock. More demanding track conditions and other track irregularities could lead to a higher impact factor.

Rail Seat Load Quantification

Once the wheel-rail loads are known, the next step in understanding the load transfer process is to estimate the rail seat loads. Van Dyk et al. [22] provided a summary of three established methodologies of calculating rail seat loads and evaluated their effectiveness on freight railroad systems. Table 1-14 contains the general equations for rail seat load with the input parameters for each equation.

Table 1-14

Rail Seat Load Equations and Variable Definitions

			Parameters Included						
Dynamic Factor	Expression for Rail Seat Load (Imperial)	Expression for Rail Seat Load (Metric)	Train Speed	Wheel Diameter	Static Wheel Load	Sleeper Spacing	Modulus of Elasticity	Moment of Inertia	Track Modulus
AREMA (2012 Manual)	$(1.5626x + 12.811)P/100$	$(61.52x + 12.811)P/100$			•	•			
Talbot (Hay 1953)	$\frac{(P + 0.01 * P(V-5)) * S * \sqrt[4]{\frac{u}{4EI}}}{2}$	$\frac{(P + 0.01P(0.62V-5)) * S * \sqrt[4]{\frac{10.41u}{EI}}}{.051}$	•		•	•	•	•	•
Kerr (2003 Edition)	$\frac{\left(1 + 0.33\frac{v}{D}\right) * P * \alpha * \sqrt[4]{\frac{k}{4EI}}}{2}$	$\frac{\left(1 + 0.52\frac{v}{D}\right) * P * \alpha * \sqrt[4]{\frac{10.41k}{EI}}}{.051}$	•	•	•	•	•	•	•

Variable	Definition
V, v	Train speed (mph)
D	Wheel diameter (in)
u, k	Track modulus (psi)
x, α, **S**	Sleeper spacing (in)
P	Static wheel load (pound)
I	Moment of inertia (in^4)
E	Modulus of elasticity of rail (psi)

Source: Adapted from Van Dyk [15]

To evaluate the applicability of these methodologies to the loads experienced by rail transit systems, a numerical analysis was performed with respect to rail transit infrastructure characteristics. Crosstie spacing of 30 in., rail section of 136 RE, wheel diameter of 33 in., and track modulus of 6,000 psi were used to represent typical conditions on concrete crosstie track. Figure 1-9 shows the predicted rail seat loads calculated using the three methods. The AREMA method has the highest rail seat values, and the Talbot and Kerr methods generate lower results, with Talbot being the lowest.

Figure 1-9

Rail seat loads as a function of wheel load

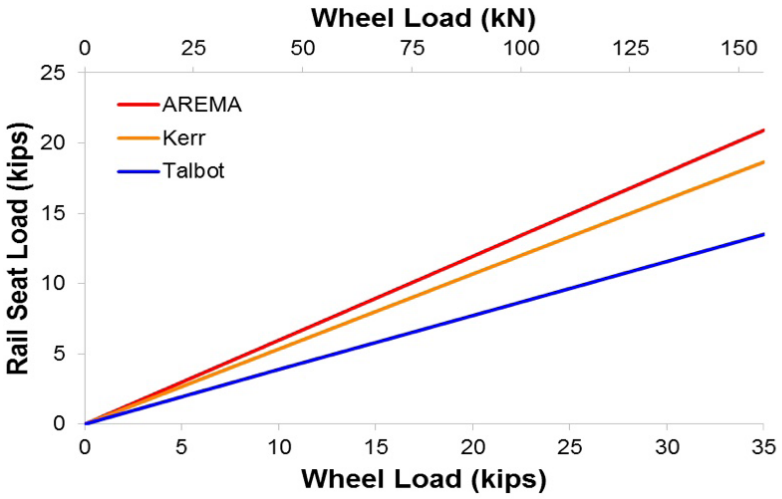

To further evaluate the applicability of the three methods to rail transit systems, four different wheel loads were used as initial input loads—10.9, 12.75, 20.7, and 33.05 kips, which represent the average loading conditions for light rail vehicles, heavy rail vehicles, commuter railcars, and commuter locomotives based on earlier investigation (Table 1-11). To compare the effect of speed into these equations, rail seat load was calculated using the three equations for three different speeds. Figure 1-10 shows the static rail seat loads calculated using the three methodologies at speeds of 0, 60, and 120 mph.

Figure 1-10

Rail seat loads for various input load values at 0, 60, and 120 mph

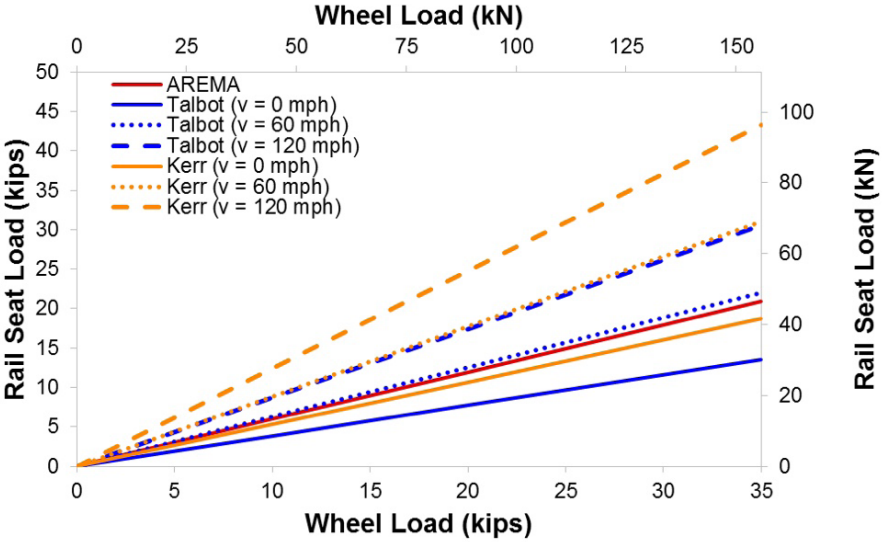

These results indicate that the AREMA method generates the highest rail seat load at low speeds. Since the AREMA method does not have speed as one of its input parameters, the rail seat loads calculated by Talbot and Kerr increase as speed increases relative to those calculated by AREMA. At 60 mph, the Talbot and AREMA methodologies generate similar rail seat load values. As speed increases to 120 mph, both the Talbot and Kerr methods predict much higher rail seat loads than AREMA.

Conclusions

A comprehensive static load quantification was conducted for light, heavy, and commuter rail transit systems in the US. Additionally, an improved understanding of rail transit loading environments was developed using industry databases and design recommendations. The applicability of several dynamic factors to rail transit loading environment was evaluated by comparing the predicted results with WILD data measured on commuter rail rolling stock. Most dynamic factors can predict peak wheel loads for commuter rail systems with high-level accuracy and precision. The effectiveness of the impact factor of 3 recommended by the AREMA manual was also studied with respect to the rail transit loading environment in the US. As shown, the impact factor of 3 is adequate for quantifying the effect of track and wheel irregularities on commuter rail transit systems and provides a conservative estimate of wheel loads. Future work (as described in Section 2) will include collection and analysis wheel-rail interface data from light, heavy, and commuter rail transit systems to evaluate the effectiveness of the dynamic and impact factors.

SECTION

2

Quantification of Rail Transit Wheel Loads and Development of Improved Dynamic and Impact Factors

Introduction

UIUC researchers studied the concept of modal variability in peak wheel-rail loads given its criticality as an input to field bending moment magnitude. The focus was on rail transit loadings because of the limited amount of research on the field of loading environment for rail transit modes, especially when compared to heavy axle load (HAL) freight railroads in the US (Table 2-1).

Table 2-1

Comparison of Rail Transit and Heavy Axle Load (HAL) Freight Railway Operations, Attributes, and Prior Research

HAL Freight	Rail Transit
Established research and findings	Limited infrastructure research
Very heterogeneous fleet in unrestricted interchange throughout network	Homogeneous fleet in closed systems
Performance-based wheel maintenance	Mileage-based wheel maintenance
Extensive field instrumentation (WILDS)	Relatively little field instrumentation
Few crosstie designs	Many crosstie designs
Crossties designed by manufacturers, based on guidance from railroads	Limited transit agency involvement in design process, largely engineering firms
Tamping cycle is tonnage-based or driven by geometry deviations	Maintenance due to poor support or geometry deviations rarely required

As such, project researchers recorded data and evaluated loads from light, heavy, and commuter rail transit properties and studied variations in the load distributions. Although it is well known that moving wheels produce higher loads than the same wheel at rest [21, 23], predicting the totality (i.e., combined static, dynamic, and impact) of the loading environment at the wheel-rail interface is non-trivial. This is because the total load is not necessarily linearly related to the vehicle's static load. Furthermore, the degree of non-linearity and overall variability may differ for different types of rail transport.

Developing accurate models for predicting dynamic and wheel impact load factors is critical to the efficient design of railway track structures and components given that load factors may be inconsistent for different types of track infrastructure and rolling stock. The current method of assessing a constant impact factor of

3 for concrete crosstie design as described by AREMA [24] and use of a wheel load dynamic factor of 0.33 to account for speed as described by Talbot and documented by Hay [25] and Kerr [23] is overly simplistic and likely inaccurate.

As a part of this project, researchers at UIUC recorded extensive wheel-rail input data on rail transit systems over a period of several years. These data allowed generation of empirical relationships reflective of the current loading environment.

For the heavy axle load (HAL) freight railroad operating environment, research has been conducted to quantify the load at the wheel-rail interface [26–29]. Relatively little comparable work has been conducted on rail transit systems, although commuter rail systems have been studied when their rolling stock operates on infrastructure owned by freight or intercity passenger rail operators [28, 30]. It is generally thought that wheel treads on rail transit rolling stock are more uniform than railroad freight car wheel treads, due to more frequent wheel trueing and other forms of vehicle and track maintenance in the transit environment. Consequently, they may be expected to generate lower dynamic and impact loads.

Beyond static load and speed, which are widely considered to be the most critical variables, total wheel-rail interface loads are shown to be influenced by wheel diameter, the portion of static load representing unsprung mass, irregularities in the track structure, track maintenance conditions, and a variety of other vehicle and track characteristics [22, 31, 32]. All of the aforementioned factors are expected to vary when comparing rail transit operations with HAL freight railroads, further emphasizing the need for research to quantify rail transit load factors.

Types of Loads

The railway track loading environment includes the application of static, quasi-static, dynamic, and impact loads [33]. The static load is the load of the rail vehicle at rest, and the quasi-static load is a low frequency oscillation applied over the static weight [34], which is the combined static load and effect of the static load at speed [35, 36]. Dynamic loads are due to the high-frequency effects of wheel/rail interaction, considering track component response and involving inertia, damping, stiffness, and mass. Impact loads that often create the highest loads in the track structure, are generated by track and wheel irregularities.

The distinctions between static, dynamic, and impact loads, their potential implications on the health of the track structure, and the ability to predict their magnitude have been discussed previously [31, 33]. This section briefly discusses rail transit static and dynamic loads and describes an approach used to quantify the totality of the track loading environment at the wheel-rail interface.

Static Loads

Lin et al. [30] conducted a data collection and processing effort to quantify static rail transit rolling stock wheel loads, as described in Section 1. In doing so, UIUC presented graphical results (Figure 3-1) for most rolling stock used on light, heavy, and commuter rail transit properties in the US. These data are useful for developing a baseline to compare the additional loads applied due to dynamic and impact forces. Additionally, they illustrate the wide variety in the three most common rail transit mode axle loads and the infeasibility of designing components and systems that are globally optimal to all three modes.

Figure 2-1

Light, heavy, and commuter rail static axle load percent exceeding distribution

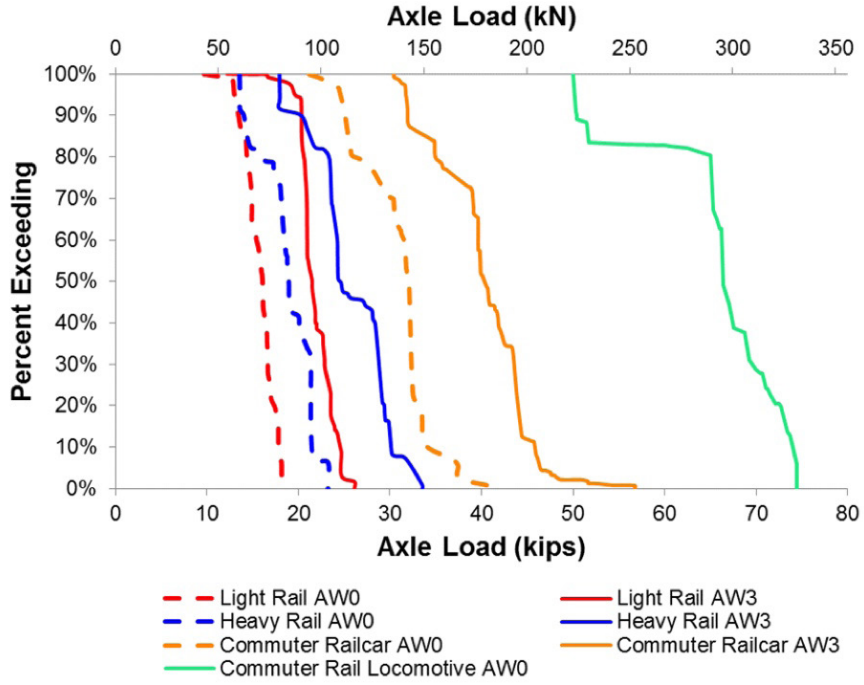

Dynamic and Impact Loads

Over the previous half-century, more than a dozen methods have been developed to predict dynamic loads, which have been summarized in prior research by Doyle [31] and Van Dyk [28]. A subset of these methods was empirically generated using field data from their respective modes of rail transport. These predictive methods include a variety of track loading, health, and rolling stock design factors, as documented by Van Dyk et al. [29]. Much of the prior research has focused on the evaluation of dynamic load factors for HAL freight trains [28, 29, 33], partially due to the widespread deployment of WILD on HAL freight railroad corridors in North America.

The prediction of impact loads and its incorporation into design is comparatively simple. Impact loads are presently incorporated into AREMA recommended design practices for concrete crossties as a 200% increase over the static load (i.e., three times the static load) [24].

Revised Dynamic and Impact Load Factors

Use of most of the dynamic factors mentioned above is restricted to a specific operating environment, thereby limiting their utility and breadth of application. Because these factors have been developed over many years in different regions of the world, they may not accurately reflect the operating conditions found in North America, especially for rail transit applications. Additionally, prior research has shown that the impact factor of 3 may overestimate the flexural demands required under revenue service train operation [29, 37].

To improve the prediction of input loads at the wheel-rail interface and address a key step in the process of executing mechanistic design for track components as outlined by Van Dyk et al. [38], this project included the development of revised predictive equations based on field data. Given that design of rail infrastructure requires knowledge of the total loading that is expected, the loading factors in this section account for static, dynamic, and impact loads. Additional consideration will be given to dynamic loads and the need to relate wheel-rail load to speed.

To generate revised formulae inclusive of both dynamic and impact loads, focused field instrumentation was deployed, and WILD data were used to compare actual loading data to predicted dynamic loads and impact factors. These data were collected or obtained for light, heavy, and commuter rail transit systems.

Data Collection Methodologies

Wheel loading data can be obtained using commercially-available systems that are present within a limited number of commuter rail corridors or by installing new, focused instrumentation that records a subset of the data provided by the commercial systems. The two methods are discussed below.

Wheel Impact Load Detector (WILD) Data

A WILD consists of rail-mounted strain gauges installed over a series of ballast cribs that are oriented in a manner that records vertical rail strain that can be related to wheel loads [26, 28] (Figure 2-2). A typical WILD site is about 50 ft (15 m) in length, with cribs instrumented at various intervals to record a single wheel's rotation five times, recording peak impact and average forces at a data collection rate of up to 25,000 H [27, 39]. There are more than 35 unique outputs obtained from a WILD [28], but this section primarily uses nominal and peak load data.

Using an algorithm that analyzes variability among strain gauges along the site, average (or nominal, as referred to by the WILD manufacturer) forces are filtered from the peak loads to obtain an estimate of static wheel load [28]. This is not a true static wheel load given the dynamic environment in which the measurements are recorded; thus, the nominal load obtained from the WILD

overestimates the typical static loading. This overestimation is acceptable for the current research given that recent field data have failed to support prevailing, empirically-derived relationships between speed and wheel load intended to estimate dynamic load factors [29, 33]. The peak wheel load is simply the highest recorded measurement from the strain gauges along the length of the WILD. Although the WILD typically has been used by infrastructure and rolling stock owners to identify poorly-performing wheels, it has also proven to be a practical means of producing reliable wheel load data useful to rail infrastructure researchers and rail industry practitioners [28, 33, 40–42].

Used to capture commuter rail train loads.

Figure 2-2

WILD on Amtrak's Northeast Corridor at Edgewood MD

WILD sites are constructed on tangent track with concrete crossties, typically with premium ballast, and well-compacted subgrade to reduce sources of load variation within the track structure due to track geometry and support condition irregularities [28]. Although loads experienced at other locations along the railway network may have higher magnitudes due to track geometry and support deviations, these data still provide relevant loading information and are useful in deriving equations for the expected loading environment [38].

Focused Loading Environment Instrumentation

Specifically-designed, focused strain gauge instrumentation was deployed to collect wheel-rail interface input loads on rail transit systems that did not have WILDs. Weldable 350-ohm half- bridge shear strain gauges (Figure 2-3) were applied to the web of the rail to create vertical load circuits with the same configuration used at a single crib of a WILD (Figure 2-4).

Figure 2-3

Weldable half-bridge shear strain gauge and loading frame used to calibrate gauges by relating strain to known system input load

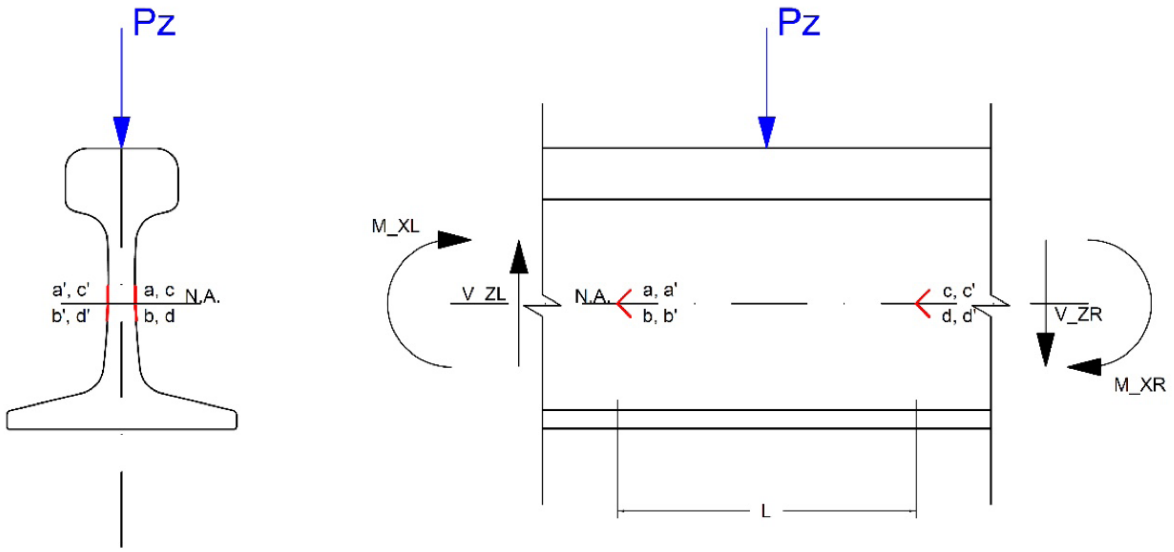

Strain gauges for quantifying lateral load also deployed but not shown.

Figure 2-4

Vertical strain gauge orientation for field testing

Installation of strain gauges required welding gauges to the rail using a portable strain gauge welding unit. This process involved first grinding the web and base of the rail to remove rust and expose pure metal, then clamping a ground wire to the base of the rail, and, finally, placing the strain gauge and using the welding electrode to send current through the material, welding the strain gauge to the rail.

A Delta Frame (Figure 2-3) uses a hydraulic cylinder to apply loads to calibrate the strain gauge instrumentation installed on the rail via application of vertical loads of up to 40,000 lbf (178 kN). Vertical loads are applied using an upward-facing steel triangular frame with loads applied in the center of the bottom side of the frame and reacting off the rail at the two bottom corners (Figure 2 3).

Vertical load and strain are collected simultaneously throughout the calibration process, providing the opportunity to relate future strain readings obtained from the instrumentation to the vertical wheel load that generated them.

Interpretation of Data and Generation of Results

Given that the data presented in this section were acquired using related but distinct instrumentation methodologies, some clarification on the data collection differences is warranted. WILD sites collect data over as many as 25 consecutive cribs to measure the full revolution of the wheel, whereas the UIUC-deployed instrumentation collects data at a single crib and does not record the full rotation of a wheel. Although the method has the limitation of being unable to determine whether the peak load from a wheel was obtained during a given train pass, it records every train pass on a captive rail transit system over long periods of time (one year or more). This volume of data helps to reduce variability and obtain readings from the entire circumference of a wheel.

Data Analysis

Comparison of Impact Factor Curves

The evaluation of rail transit wheel-rail interface input loading conditions was performed using data from three rail transit field sites in the US:

- Light rail transit – St. Louis MetroLink at Fairview Heights, IL (MetroLink)
- Heavy rail transit – Metropolitan Transportation Authority (MTA) New York City Transit Authority (NYCTA) at Far Rockaway, NY (NYCTA)
- Commuter rail transit – Maryland Area Regional Commuter (MARC) at Edgewood, MD (MARC)

MetroLink and NYCTA used focused instrumentation described previously, and MARC is a WILD site owned by Amtrak. For data collected from instrumentation on MetroLink and NYCTA, there were not enough instrumented cribs to record and estimate the nominal wheel load as in a full WILD site. For these sites, the AW0 weight provided in the NTD [7] was used as the nominal load. The measured loads were then used for the "peak" load, which was divided by the nominal AW0 weight to obtain the load factor. As-delivered wheel loads were supplied by MetroLink and were used for the nominal loads in lieu of AW0 loads at the MetroLink site, given the need to better account for wheel-to-wheel nominal load variability of the LRVs. These assumptions are conservative with respect to estimation of impact load factors given that the actual weight of the railcar could be as high as its AW3 load depending on passenger loading.

A histogram of peak wheel loads for each rail transit mode (Figure 2-5) reveals the variety in input loads as measured in the field, and further emphasizes the disparity in loading when only nominal loads are used (Figure 2-1). Additionally, when plotting the total (dynamic and impact) load factors for each rail transit mode

(Figure 2-6), it is evident that the distributions of impact factors for the three rail transit systems are distinct. These reflect the unique relationships that describe the total loading environment that is applied above the static (AW0) loads.

Figure 2-5

Histogram showing distribution of vertical wheel-rail loads from three rail transit systems (MetroLink, NYCTA, MARC)

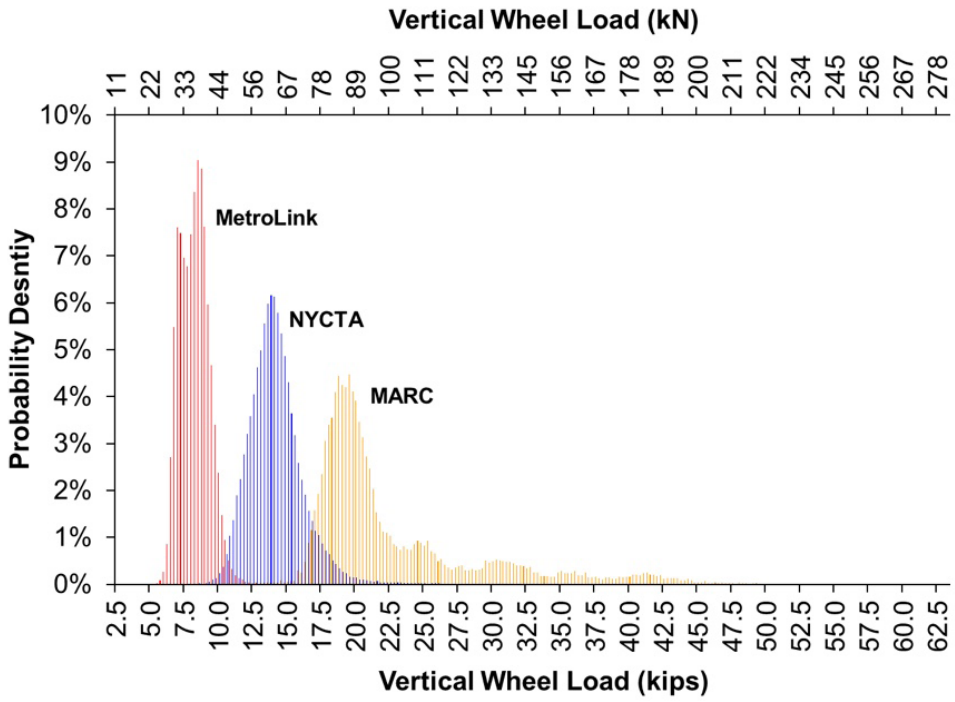

Figure 2-6

Histogram showing distribution of dynamic and impact load (total load) factors from three rail transit systems (MetroLink, NYCTA, MARC)

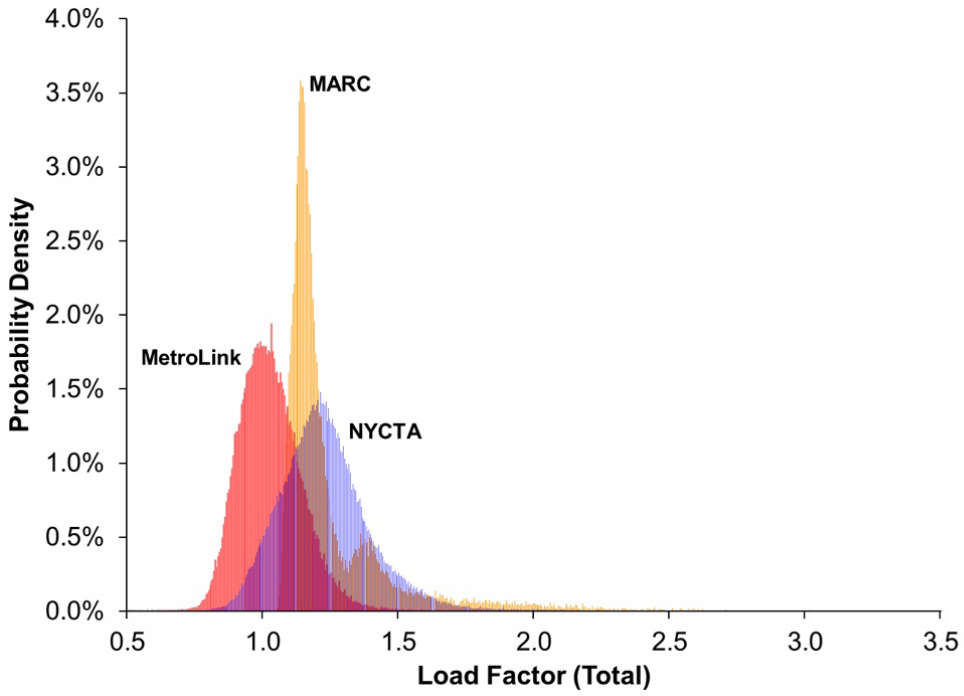

The MetroLink distribution and, to a lesser extent, the NYCTA distribution, raise questions given the presence of impact factors that are less than 1.0 indicating a dynamic load lower than static. This is not reasonable and, based on conversations with MetroLink's mechanical maintenance leadership, can be attributed to several factors. First, MetroLink operates a closed system and has an aggressive wheel truing maintenance program. This reduces the range between static and dynamic loads and, thus, the expected impact factor. Additionally, each wheel on a MetroLink's LRV has a unique, as-delivered weight associated with it. Weights vary among axles and between wheels on a single axle due to the placement of mechanical devices on the LRV. The data collected in the field are processed using the MetroLink-supplied wheel weights and known direction of travel for each train. These loadings, however, may not be reflective of the current weight due to minor changes in the arrangement of equipment on the LRV. For NYCTA, the field site is located on curved track, resulting in varying loads on the high and low rail depending on the operating speed of any given train. Nevertheless, when taken as a whole, data in Figure 2-6 demonstrate that on all three systems the measured load factors were well below the AREMA manual value of 3.0. This is true even when a safety factor is applied to account for the aforementioned concerns related to the MetroLink data.

Descriptive statistics were used to compare the three distributions of impact factors and to determine how they differed (Table 2-2).

Table 2-2

Descriptive Statistics Comparing Rail Transit Impact Factor Data

Statistic	Units	MARC	MetroLink	NYCTA
Sample Size	Number	28,920	62,472	131,062
Range	Load factor	2.997	1.537	4.652
Mean	Load factor	1.258	1.023	1.229
Variance	Load factor^2	0.057	0.013	0.037
Standard deviation	Load factor	0.240	0.115	0.192
Coefficient of variation	Decimal percent	0.190	0.112	0.156
Standard error	Load factor	0.001	0.000	0.001
Skewness	Unitless	3.284	0.616	2.437
Excess kurtosis	Unitless	15.038	1.469	17.537

In comparing the three distributions, the means were found to be similar between MARC (1.26) and NYCTA (1.23), but the variance and skewness were notably higher for the MARC data.

Additionally, the standard deviations were quite different, as would be expected based on visual inspection of the plotted data. These statistics show that the three distributions are unique and cannot be accurately represented using a single distribution. A single impact factor estimate cannot adequately reflect these differences.

Additional statistical tests were used to evaluate the null hypothesis that the impact factor data for the three rail transit modes do not differ (e.g., distribution function) [43]. The Kolmogorov- Smirnov (K-S) test was used to make pair-wise comparisons of each of the three modes. All K-S p values were zero, indicating that the null hypothesis that the three distributions are the same can be rejected. All three types of rail transit systems surveyed had unique impact factor distributions. This dissimilarity has important implications for track component design and the need for different factors for each mode.

Distribution Fitting and Quantification of Goodness of Fit

The focus of this research is to develop generalized relationships to fit the distributions of impact factors for the three rail transit modes to estimate the percentage of loads to be included when selecting future impact factors. This evaluation was made using the distribution fitting feature in the commercially-available software EasyFit (MathWave Technologies), which is able to determine the most appropriate distribution(s) for a set of continuous data using approximately 65 typical distributions (e.g., log-logistic, Gamma, normal, Weibull, etc.) for comparison and fitting purposes.

In addition to the K-S test, the Anderson-Darling statistical procedure was used to compare the distribution of load factors for each transit system to common distributions. The Anderson- Darling method is particularly useful for this application given that it increases the power of the K S statistic to investigate the tails of the distribution and produces a weighted statistic [44, 43]. This is important given the criticality of the tail of the impact-factor distribution in selecting a value for the design of track components.

The best-fit (optimal) impact factor distribution was selected using the Anderson-Darling criteria and was plotted with each rail transit impact factor field data set (Figure 2-7). Of particular interest is how the tails are fitted (shown in greater detail in Figure 2-8) for the maximum 0.10% of impact factors. The extreme values for impact loads also show significant scatter for the MARC commuter rail loading environment. It is likely that this greater variability is due to recorded data from multiple cribs at the WILD location.

Figure 2-7

. Total load factors for three rail transit systems (MetroLink, NYCTA, MARC) and overlay of best-fit distributions

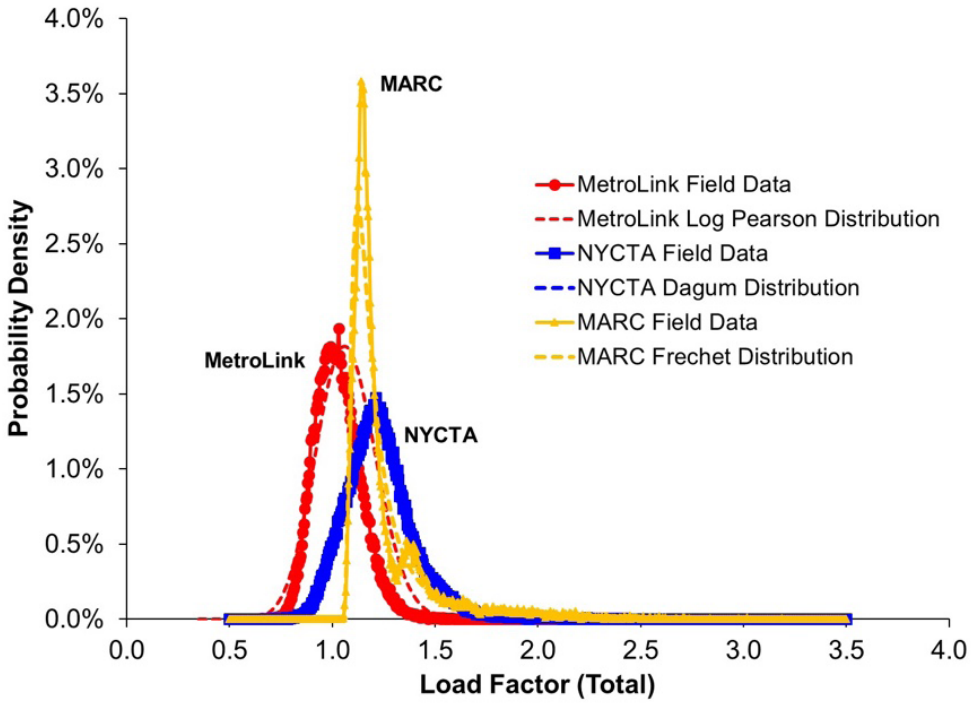

Figure 2-8

Extreme values (highest 0.10%) of total load factors for three rail transit systems (MetroLink, NYCTA, MARC) and overlay of best-fit distributions

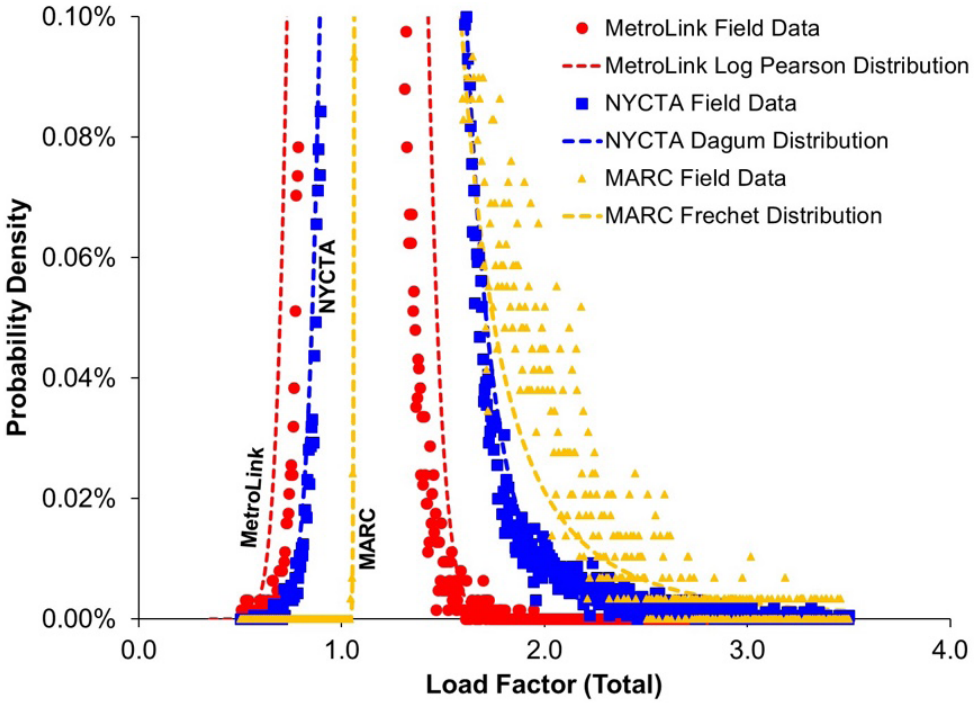

Goodness-of-fit rank-order values for the K-S method and Anderson-Darling were summarized for the three rail transit modes (Table 2-2).

Table 2-3

Goodness of Fit Comparisons of Rail Transit Impact Factor Distributions Using K-S & Anderson-Darling Methods

	Kolmogorov-Smirnov (K-S)			Anderson-Darling		
Distribution	***MARC***	***MetroLink***	***NYCTA***	***MARC***	***MetroLink***	***NYCTA***
Log-Pearson 3	14	2	25	44	1	37
Pearson 6 (4P)	7	5	11	4	2	9
Lognormal (3P)	11	6	12	8	3	11
Pearson 6	26	7	16	23	4	14
Pearson 5	28	3	15	24	5	12
Dagum (4P)	24	13	1	22	7	1
Pearson 5 (3P)	2	4	10	2	8	10
Gamma (3P)	22	12	20	14	13	17
Dagum	35	15	6	54	14	5
Burr (4P)	10	17	4	12	15	3
Log-Logistic (3P)	6	19	3	5	17	2
Beta	31	18	14	13	18	13
Burr	12	21	2	13	19	4
Gen. Extreme Value	3	1	9	3	20	8
Frechet (3P)	1	38	38	1	37	34

*Sorted by Anderson-Darling MetroLink ranking

Based on these results, it is evident that the three distributions' tails are best fit using a variety of different functions, with little overlap among the generalized distributions. This further illustrates that the variables affecting total load factor were unique for each rail transit mode.

The generalized distributions that provided the best fit as ranked by the Anderson-Darling criteria for each of the three modes were as follows: Log Pearson for MetroLink (Eq. 2-1), Dagum for NYCTA (Eq. 2-2), and Frechet for MARC (Eq. 2-3). These distributions are shown in Figure 2-7 and Figure 2-8, along with a histogram of the field data, and the generalized distributions are given by Eqs. 2-1, 2-2, and 2-3. Eqs. 2-4, 2-5, and 2-6 provide the specific distributions representing the data for MetroLink, NYCTA, and MARC, respectively, by inclusion of distribution parameters that best fit the data.

Despite the large number of common distributions checked, the p-values for all data except MetroLink do not allow rejection of the null hypothesis using α = 0.05. The Anderson-Darling rejection critieria were not met for any of the three distributions shown; thus, the distributions are all considered to be different than the sample data. Specifically, the equations allow for future calculations of impact loads considering different percentile loading conditions (e.g., designing to the 99th percentile load). This type of calculation is an integral part of a probabilistic or mechanistic design process.

Log Pearson Distribution

$$F(x) = \frac{\Gamma_{(\ln(x)-\gamma)/\beta}(\alpha)}{\Gamma(\alpha)} \quad (2\text{-}1)$$

Dagum Distribution

$$F(x) = \left(1 + \left(\frac{x-\gamma}{\beta}\right)^{-\alpha}\right)^{-k} \quad (2\text{-}2)$$

Frechet Distribution

$$F(x) = \exp\left(-\left(\frac{\beta}{(x-\gamma)}\right)^{\alpha}\right) \quad (2\text{-}3)$$

MetroLink Best Fit

$$F(x) = \frac{\Gamma_{(\ln(x)+1.593)/0.0076}(211.83)}{\Gamma(211.83)} \quad (2\text{-}4)$$

NYCTA Best Fit

$$F(x) = \left(1 + \left(\frac{x-0.55114}{0.6611}\right)^{-7.2334}\right)^{-0.95689} \quad (2\text{-}5)$$

MARC Best Fit

$$F(x) = \exp\left(-\left(\frac{0.14201}{(x-1.0094)}\right)^{1.9514}\right) \quad (2\text{-}6)$$

In addition to the previous analysis of load factors, vertical load percentiles (Tables 2-4 and 2-5) and their load factors (Table 2-6) are presented below. MetroLink had both a lower load and lower impact factor than either NYCTA or MARC. Although this is expected due to the corresponding static wheel loads, the lower impact or dynamic load factor was not necessarily expected. These values could also be used to estimate the percentage of loads that would be covered by a given design factor.

Table 2-4

Percentiles of Rail Transit Vertical Loads (kips)

Mode	Mean	10%	50%	75%	90%	95%	97.5%	99.5%	100%
MetroLink	8.1	6.8	8.1	8.8	9.5	9.9	10.2	11.2	18.6
NYCTA	14.0	11.7	13.8	15.0	16.4	17.5	18.6	24.0	59.3
MARC (Nominal)	18.1	15.1	16.7	17.7	26.8	30.7	35.2	38.0	41.1
MARC (Peak)	22.7	17.5	20.1	24.4	32.2	37.8	41.5	46.7	64.6

Table 2-5

Percentiles of Rail Transit Vertical Loads (kN)

Mode	Mean	10%	50%	75%	90%	95%	97.5%	99.5%	100%
MetroLink	36.1	30.1	36.2	39.3	42.2	43.9	45.6	49.8	82.6
NYCTA	62.3	51.9	61.3	66.6	72.9	77.8	82.8	106.6	263.9
MARC (Nominal)	80.7	67.1	74.2	78.7	119.1	136.6	156.5	168.9	182.9
MARC (Peak)	100.8	78.1	89.3	108.5	143.1	168.1	184.4	207.9	287.4

Table 2-6

Percentiles of Total Load Factors from Rail Transit Systems)

Mode	Mean	10%	50%	75%	90%	95%	97.5%	99.5%	100%
MetroLink	1.02	0.89	1.01	1.09	1.17	1.22	1.27	1.39	1.94
NYCTA	1.23	1.03	1.21	1.32	1.44	1.54	1.64	2.11	5.21
MARC	1.26	1.10	1.17	1.28	1.50	1.76	1.99	2.47	4.04

Although further study is warranted as to why the impacts are lower for MetroLink's LRVs, the authors of this report surmise that differences in the suspension system of the trucks, wheel health, resilient (i.e., sandwich composite) wheel construction, and track health and degradation rates play a role in reducing these impacts compared to the other two systems. These factors are also noted in many of the aforementioned dynamic load factor equations summarized by Doyle and Van Dyk [28].

Development of Improved Speed Factor

To determine the influence of speed on the vertical loads imparted into the track structure, an accurate measurement of speed was needed for each vertical load reading. Speed is provided as a direct output of WILD systems and speeds from trains passing instrumented locations were calculated using the time between measured loads and known axle spacing. Using the speed and wheel load data, loads were categorized into 5 mph (8 kph) speed bins for UIUC-installed instrumentation and 10 mph (16 kph) bins for the WILD data. Bins with more than 20,000 data points were subdivided until no bin contained more than 20,000 data points. Each speed bin was analyzed to find several relevant percentiles (e.g., 90th, 95th, 99th, and maximum) of wheel loads.

Wheel load data were next used to estimate the effect of speed using an approach similar to [29]. The Talbot equation slope [23, 25, 45] was modified to minimize the sum of percent exceeding and root mean square deviation for each rail transit dataset. The change in dynamic factor due to the aggregate factors experienced in the field on the three systems surveyed can be expressed in the three equations shown in Table 2-7.

Table 2-7

Summary of Impact Factor Equations for Prediction of Light, Heavy, and Commuter Rail Transit Wheel Loads as a Function of Speed and Wheel Diameter

Rail Transit Mode	Total Load Factor Equation	
	SI Units	US Customary Units
Light	$1+0.067\frac{Speed\ (kph)}{Wheel\ Diameter\ (cm)}$	$1+0.105\frac{Speed\ (mph)}{Wheel\ Diameter\ (inches)}$
Heavy	$1+0.323\frac{Speed\ (kph)}{Wheel\ Diameter\ (cm)}$	$1+0.510\frac{Speed\ (mph)}{Wheel\ Diameter\ (inches)}$
Commuter	$1+0.198\frac{Speed\ (kph)}{Wheel\ Diameter\ (cm)}$	$1+0.313\frac{Speed\ (mph)}{Wheel\ Diameter\ (inches)}$

Based on the slopes of these three lines, it is evident that the wheel health and track maintenance vary for each mode. The MetroLink data displayed the lowest slope (Figure 2-9)—thus, the least influence of speed on wheel-rail loads. This factor of 0.067, roughly 20% of the Talbot factor, may indicate that the dynamic factor for light rail can be considerably reduced from its current value of 0.33. The NYCTA data, on the other hand, tend to indicate that a higher dynamic factor is required to adequately account for increased loads that vary as a function of speed.

Figure 2-9

Raw data and predictive curves generated from field data from three rail transit modes

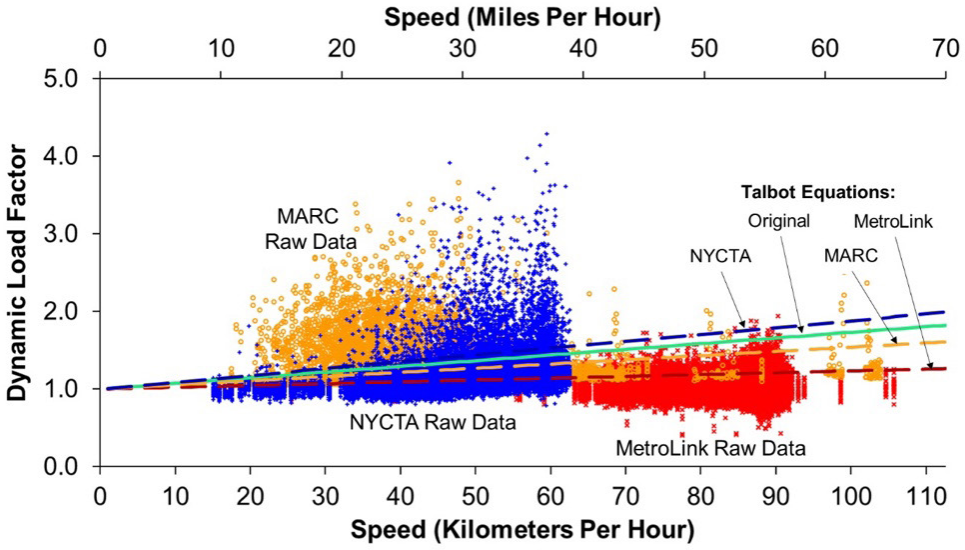

Conclusions

In this section, the aggregate effect of speed and other vehicle and track irregularities was quantified to generate accurate dynamic and impact load factors for rail transit systems. Specifically, the following conclusions were drawn:

- Total load factor distributions for the three rail transit systems significantly differed, demonstrating that unique, specific load factors are needed to adequately represent the existing wheel loads on rail transit infrastructure and improve design of the critical components that make up the track structure. All distributions indicate that the current AREMA impact factor of three should be reduced, possibly by as much as half.
- Existing dynamic load factors were analyzed, and the Talbot approach to estimating dynamic loading due to speed and wheel diameter was found to be quite conservative, with the light rail transit loading environment being over-estimated by a factor of three. Conversely, heavy rail transit factors were underestimated by approximately 50%. Finally, commuter rail transit factors matched the Talbot prediction quite well.
- For a given mode, in the absence of field data related to the track loading environment, the selection of an appropriate load factor should be based

- on knowledge of a particular rail transit system's track and rolling stock maintenance practices.
- Focused load-related field instrumentation can be deployed to answer system-specific loading questions within a given rail transit mode. The relatively modest effort required to install instrumentation and process data from such an installation could provide significant returns on investment with respect to mechanistically designing track components.

SECTION

3

Quantification of Rail Transit Concrete Crosstie Field Bending Moments

Background and Introduction

This section presents results from a field study quantifying flexural demands on concrete crossties on both light rail transit (LRT) and heavy rail transit (HRT) systems. The research uses the surface strain measurement methodology described by Edwards et al. [46] to obtain bending moments, developed, in part, through funding from this FTA cooperative agreement.

Prestressed concrete crossties are commonly used in rail transit applications due to their improved ability to maintain track gauge and higher reliability that reduces the time needed for track maintenance activities [28, 47, 48]. Although useful input data for the mechanistic design of concrete crossties in heavy axle load (HAL) freight systems were documented in earlier research efforts [49], additional effort is required to generate a robust dataset for rail transit loads, bending moments, and displacements.

The majority of North American design practices used for rail transit are borrowed from HAL freight railroad engineering; thus, the potential for incorrect and inefficient application of these standards exists. This potential inefficiency (over-design) was addressed by developing methods and practices for mechanistically designing track components based on actual field loading conditions.

Most of the overly-conservative rail transit crosstie designs have demonstrated reasonable service lives to date. However, challenges can emerge from concrete crossties that have been over-designed with unnecessarily high levels of prestress, contributing to brittle failures [50].

Additionally, striving for concrete with excessively high levels of compressive strength (in excess of 10,000 psi) could also contribute to premature failures of crossties [51] and necessitate the use of premium (and more costly) mixture designs. Finally, prestress forces have been known to generate bursting stresses around wires or strands that leads to cracking at the ends of crossties [52]. Reducing these stresses would prevent at least a portion of this type of failure.

Whereas the extent of these concerns remains to be quantified, there is an economic benefit to designing and manufacturing crossties that are optimally

sized in terms of the component itself and the equipment needed to install crossties.

Although the design of prestressed, precast monoblock crossties has many different facets (e.g., material selection, economic impact, overall performance criteria, etc.), the flexural design is considered to be the most critical design element given its linkage to the structural integrity of the crosstie. Beyond quantifying bending moment magnitude, which could be incorporated into future mechanistic designs [38], both researchers and practitioners are interested in understanding the variability in flexural demands among crossties to plan and prioritize tamping operations. Additionally, variability in temperature can affect bending moments [53].

Among other critical topics, this section documents the quantification of seasonal variation in bending on rail transit systems. Flexural reserve capacity (i.e., ratio between crosstie design capacity and moment observed) and seasonal variability of moments have the potential for being more pronounced in the rail transit loading environment due to the ratio between the average wheel loads and flexural resistance of crossties being lower than that seen in the HAL freight railroad operating environment. In other words, seasonal and other sources of variation that are independent of load may be more critical in rail transit applications than has been observed in HAL freight service [53, 54] due to the distinctly different loading magnitudes, yet relatively similar sectional properties of the crossties.

To address crosstie flexural reserve capacity quantification, crosstie-to-crosstie variability, and seasonal variation of moments, concrete surface strain gauge instrumentation was deployed in the field on both LRT and HRT systems. This method was previously developed, deployed, and validated by Edwards et al. [46] and has proven useful in answering similar questions for HAL freight applications [46].

Instrumentation Technology

Previous research has used either embedded or surface strain gauges to quantify field bending moments of concrete crossties [49, 52, 55–57]. These projects focused almost exclusively on the freight and intercity passenger rail domain, with little mention of rail transit applications.

A minimum sampling rate for rail transit data collection was determined based on the maximum authorized train speed at each field location and the desired data sampling resolution, where the sampling resolution is the distance the train travels between collection of consecutive samples. The sampling resolution desired for the application discussed in this section was 0.5 in. (12.7 mm). Based on these requirements, prior experience, and expert recommendation a sampling rate of 2,000 H was used.

Field Deployment

Example Field Instrumentation Deployment

The specific field tests discussed were conducted at ballasted track field sites on two rail transit systems, MetroLink and NYCTA. Because of the variability in support conditions observed in past field experimentation [46, 54, 58], instrumentation was placed on five consecutive crossties at each field test location (Figure 3-1).

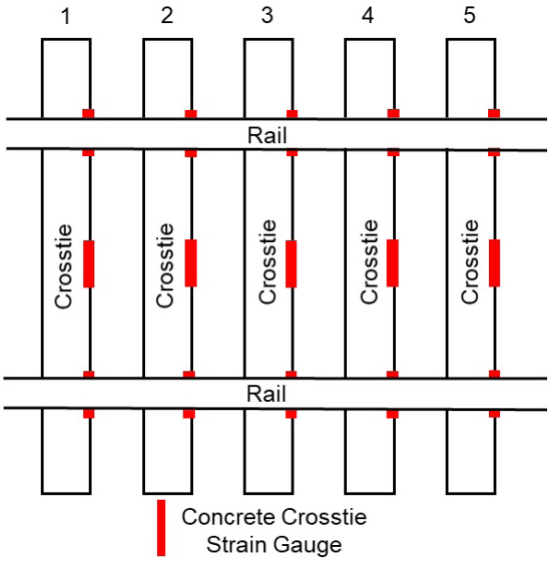

Figure 3-1

Typical field experimentation site layout with five crossties showing locations of concrete surface strain gauges

Instrumentation Deployment on Crosstie

Bending strains at critical locations along the length of the crosstie were measured to quantify the flexural behavior of the crosstie under revenue service train loading. Three strain gauges (labeled A, C, and E) were used on each crosstie, with one applied at each of the two rail seats and one at the center (Figure 3-2). Additional relevant dimensions and properties for the two types of rail transit crossties investigated are shown in Table 3-1, which includes a typical crosstie used in HAL freight service for comparison. All three types of crossties in Table 3-1 use a prestressing tendon that is 0.209 in. (5.32 mm) in diameter and similar concrete mixture designs. Specification design capacities in Table 3-1 refer to the transit agency value that must be met or exceeded for flexural strength. Design values are the capacities associated with the unique crosstie designs produced by the manufacturers.

Figure 3-2

Profile view of instrumented crosstie showing locations of strain gauges and image showing example of rail seat with gauge A installed

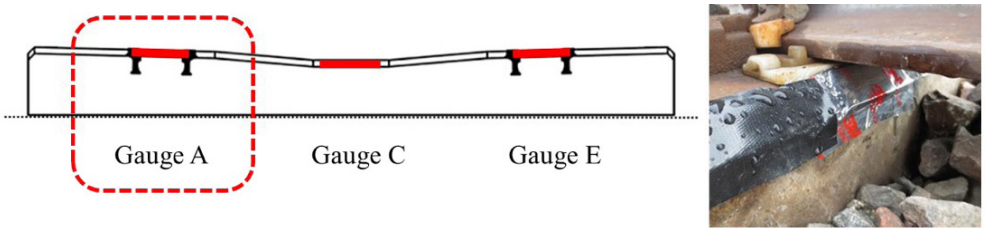

Table 3-1

Characteristics of Rail Transit Crossties and Comparison to Typical HAL Freight Concrete Crosstie

Crosstie / System Characteristic			Light Rail (MetroLink)		Heavy Rail (NYCTA)		HAL Freight	
			SI	Imperial	SI	Imperial	SI	Imperial
Static Wheel Loads*	Maximum (AW3)		41.8 to 55.6 kN	9.4 to 12.5 kips	62.9 kN	14.1 kips	35.8 kips	159 kN
	Minimum (AW0)		28.9 to 42.7 kN	6.5 to 9.6 kips	50.6 kN	11.4 kips	Varies	Varies
Crosstie Geometry Crosstie	Length		2.51 m	8' 3"	2.59 m	8' 6"	2.59 m	8' 6"
	Tie Spacing		0.76 m	30"	0.61 m	24"	0.61 m	24"
Crosstie Prestressing	Number of Wires		12		18		20	
	Jacking Force		31.1 kN	7 kips	31.1 kN	7 kips	31.1 kN	7 kips
	Precompression (Crosstie Center)		10,204 kN/m^2	1.48 ksi	13,858 kN/m^2	2.01 ksi	15,444 kN/m^2	2.24 ksi
Crosstie Design Capacity	Center Negative	Specification	16.3 kN-m	144 kip-in	19.0 kN-m	168 kip-in	26.0kN-m	230 kip-in
		Design	16.6 kN-m	147 kip-in	21.9 kN-m	194 kip-in	26.0 kN-m	230 kip-in
	Center Positive	Specification	10.5 kN-m	93 kip-in	13.3 kN-m	118 kip-in		
		Design	16.3 kN-m	105 kip-in	14.9 kN-m	132 kip-in	21.0 kN-m	186 kip-in
	Rail Seat Positive	Specification	20.2 kN-m	179 kip-in	28.3 kN-m	250 kip-in	33.9 kN-m	300 kip-in
		Design	25.0 kN-m	221 kip-in	32.0 kN-m	283 kip-in	43.1 kN-m	381 kip-in
	Rail Seat Negative	Specification	12.0 kN-m	106 kip-in	15.6 kN-m	138 kip-in		
		Design	15.4 kN-m	136 kip-in	20.1 kN-m	178 kip-in	24.7 kN-m	219 kip-in

*AW0 loads are as-delivered, ready-to-operate static loads; AW3 loads (crush load) represent AW0 load plus weight of seated passengers and additional "live load" of 6 standing passengers/square meter, a common load used for passenger vehicle design

The process of instrumenting crossties in the field, including the protection of strain gauges, is shown in Figure 4-3. To relate the field-measured strains to a bending moment, calibration factors were generated using laboratory tests conducted at UIUC's Research and Innovation Laboratory (RAIL) using the processes described by Edwards et al. [46].

Figure 3-3

Crossties instrumented with concrete surface strain gauges and completed St. Louis MetroLink light rail field experimentation location

Data Analysis

To quantify the bending moments concrete crossties experience in revenue service, peaks in the strain gauge signal caused by crosstie bending due to a wheel or axle load must be extracted from the data stream collected at 2,000 H. This was accomplished using a modified version of the "findpeaks" function in MATLAB (2012) that is detailed in Edwards et al. [46]. To improve the performance of this function for this application, several built-in options were used, and additional modifications were made to the code originally developed by Wolf [54].

Before the peaks were obtained, the strain signal was zeroed using data captured before the arrival of the first axle, and a linear baseline correction was applied to adjust for any signal drift over the course of a single train pass. As such, data collection was initiated several seconds prior to the arrival of the leading axle to provide a stable zero point for the crosstie under no applied load. Additionally, the data collection was ended several seconds after the final train axle passed to serve as an end point for the baseline correction. To ensure that the true peaks were being captured by the program, as opposed to false peaks that did not represent the extreme strain reading for a given axle pass, a minimum spacing between the peaks was specified and a minimum value for all peaks was set. Additional detail on filtering and processing of data was previously documented by Edwards et al. [46].

Figure 3-4 (left y-axis) shows an example of a typical strain gauge signal for a center gauge for a single MetroLink train pass made up of two, six-axle LRVs. The signal was zeroed out and the peaks were numbered in sequence, which were then converted into bending moments using the laboratory moment calibration factors described previously (Figure 3-4, right y-axis).

Figure 3-4

Typical crosstie center strain signal and resulting center bending moment captured under passage of 12-axle St. Louis MetroLink light rail trainset

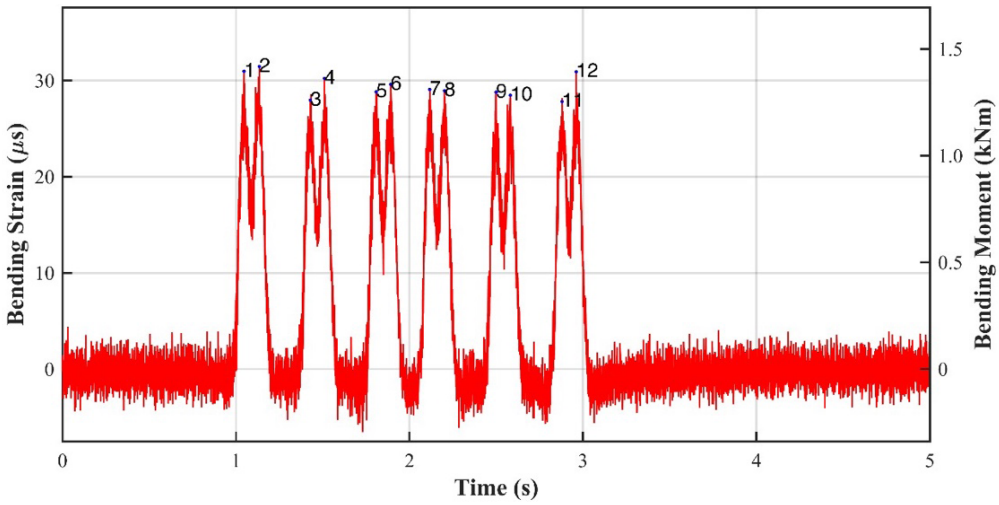

Results

The instrumentation plan described in this section was deployed for approximately one year on each of the two rail transit properties. In total, 27,092 light rail train passes were recorded at the MetroLink site from March 18, 2016, to May 19, 2017, and 11,597 heavy rail train passes were recorded at the NYCTA site between April 26, 2016, and February 27, 2017. For the duration of these deployments, the instrumentation described in this section functioned properly. Other field sites have experienced similar successes [49]. Using these data from MetroLink and NYCTA, bending moments induced by loaded axles from the signals of the center and rail seat strain gauges were analyzed.

Magnitude of Bending Moments and Comparison to Design Standards Capacities

The concrete crosstie center negative (C-) bending moment distributions for the trains show both the overall magnitude and variability of moments (Figure 3-5). It is evident that the variability and range associated with NYCTA moments exceeds that of MetroLink, as evidenced by the shallower slope of the NYCTA data. Additionally, similar plots are shown for the rail seat positive bending moments in Figure 3-6, with greater variability and range seen in the NYCTA data. These distributions are also shown in comparison to the specifications and design capacities for both rail seat positive and center negative cracking, which are most commonly based on limits generated using AREMA-recommended design practices [24]. These values, as generated using the AREMA method [24], define a threshold that a bending moment would need to exceed before a crack propagates to the first level of prestress.

Figure 3-5

Distribution of MetroLink and NYCTA center negative (C-) bending moments for each axle and comparison with design capacity and transit specifications

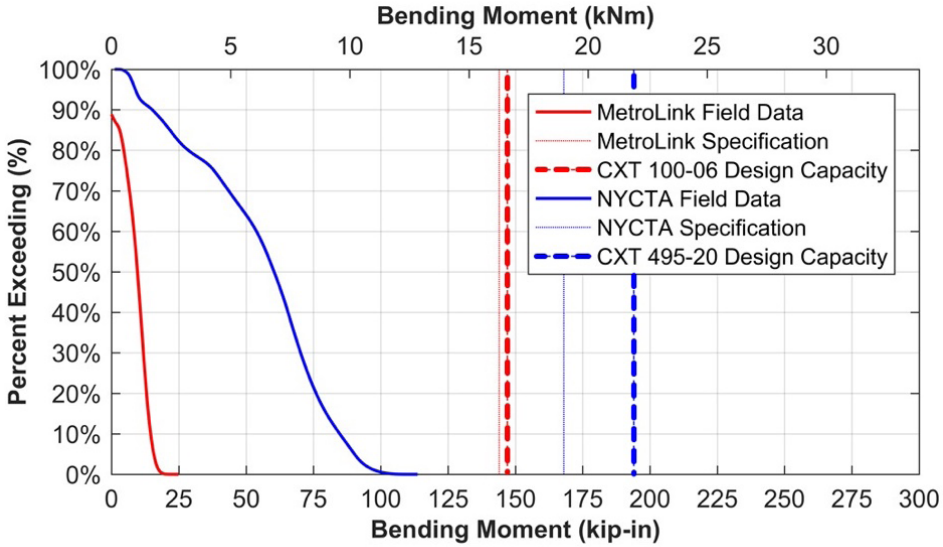

Figure 3-6

Distribution of MetroLink and NYCTA rail seat positive (RS+) bending moments for each axle and comparison with design capacity and transit specifications

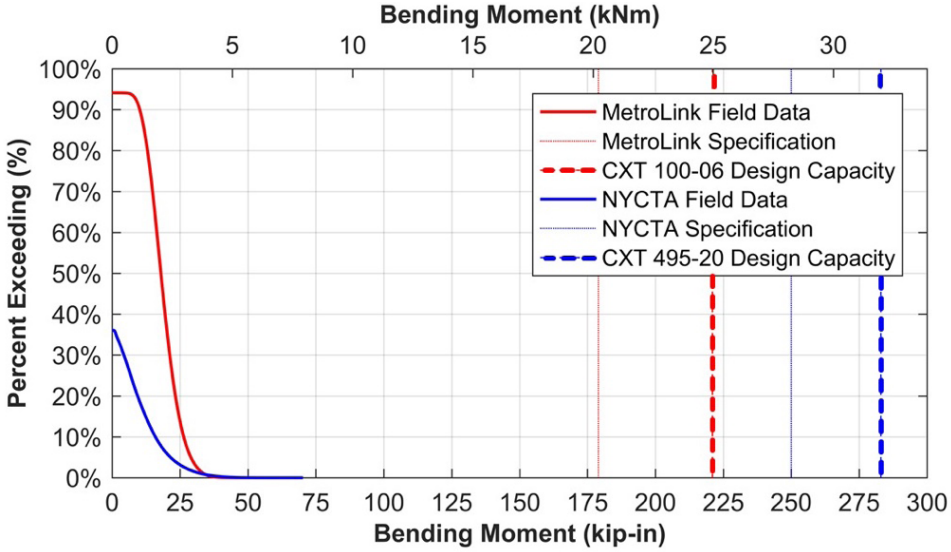

None of the crosstie bending moments recorded reached the specification or design limit (shown by the vertical lines in Figures 3-5 and 3-6). This is especially evident at the rail seats, as the 95th percentile rail seat positive (RS+) moment values were less than 10% of the 179 kip- in. (20.2 kNm) and 250 kip-in. (28.2 kNm) specification limits for crosstie flexural design for MetroLink and NYCTA, respectively. When combined with high estimates for input wheel loads in design specifications, AREMA [24] recommendations can overestimate the flexural demand at the crosstie rail seat (Figure 3-6). Compared to rail seat positive (RS+) moments, 95th percentile center negative (C-) bending moments were closer to the specification values, reaching as much as 50% of the 144 kip-in. (16.3 kNm) and 168 kip-in. (19.0 kNm) values for MetroLink and NYCTA, respectively.

This indicates that center bending conditions may govern the design in terms of factors of safety (Figure 3-5). This finding is also in agreement with a previous survey of industry experts that suggested that center cracking of concrete crossties was more commonly seen in the field, albeit in HAL freight railroad applications [28]. This type of failure may be preferable to infrastructure owners given they are more easily detected through visual inspection.

A measure of reserve capacity was generated by dividing the design capacity of the crosstie at the center or rail seat by the observed field moments at varying percentiles (Table 3-2). Current crosstie designs, even when compared with the maximum bending moments experienced in the field, have a reserve capacity exceeding 3.2 in. rail seat positive bending (RS+) for MetroLink and 1.7 in. center negative (C-) bending for NYCTA. These respective reserve capacity factors further increase to 7.6 and 2.2 when considering 95th percentile bending moments.

Table 3-2

Reserve Capacity for Light Rail (MetroLink) and Heavy Rail (NYCTA) Crossties

Bending Moment Percentile	Light Rail		Heavy Rail	
	Center	Rail Seat	Center	Rail Seat
Minimum	-4.9	-3.4	168.5	-2.7
0.10%	-7.9	-5.9	49.4	-4.9
1%	-9.9	-8.1	32.2	-6.1
5%	-18.3	-14.7	21.9	-7.6
10%	-95.9	21.7	12.8	-8.8
90%	10.1	8.4	2.3	17.8
95%	9.4	7.6	2.2	13.2
99%	8.4	6.5	2.0	8.6
99.90%	7.5	5.7	1.9	6.3
Maximum	5.9	3.2	1.7	4.0

Reserve design capacities are consistently higher for MetroLink than NYCTA. There are a variety of factors that likely influence this, including crosstie design and its related assumptions, input rail seat loads (primarily a function of wheel tread condition and maintenance), and crosstie support conditions (primarily a function of track quality).

Of additional interest is that positive center moments were recorded on MetroLink and negative rail seat moments were recorded on NYCTA. Negative values of reserve design capacity in Table 3 2 indicate that the "opposite" moment was recorded (e.g., rail seat negative and center positive). Whereas these values are expected to occur infrequently, they do occur, and these data provide insight regarding their occurrence. It is interesting to note that the lowest reserve capacity ratios are found for rail seat negative (RS-) as opposed to rail seat positive (RS+) for NYCTA and for center positive (C+) as

opposed to center negative (C-) for MetroLink. These apparent contradictions of conventional thinking are due to the specific support conditions that were present where the instrumentation was deployed, with the MetroLink crossties being well-supported at the rail seat and NYCTA crossties having more support at the center, as evidenced by the high center negative (C-) bending moments. Furthermore, this finding can provide a method for future estimation of support conditions and a process to infer whether center binding is present.

Crosstie-to-Crosstie Moment Variability

A critical question is the extent of variability in bending moments for consecutive crossties. This question was addressed in earlier work aimed primarily at the HAL freight environment [46], but no previous research has focused on concrete crossties used in rail transit systems.

Figure 3-7 and Figure 3-8 show the distribution of center negative (C-) and rail seat positive (RS+) bending moments, respectively, under MetroLink light rail transit loading for 5 crossties and 10 rail seats. Figure 3-9 and Figure 3-10 show the same distributions under heavy rail traffic on NYCTA.

Figure 3-7

Distributions showing crosstie-to-crosstie variability of center negative (C-) bending moments for light rail transit loading on St. Louis MetroLink

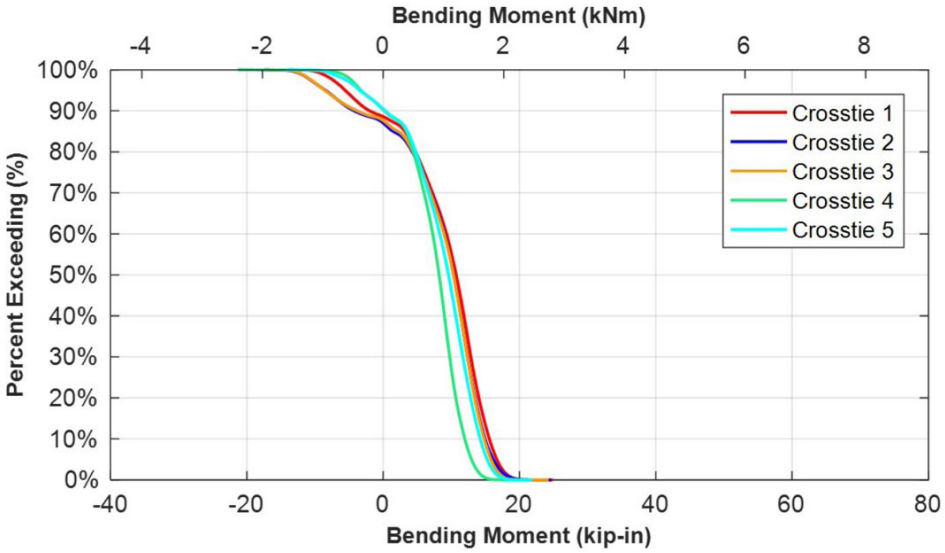

Figure 3-8

Distributions showing crosstie-to-crosstie variability of rail seat positive (RS+) bending moments for light rail transit loading on St. Louis MetroLink

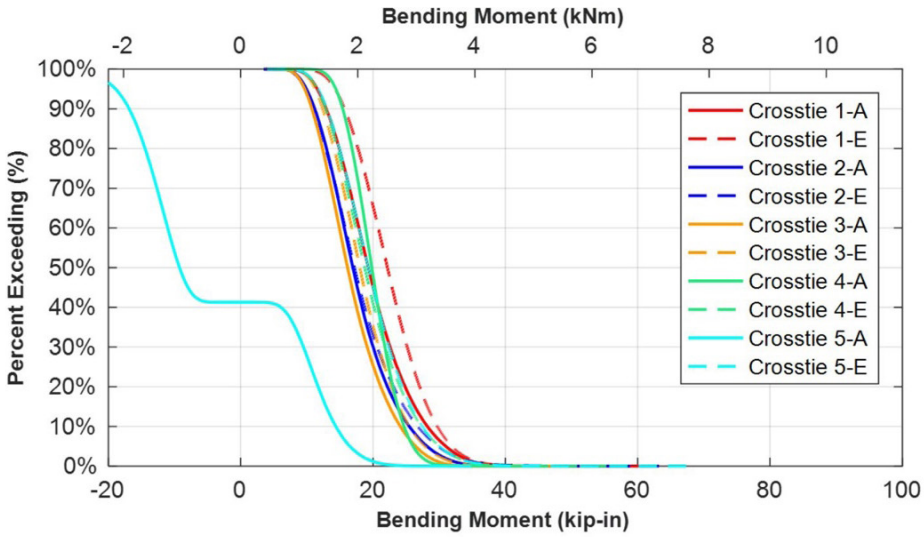

Figure 3-9

Distributions showing crosstie-to-crosstie variability of center negative (C-) bending moments for heavy rail transit loading on NYCTA

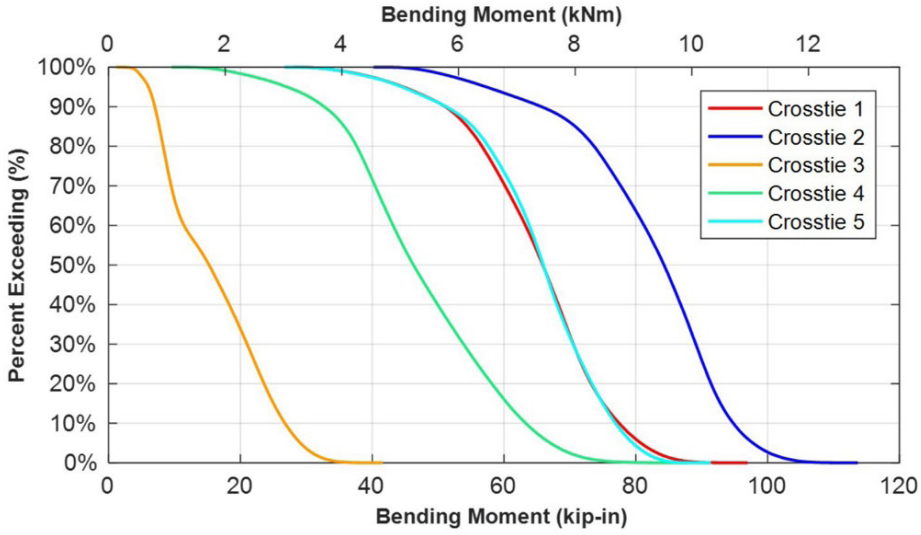

Figure 3-10

Distributions showing crosstie-to-crosstie variability of rail seat positive (RS+) bending moments for heavy rail transit loading on NYCTA

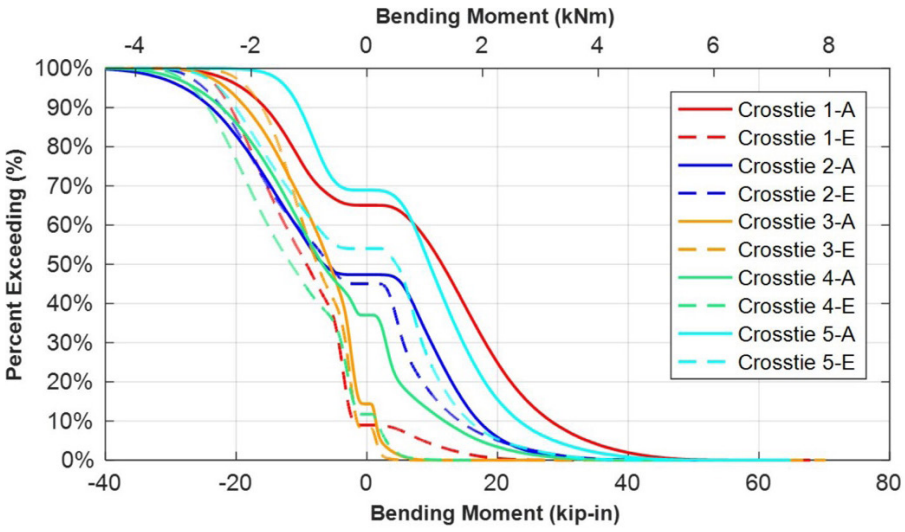

With the exception of Crosstie 5-A, the crosstie-to-crosstie variability of the bending moments experienced on MetroLink were as low as 10%. The variability of the bending moments at both the rail seat (RS+) and crosstie center (C-) were considerably higher at NYCTA, reaching as high as 100% (factor of 2). This range in variabilities is likely due to different support conditions generated by higher unique track deterioration rates due to the much heavier static railcar axle loads on NYCTA (approximately twice the magnitude of MetroLink). Additionally, the MetroLink track is newer; it was constructed in 2003 and has required little (if any) tamping since construction. Similar variability has been noted around other areas of special trackwork or track transition zones due to the higher loads and corresponding dynamic response of the track structure to these loads [59, 60].

Seasonal Effect on Bending Moments

Temperature-induced curl of the crosstie due to different temperatures on the top and bottom (i.e., temperature gradient) has been shown to influence the flexural demand placed on the crosstie [53]. Initially, curl was found to change over the course of the day as the temperature gradient changed, which was noted in both laboratory and field settings [54]. Temperature gradients also were found to vary over the course of the year under HAL freight operations. These changes affected the bending moments induced in the concrete crossties [53, 54], a behavior similar to that noted in rigid pavement applications [61].

Figure 3-11 shows the seasonal variation of bending moments throughout a year of data collection at MetroLink with single data points representing the average of a train pass over the site; Figure 3-12 shows similar data for NYCTA. For graphical clarity, these data represent only one crosstie at each field-testing location, but the crosstie selected was indicative of the overall behavior noted at each site.

Figure 3-11

Distributions showing seasonal variation of center negative (C-) bending moments for light rail transit loading on St. Louis MetroLink

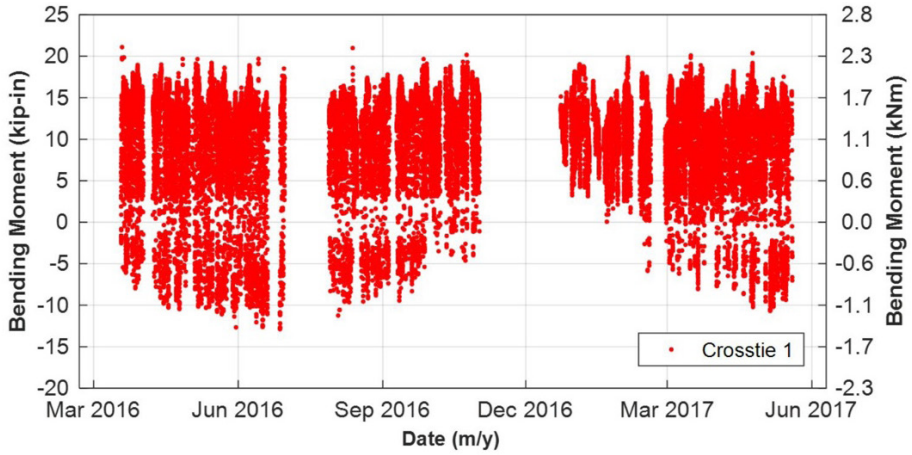

Figure 3-12

Distributions showing seasonal variation of center negative (C-) bending moments for heavy rail transit loading on NYCTA

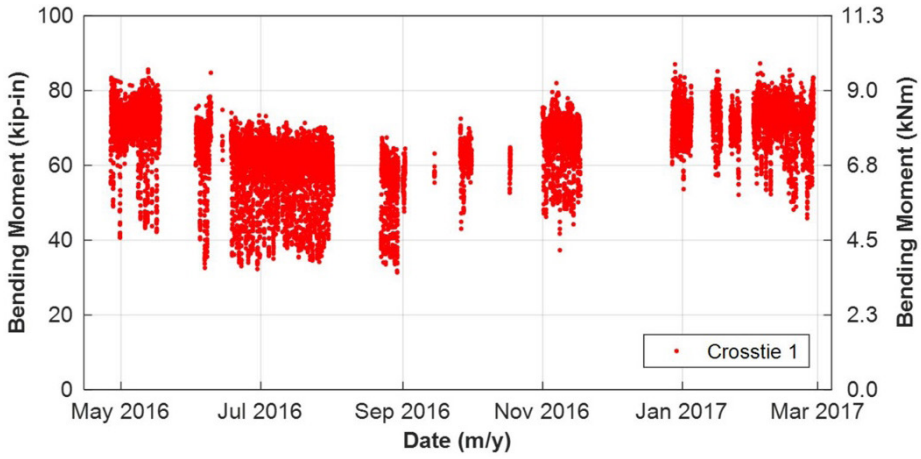

Seasonal variation is further demonstrated by extracting the daily average for each of the center gauges on the two rail transit systems, shown in Figure 4-13 for MetroLink and Figure 4-14 for NYCTA. The variation in absolute bending moment values seen in Figure 4-14 maps to the variability that was seen at the NYCTA field site as discussed above.

Figure 3-13

Distributions showing crosstie-to-crosstie variability of average train pass center negative (C-) bending moments for light rail transit loading on MetroLink

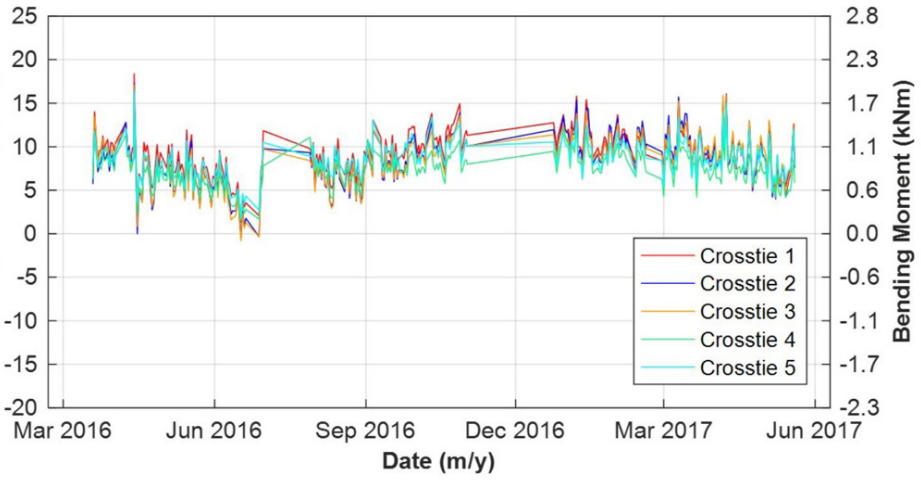

Figure 3-14

. Distributions showing seasonal variation of average train pass center negative (C-) bending moments for heavy rail transit loading on NYCTA

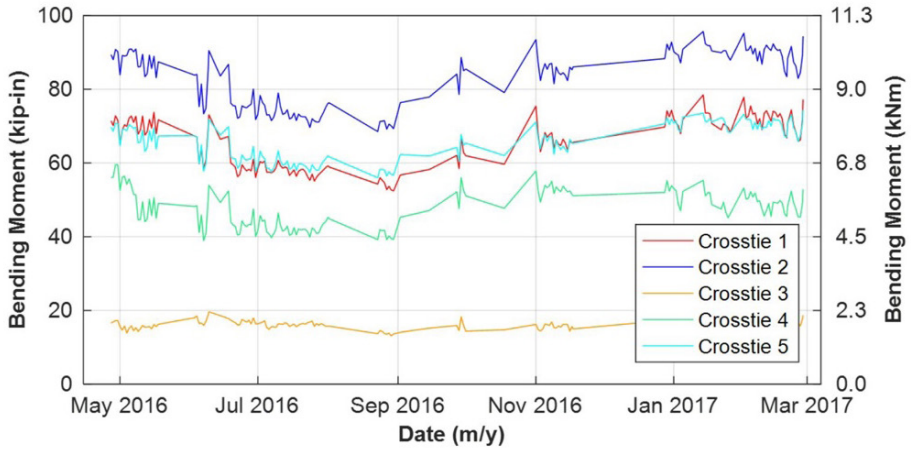

The daily average train pass fluctuations in bending moments ranged by as much as 30 kip-in. (3.3 kNm) and 40 kip-in. (4.5 kNm) for MetroLink and NYCTA, respectively. Despite these seasonal effects, the fluctuations in center negative (C-) bending moments due to daily temperature fluctuations exceeded seasonal variability by a factor of approximately 2.

The data show a modest seasonal trend (Figures 3-13 and 3-14) with higher absolute center negative bending moments occurring during the winter months consistent with the idea that track support is stiffer during cold weather [21, 62]. Additionally, although not investigated in this phase of the research, the physical deterioration of the crosstie is another factor that could affect the long-term flexural behavior of crossties. Temperature-induced curl and bending moment relationships were also documented by Canga Ruiz [63], albeit over shorter time durations, who observed a change in bending moments of up to 30 kip-in. (3.3 kNm) for MetroLink and 40 kip-in. (4.5 kNm) for NYCTA (Figure 3-15).

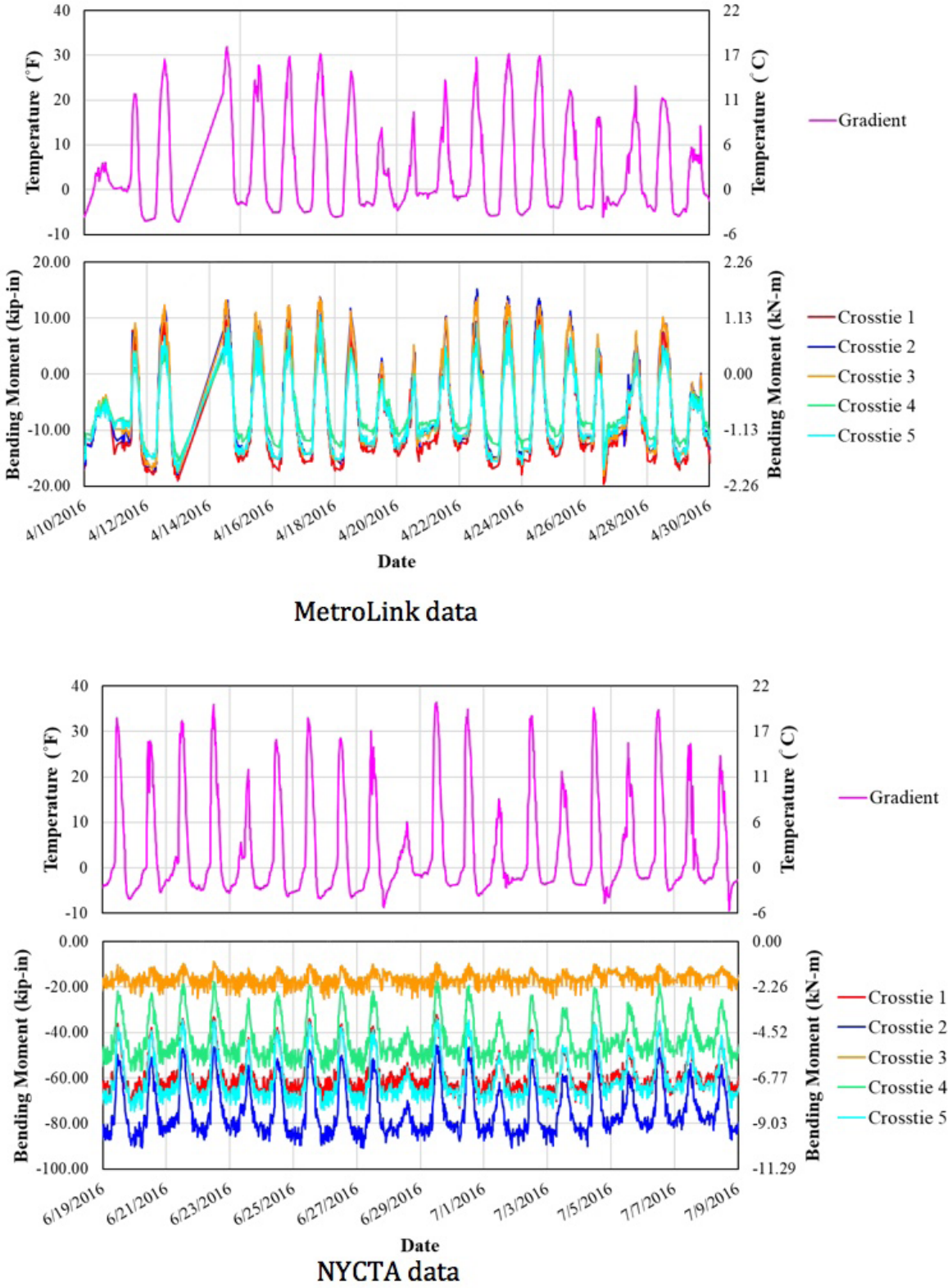

Figure 3-15

Comparison of temperature gradient and center bending moment variation as function of time [63]

Conclusions

Concrete surface strain gauge instrumentation methodology and deployment successfully measured concrete crosstie bending strains and the resulting moments experienced by two rail transit modes in the US. Field deployments at MetroLink and NYCTA were used to answer questions related to crosstie-to-crosstie variability and the occurrence and magnitude of temperature-induced curl. The following conclusions can be drawn from this research:

- The magnitude of maximum center negative bending moments ranged from 25 kip-in. (2.8 kNm) on MetroLink to 120 kip-in. (13.5 kNm) on NYCTA. Significant residual capacity was found in both systems. Considering the 99th percentile center negative (C-) bending moments, residual load capacities of approximately 6 and 2 were found for light and heavy rail transit systems, respectively.
- Bending moments vary widely from crosstie-to-crosstie. This was demonstrated on a HAL freight railroad, showing bending moments at the crosstie center that ranged from 0 kNm (0 kip-in.) to 22.8 kNm (202 kip-in.). This is consistent with prior research [54, 64, 58].
- Temperature-induced curl (e.g., warping of the crosstie due to different temperatures on the top and bottom) has a quantifiable impact on concrete crosstie flexural demand. Curl in concrete crossties was found to change over the course of the day as the temperature gradient changed. These changes affected the bending moments induced in the concrete crossties [53, 64], a behavior similar to that which has been noted in rigid pavement applications [61].

SECTION

4

Rail Transit Concrete Crosstie Design Considerations and Analysis

Introduction

Existing concrete crossties designs used by rail transit operators are based largely on empirical design practices that have resulted in significantly overdesigned crossties. Research conducted at UIUC has shown that the ultimate capacity of concrete crossties is more than double the demand imposed by even the heaviest rail traffic [65]. This study aimed to mechanistically optimize the design of concrete crossties to not only address the serviceability and ultimate limit state concerns but also to achieve more cost-effective designs. The results reported represent an initial step toward this goal and should be interpreted with the understanding that further options and parametric studies should be executed to generate an optimal design solution.

The specific focus of this section and the prototypes that are being developed in this research are concrete crossties for light rail transit applications. The flexural capacity of crossties is widely considered to be the most important characteristic. As a result, typical rail transit crossties tend to be excessively overdesigned for flexure. However, this forces the predominant failure mode to be in shear both at the rail seat and at the crosstie center. Shear failure is not often considered desirable because of its sudden and brittle nature. The current CXT-100 design that is the initial focus of this project's investigation lacks provisions to develop any residual capacity after failure. It is not unlike any other rail transit concrete crossties. Given that failure could bring catastrophic consequences in terms of sudden and brittle failure, the main goal of the design optimization is to safely reduce the ultimate flexural capacity of current CXT-100 crosstie designs to levels more representative of actual field conditions and to enforce more ductile modes of failure. Many interacting elements must be considered in the design of a concrete crosstie. In the initial stages of this project, researchers attempted to identify the most critical facets of the design that should be addressed. At a high level, these include the crosstie's geometry, nature of prestressing, and concrete materials selection.

As a part of this portion of the project, extensive finite element analysis (FEA) was conducted to incrementally alter the existing CXT 100 design and numerically assess the effectiveness of three different approaches: 1) reducing the prestressing level, 2) introducing flexural reinforcement, and 3) introducing shear reinforcement. The three options were systematically evaluated to develop prototypes that were produced and experimentally tested to validate the results. Center negative and rail seat positive testing, both widely accepted measures of crosstie performance, were used to develop the prototypes.

Optimization of concrete crosstie flexural design requires knowledge of the following items:

- Input loading conditions that characterize the loading conditions at the wheel rail interface, which are subsequently passed to the rail seat
- Support conditions beneath the crosstie, predicted support conditions in the future, and the resulting reactions stemming from these support conditions
- Preferred failure modes at critical regions of the crosstie (center and rail seats)
- Method of stressing, and magnitude as well as positioning of tendons

Design Optimization using FE Methods

FE Model

The first part of the design optimization process was developing an FE model (FEM) of the CXT 100 crosstie to predict its baseline behavior and evaluate various design modifications. The commercial FE analysis software ABAQUS was used for the numerical modeling. Figure 4-1 shows the CXT-100 crosstie model developed in ABAQUS.

Figure 4-1
CXT-100 crosstie model in ABAQUS

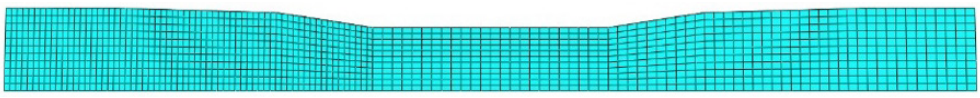

The accuracy of the FEM was first verified by comparing the behavior of the conventional, unaltered crosstie under center negative and rail seat positive bending to experimental test results. As shown in Figure 4-2, results from the FEM were in good agreement with the test results.

Figure 4-2

Comparison between experimental and FEM results: center negative load-displacement curve of baseline (specimen 3-A) and center negative load-displacement curve of stirrup reinforced tie (specimen 3-C)

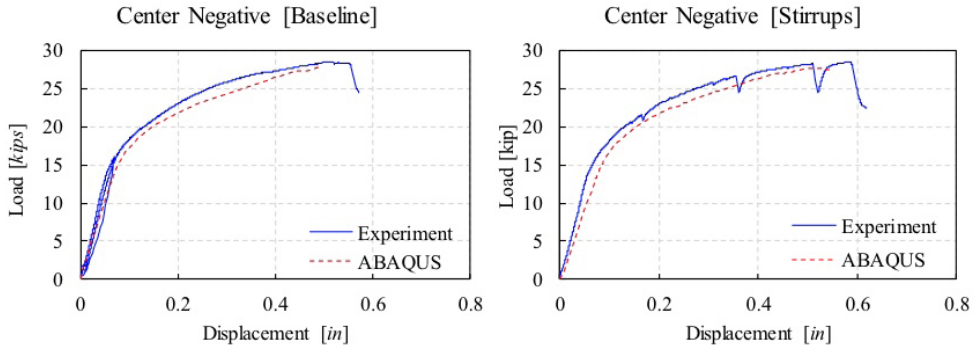

Proposed Changes to Existing Design

As noted, three categories of design alternatives were considered for effectively reducing the ultimate flexural capacity of the existing CXT-100 design and promoting more ductile failures modes. These alternatives were 1) reducing total prestressing levels (magnitude and number of wires), 2) introducing conventional flexural reinforcement (Figure 4-3), and 3) introducing shear reinforcement (Figure 4-3).

Figure 4-3

Conventional flexural reinforcement, shear reinforcement

The rationale behind reducing prestressing levels was to reduce the ultimate capacity of the crosstie and the introduction of flexural and shear reinforcement was to avoid a brittle failure mechanism. The ultimate capacity of the crosstie can be reduced by either reducing the cross- sectional area of the crosstie, using concrete with lower compressive strength (ff_{cc}'), or reducing the prestressing levels. Reducing prestressing levels was the only option considered in the first phase of this study. Two methods of reducing the prestressing levels are studied in an FEM parametric study: 1) reduction in the number of wires in the section and 2) reduction of the prestressing force applied to the strands. Based on the results of this parametric study, prestressing levels were varied throughout the test specimens, as shown in Table 4-1.

Table 4-1

Design Specimens and Design Variables reinforced tie (specimen 3-C)

Specimen	Prestressing (# of Wires / Jacking Force)	Concrete Material	Shear Reinforcement (Stirrups)	Flexural Reinforcement (Rebars)	Confinement (Stirrups)	Test
3-A (baseline)	12 wires/100%	Normal Concrete	–	–	–	C-, RS+
3-B (fiber)	12 wires/100%	FRC	–	–	–	C-, RS+
3-C (Stirrup)	12 wires/100%	Normal Concrete	4 x #3	–	–	C-
4-A-R	8 wires/100%	Normal Concrete	–	–	–	RS+
4-A-L	8 wires/100%	Normal Concrete	–	2 x #3	–	RS+
4-B-R	8 wires/70%	Normal Concrete	–	–	–	RS+
4-B-L	8 wires/70%	Normal Concrete	6 x #3	–	–	RS+
4-C-R	8 wires/60%	Normal Concrete	6 x #3	–	–	RS+
4-C-L	8 wires/60%	Normal Concrete	6 x #3	–	2 x #3	RS+
4-D-R	6 wires/80%	Concrete	–	–	–	RS+
4-D-L	6 wires/80%	Concrete	–	2 x #3	–	RS+

The flexural reinforcement was introduced to avoid brittle failure and to improve the flexural performance under service and ultimate loads. The flexural performance of the crosstie can be improved either strengthening regions where the tensile stress and high compressive stress are distributed under load condition of interest. Along these lines, the conventional flexural reinforcements were introduced to carry tensile stresses at the bottom of the crosstie where the tensile stresses are concentrated. In addition, stirrups for confinement were placed below the rail seat region where the high compressive stresses are located. The rail seat region is vulnerable to the crushing of the concrete in the ultimate load levels which was shown in the experiment (Figure 4-8c).

Shear reinforcement was introduced to prevent shear failure. By increasing the ultimate shear capacity of the section, the mode of failure may be altered from shear to flexure when the shear capacity surpassed the flexural capacity. The failure mechanism is dictated by the minimum capacity. The three alternatives were evaluated in a parametric study. Table 4-1 shows the design variables considered in the study, and the output characteristics considered for each design iteration. The iterative modeling process will be explained in detail in the following section.

Design Iterations using FEM

Optimizing the prototype design was an iterative process that was based on the use of FEM. Using the CXT 100 prototype design manufactured in the Newmark Civil Engineering Laboratory (NCEL) at UIUC as the baseline (specimen 3-A in Table 4-1), three design elements (reducing prestressing level, introducing flexural reinforcement, introducing shear reinforcement) were varied. The baseline design is comprised of 12 prestressing wires where jacking force was 6.5 kip/wire. The performance of the tie was evaluated by the tests specified in the AREMA manual (Chapter 30, center negative test and rail seat positive test [24]). The FEM was validated in the center negative test, where the analysis results showed good agreement with the test results (Figure 4-2).

Center Negative Test

The dominant failure mode of the baseline design under the center negative test was shear. Shear failure is not a desirable mode, because it occurs suddenly and, after the shear crack propagated, there is no residual strength. However, flexural failure is a desirable mode because it occurs more gradually with multiple cracks as an alarm that the failure is near which enables the replacement of the damaged crosstie. To enhance the crosstie's shear performance, two options were considered—introducing fiber reinforced concrete (FRC) and including shear reinforcement.

Shear reinforcement was designed based on the experimental result of baseline design (Figure 4-9). The ultimate shear capacity of the center section was 27 kips, and UIUC's baseline design failed in pure shear. The shear reinforcement was designed based on the shear capacity following ACI [66]. Two #3 rebars were selected to carry 27 kips of shear forces along the section. Thus, four #3 rebars are placed throughout the crosstie, and the geometry of the stirrups are designed to have ¾-in. covers. Depending on the location of the stirrup, different crack patterns are predicted and determine the optimum location is determined. A parametric study on the location of shear stirrups was conducted (Figure 4-4), which indicated that the ultimate strength and ductility of the crosstie were similar regardless of the location and the number of stirrups. FRC is known to mitigate crack propagation, and the volumetric reinforcement ratio of the fiber was selected as 8 lb/yd^3 based on previous small-scale experimentation at UIUC.

Figure 4-4

Parametric study for determining location of stirrups: center negative load-displacement curve with stirrups at different locations and ultimate strengths and displacements of different stirrup locations

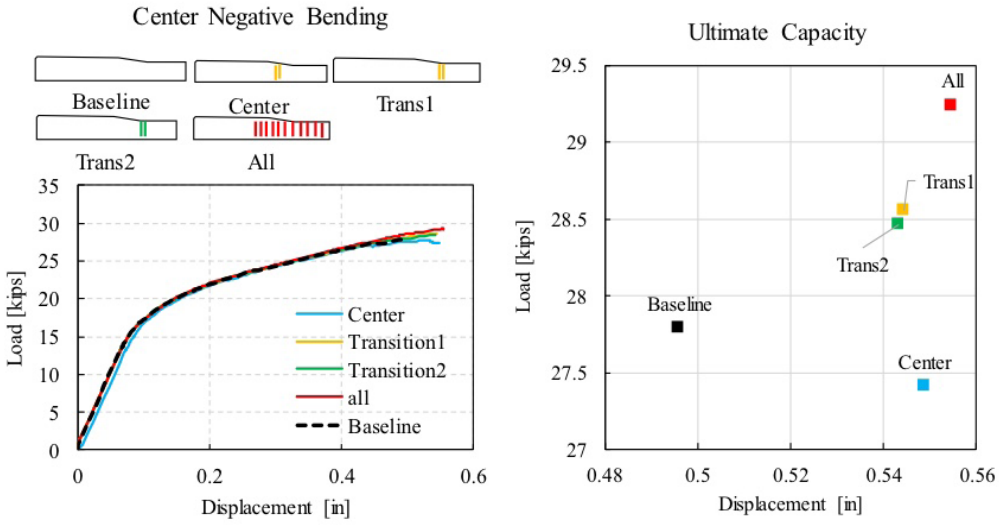

Figure 4-5

Schematic representation of test specimens for center negative test

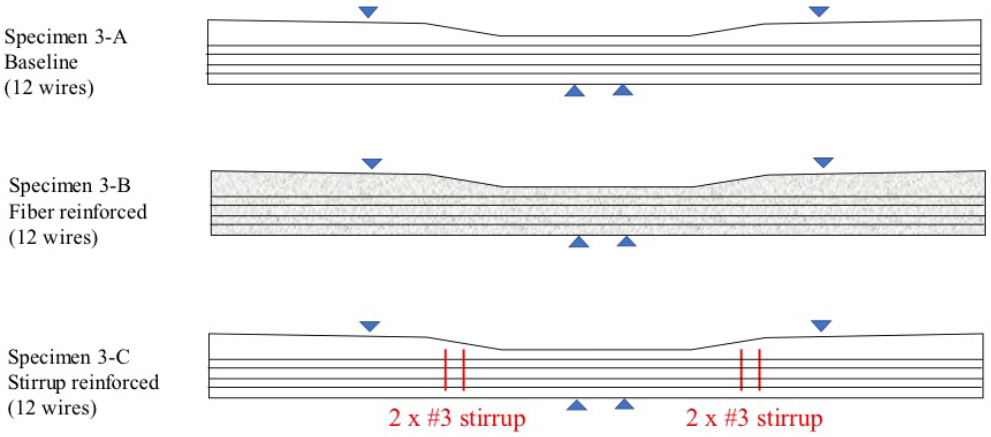

Rail Seat Positive Test

Combinations of the three design elements shown previously were evaluated by FEM to develop specific designs for all types of test specimens listed in Table 4-1. Each combination was evaluated in terms of failure modes and the reduction in service and ultimate strength. The target flexural capacity was set based on the maximum bending moment recorded in the field. The field maximum bending moments were 25 kip-in. for center negative and 62 kip-in. for rail seat positive.

First, reducing prestressing levels was studied by eliminating the number of wires used. The preliminary FE analysis showed that eliminating 6 wires would reduce the ultimate capacity to 60% of the baseline. However, the analysis predicted that eliminating strands without any reinforcement would fail due to the rupture of the strands. The rupture of the strands is a brittle type of failure mode and leads to disastrous drop in strengths. Since the crossties with 6 wires were predicted inadequate, the crossties with 8 wires were studied further by varying other variables. Three specimens (4-A, 4-B, and 4-C) eliminated 4 out of 12 wires,

and specimen 4 D eliminated 6 out of 12 wires. Specimens 4-A-R and 4-D-R (Table 4-1) were designed to test the effect of eliminating wires without any reinforcement.

Second, reducing the jacking force was studied. The jacking force was varied to 70% and 60% of the baseline for the crossties with 8 prestressing wires—specimens 4-B-R, and 4-C-R, respectively. For the crossties with 6 wires, the jacking force was 80% of the baseline.

Reduced jacking force would not only decrease the ultimate and service flexural capacity of the crosstie, but also delay the prestressing strand rupture. Once jacking force is reduced, strands have more room to be stretched when they are subjected to the tensile stresses.

Since the rail seat positive test can be conducted in both sides of the crosstie separately, each side was designed differently. Left-side ties are designed to be reinforced to explore the effect of each reinforcement options. Flexural reinforcement was introduced to prevent prestressing strand rupture and improve the flexural performance of the crosstie.

Flexural reinforcement would not only increase the flexural capacity of the tie but also provide some ductility to the crosstie at the ultimate stage. Flexural reinforcement can carry tensile stresses at the bottom of the crosstie, thus compensating for the effect of eliminating prestressing strands. Specimens 4-A-L and 4-D-L were both reinforced with 2 #3 rebars. However, FEM predicted that the shear would be the governing failure mechanism for those specimens since the flexural capacity was increased and the risk of prestressing strand rupture was alleviated.

Shear reinforcement was introduced for the ties with reduced jacking force (specimens 4-B-L, 4-C-R, 4-C-L). Shear stirrups were designed based on the FEM result of specimen 4-B-R, which was predicted to fail in shear; thus, the ultimate shear capacity of the section was set as the strength of 4-B-R. Shear reinforcements were designed following ACI provisions. Six #3 rebar were used to reinforce to specimens 4-B-L, 4-C-R, and 4-C-L where the jacking forced was reduced to 70% and 60% to the baseline.

Flexural confinement was introduced to provide confinement at high compressive stress region. Under high compressive stress, the crosstie rail seat is prone to crushing (Figure 4-8c). Once crushing initiated, the effective cross-sectional area decreased and led to the shear failure. To improve the flexural performance and ductility of the tie, specimen 4-C-L was designed with six #3 stirrups and two #3 confinements.

Figure 4-6

Schematic representation of test specimens for rail seat positive test

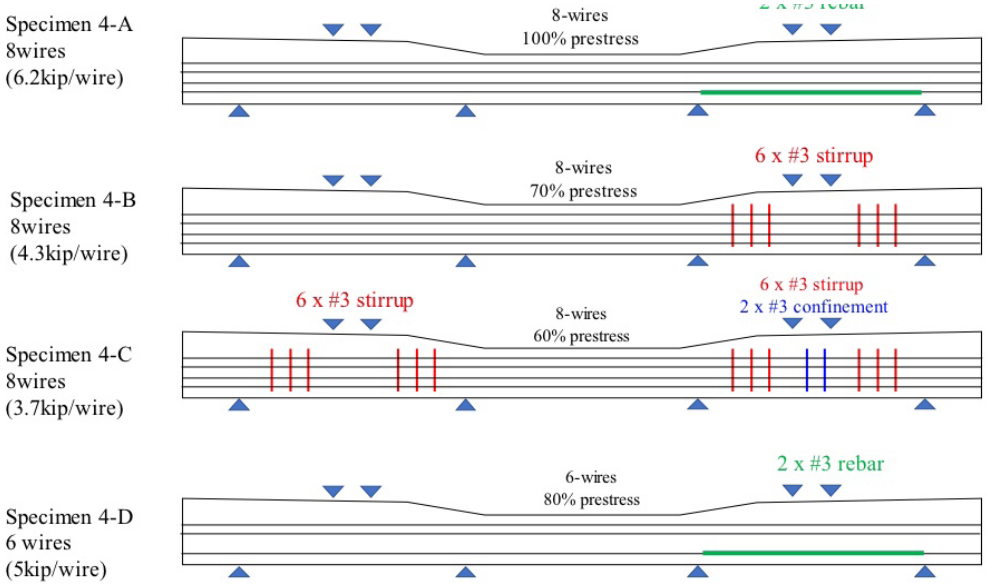

Figure 4-7

Rail seat positive load-displacement curve with different configurations and percentile of ultimate strengths of different configurations to current configuration

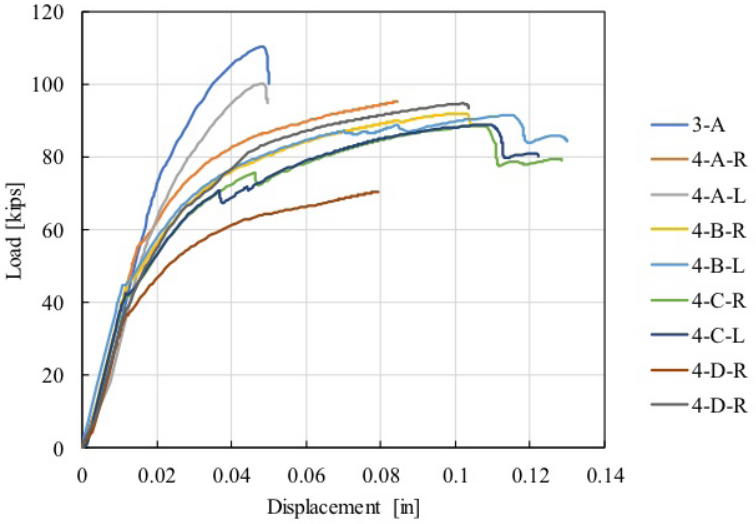

Results

Center Negative Tests

Figure 4-8 shows the specimens at the ultimate load level. The baseline design (3-A) showed a clear shear crack without any sign of flexural crack which can be concluded that the failure mode was pure shear. The fiber reinforced tie (3-B) exhibited multiple flexural cracks at the center bottom of the crosstie, and the crushing of the concrete at the center top of the section. The shear reinforced crosstie (3-C) showed both flexural and shear cracking. The crushing of the concrete was observed at the center top of the tie, and the diagonal shear crack pin crossing the load pin to support was observed. After monitoring a video of the testing, especially at failure, the shear crack was propagated right after the center

crushing happened. This was because the effective section area decreased due to the crushing at the center, thus load path from load pin to support become critical.

Figure 4-8

Test specimens at ultimate stage under center negative test—(a) 3-A, (b) 3-B, (c) 3-C

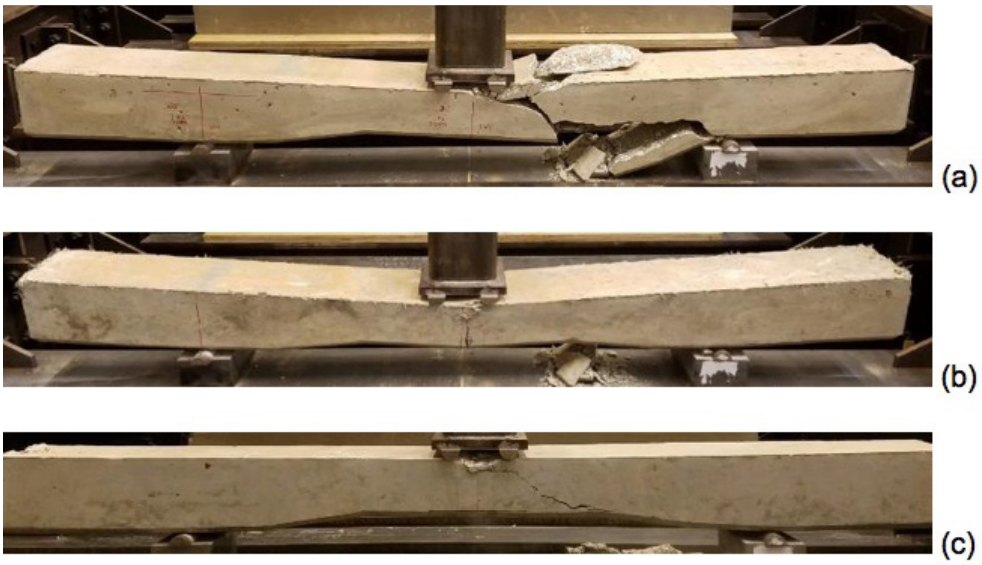

Figure 4-9 shows the load-deflection curves of 3-A, 3-B, and 3-C under the center negative test. For all three cases, the ultimate strengths at failure were almost identical. This means the ultimate capacity triggered failure was nearly identical. The fiber and shear reinforcement did little to increase the ultimate capacity. Additionally, the ultimate load and displacement of 3-B and 3-C are almost identical, which means the same failure mechanism was developed. Since the failure mode of 3-B was undoubtedly flexure, the flexure was the trigger that lead 3-C to failure. It can be concluded that the failure mechanisms for 3-A, 3-B, and 3-C were pure shear, flexural, and flexural-shear, respectively. Thus, the ultimate flexure and shear capacity of the section was almost identical.

Figure 4-9

Center negative test results

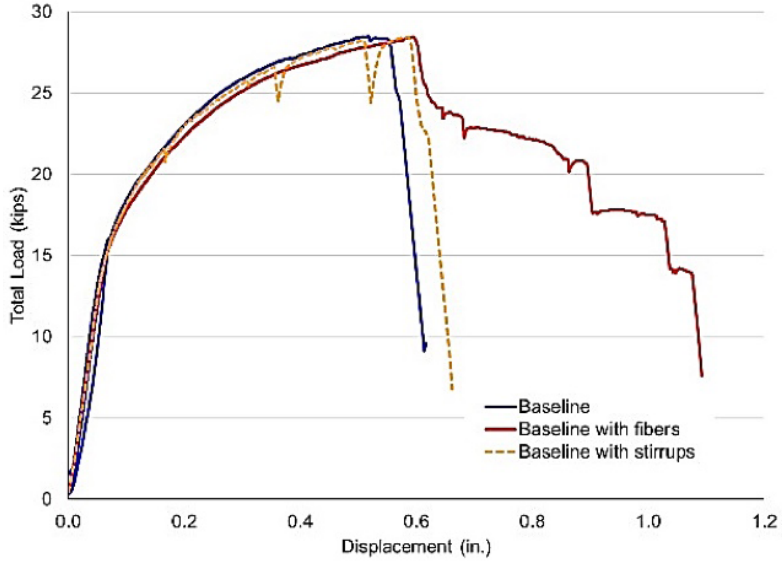

Rail Seat Positive Test

The load-deflection curves for rail seat positive tests are shown in Figure 4-10. The test specimens at ultimate load levels are also shown in Figure 4-11. The failure modes and the ultimate capacity of the specimens are listed in Table 4-2.

In Figure 4-10a, the effect of fiber reinforcement was shown. The ultimate load and displacement for both baseline and FRC crosstie was almost identical, 93.2 kips and 92.3 kips, respectively, yet the post-peak behavior was different. FRC provided some residual strength after reaching the peak load. However, in Figure 4.11a and b, both ties showed a clear shear crack pattern at ultimate stage. Unlikely to impact the center negative test result (Figure 4-8b), FRC did not prevent shear failure. This was because the ultimate shear capacity under rail seat positive test (93.2 kips) was much greater than the counterpart of center negative test (27 kips), fiber could not hold cracks from opening. In this case, more aggressive applications of reinforcement (e.g., shear stirrups) is required to prevent shear failure.

Figure 4-10b shows the effect of eliminating the number of wires. All three specimens failed in tendon rupture and the only difference was the ultimate strength. Eliminating 4 out of 12 wires lead to 29% reduction and 6 out of 12 wires with 20% reduction in jacking force led to the 42% reduction in the ultimate capacity.

In Figure 4-10c, the effect of reducing jacking force was compared. Reducing jacking force in specimen 4-B-R was 70% of 4-A-R. It led to the greater ultimate displacement which is more flexible behavior. This is because there are more room for strands to be stretched in specimen 4-B-R. This delay of ultimate displacement led to change of failure modes from strand rupture to shear.

Figure 4-10d depicts the effect of flexural reinforcement. As expected from FEM results, flexural reinforcement provided extra flexural capacity and alleviated the possibility of the strand rupture, yet the crossties failed in shear. With flexural reinforcement (specimens 4-A-L, and 4-D-L), the crossties behaved stiffer than the crossties without the reinforcement.

The effect of shear reinforcement was shown in Figure 4-10e. Flexural failure mode was observed given the presence of shear reinforcement (specimens 4-B-L and 4-C-R). In addition, the post peak behavior was clearly different from that of counterpart (specimen 4-B-R).

Specimens 4-B-L and 4-C-R showed more gradual decrease in the strength that is more ductile response. After the gradual decrease, the crosstie still had a residual strength about 83% of the peak strength.

Figure 4-10f demonstrates the effect of flexural confinement. With the flexural confinement (specimen 4-C-L), the response of the crosstie was even more ductile with higher ultimate strength. The ultimate strength of specimen 4-C-L was 69.9 kips, whereas specimen 4-C-R was 60.4 kips. The ductility ratio of

specimen 4-C-L was greater than that of counterpart (specimen 4-C-R). This was because confinement confining the concrete at high compressive stress region, provided extra flexural capacity to the crosstie.

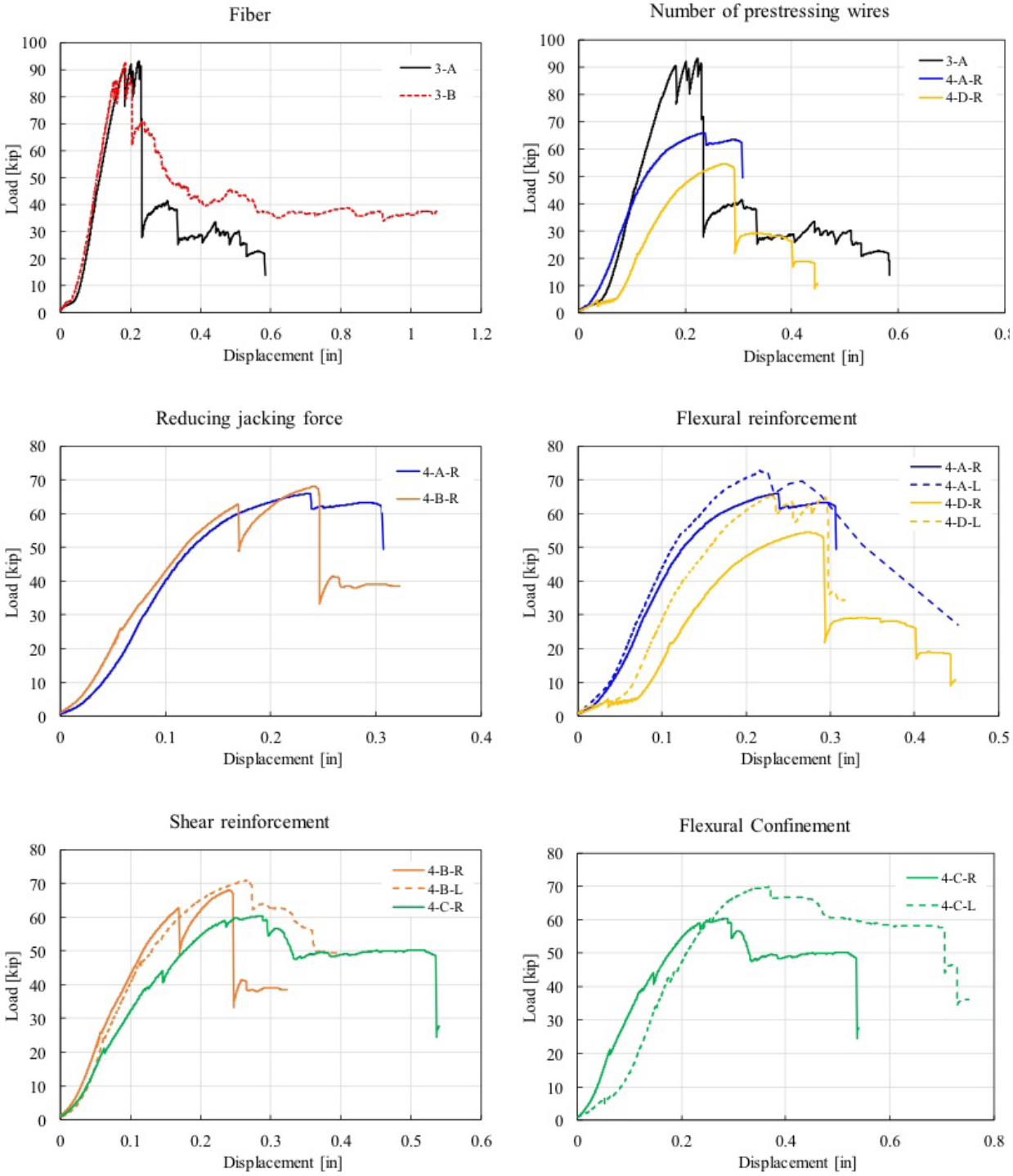

Figure 4-10

Load-deflection curve for specimens under rail seat positive tests: (a) Fibers, (b) number of prestressing wires, (c) reducing jacking force, (d) flexural reinforcement, (e) shear reinforcement, (f) flexural confinement

Figure 4-11

Test specimens at ultimate stage under rail seat positive test

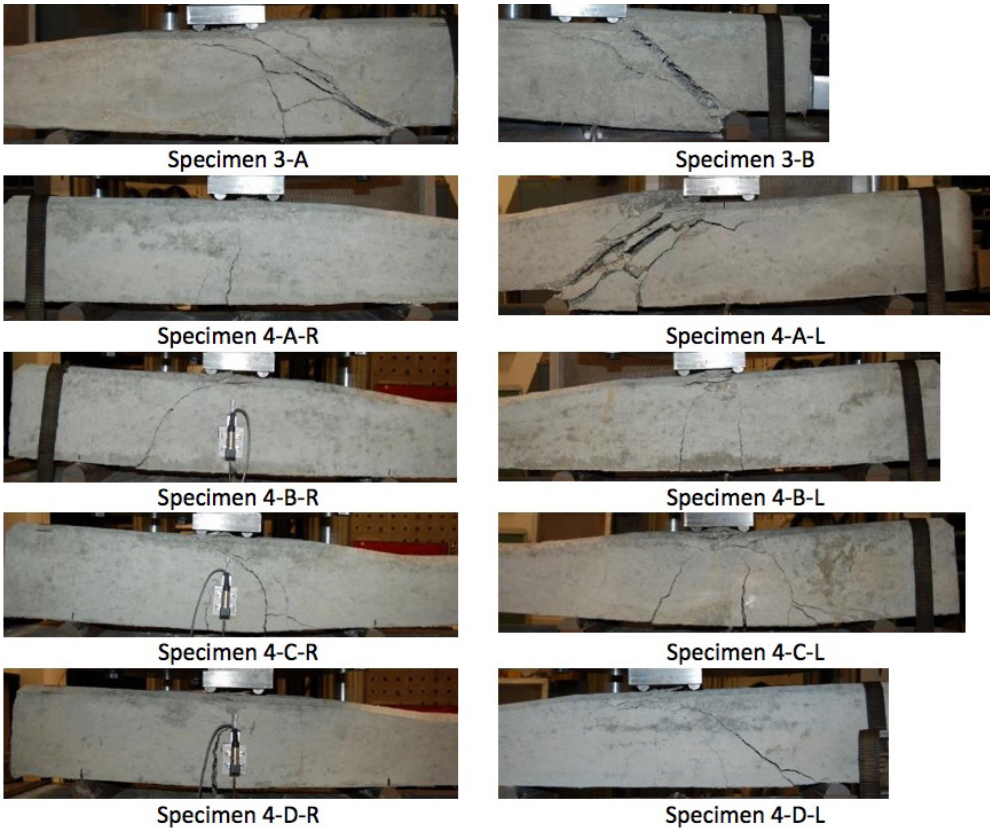

Table 4-2 presents rail seat positive test results along with the failure mode and ultimate strength of each specimen. In Figure 4-12, the FEM predicted ultimate strength reduction ratio, and the experimental ultimate strength reduction ratio was compared. The overall trend of strength reduction was matched between the laboratory results and FEM analysis.

Table 4-2

Rail Seat Positive Test Results

Specimen	Prestressing (# of Wires [Jacking Force])	Reinforcement	Failure Mode	Ultimate Strength(kips)	Ultimate Strength Reduction (%)
3-A (Baseline)	12 wires/ (6.5kip/wire)	–	Shear	93.2 kips	0%
3-B (fiber)	12 wires/ (6.5kip/wire)	Fiber (8lb/yd^3)	Shear	92.3 kips	-0.94%
4-A-R	8 wires / (6.5kip/wire)	–	Strand rupture	65.9 kips	-29.28%
4-A-L	8 wires/ (6.5kip/wire)	2 #3 flexural reinforcement	Shear	72.8 kips	-21.9%
4-B-R	8 wires/ (4.7kip/wire)	–	Strand rupture	68.1 kips	-26.92%
4-B-L	8 wires/ (4.7kip/wire)	6 #3 shear reinforcement	Flexure	70.9 kips	-23.91%
4-C-R	8 wires/ (4.1kip/wire)	6 #3 shear reinforcement	Flexure	60.4 kips	-35.22%
4-C-L	8 wires/ (4.1kip/wire)	6 #3 shear reinforcement, 2 #3 flexural confinement	Flexure	69.9 kips	-25%
4-D-R	6 wires/ (5.6kip/wire)	–	Strand rupture	54.4 kips	-41.61%
4-D-L	6 wires/ (5.6kip/wire)	2 #3 flexural reinforcement	Shear	65.4 kips	-29.92%

Figure 4-12

Ultimate capacity ratio comparison between experimental designs and baseline

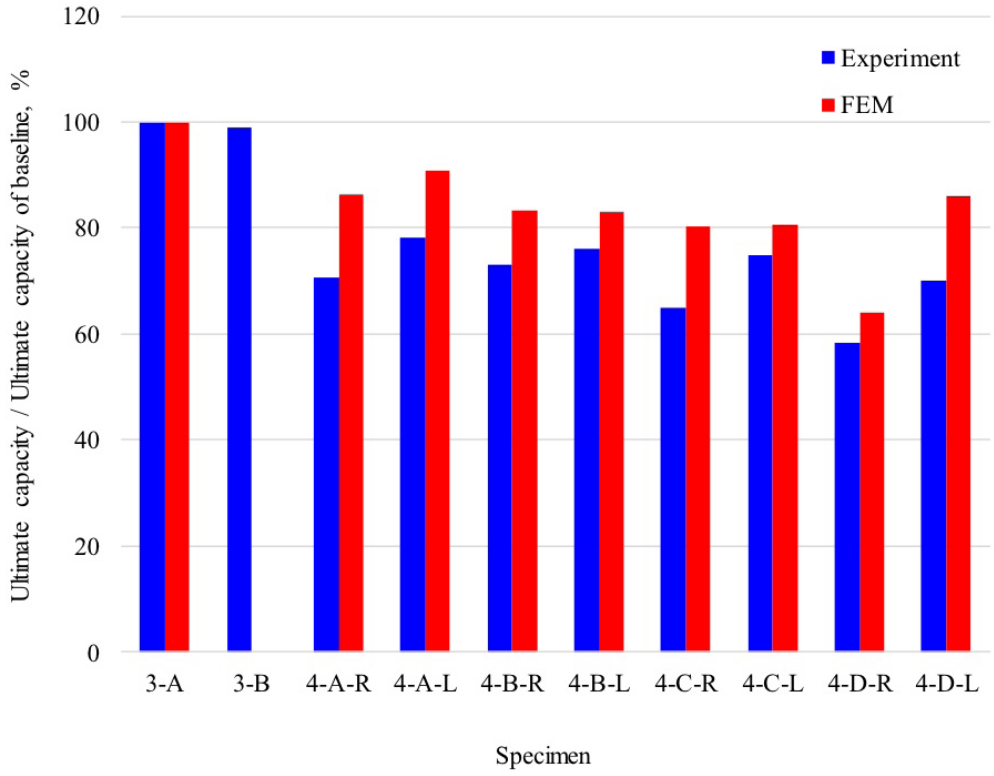

Initial Conclusions

Three critical design elements were studied in the initial design phase of this project: 1) reducing prestressing levels, 2) introducing flexural reinforcements, and 3) introducing shear reinforcements. Accordingly, test specimens were designed based on FEM results and the aforementioned design elements.

In the center negative tests, two design options were studied to reinforce the crosstie—shear reinforcement and synthetic fiber, both of which changed the mode of failure of the crosstie from pure shear to flexure and flexural-shear. In the rail seat positive test, reducing prestressing levels by eliminating wires led to the reduction in capacity about 30%. Reducing the jacking force of the wire led to the delay of strand rupture and made the tie more flexible. Introducing flexural reinforcement alleviated the risk of strand rupture yet led to shear failure. Introducing shear reinforcement led the ties to have more ductile behavior, and there was significant residual strength after the peak. Introducing flexural confinement improved the ductility of the tie and also strengthened the ultimate capacity.

Final Prototype Design, Manufacture, and Testing

Valuable feedback was provided by the project's industry partners on November 1, 2017, at a scheduled annual project status update meeting in Victorville, California. This feedback, combined with further advancements in the UIUC team's FEM model and lab experimentation, led to proposing the following set of prototype designs.

Objective

The objective for the new vision for the prototype design was to reflect comments from the industry partners at the Victorville meeting. Instead of enhancing the ultimate stage capacity as was described previously and focusing on controlling the failure mechanism, the revised objective focuses on the behavior of the crosstie at the service load level and optimization of its cost effectiveness. According to data recorded in the field, the maximum field moment was far below the service level capacity of the current crosstie design. Thus, reducing the service level capacity of the crosstie within a reasonable range of safety factors was undertaken.

Design Variables

The variables for the revised project objective were 1) section depth, 2) location and arrangement of the prestressing tendons, and 3) number of prestressing tendon used. The section depth can be reduced from the bottom of the crosstie so the same form can be used. The location and arrangement of the prestressing

tendons govern the prestressing force induced by the eccentricity between the centroid of the tendons and the centroid of the section. The number of prestressing tendon used governs the prestressing force, since the jacking force per wire (6.5kip/wire) and the diameter of the tendon (5.32mm) are kept constant.

These three variables are independently related to the cracking moment capacity (M_{cr}). The optimization of the design is to find the optimal combination of the three variables. Thus, each contribution of variability from each design change must be considered independently. In conventional parametric study using FEM, varying the parameter of interest where other variables are fixed is not efficient for finding the optimal values given that there are too many possible combinations. Thus, the new optimization framework that simultaneously evaluates three independent variables is proposed.

Target Values

The most critical target value of the revised objective is service level capacity. The service level safety factor (Φ_{cr}) is introduced to quantify the reserved capacity in the tie at the maximum load recorded in the field. The service level safety factor (Φ_{cr}) is defined as the moment at cracking (M_{cr}) with the maximum field moment ($M_{max.field}$) (Eq. 4-1).

$$\Phi_{cr} = M_{cr} / M_{max.field} \quad (4\text{-}1)$$

If the Φ_{cr} is greater than 1, the crosstie is in the elastic region. The current design prototype has a Φ_{cr} of 5 and 3 under center negative and rail seat positive settings, respectively. In this project, the target safety factors were 3.0 and 2.0 for the rail seat positive and the center negative, respectively. Cost effectiveness was also an important factor in design optimization. The design with the least cost among the alternatives having same target safety factors will be selected as the final optimized design.

Proposed Optimization Framework

The new design optimization framework is proposed to efficiently find the optimal combinations of design variables. Preliminary analysis was introduced to find the preliminary optimal combination with simplified force equilibrium equations instead of varying three variables randomly. The flowchart for the new design optimization framework is shown in Figure 4-12.

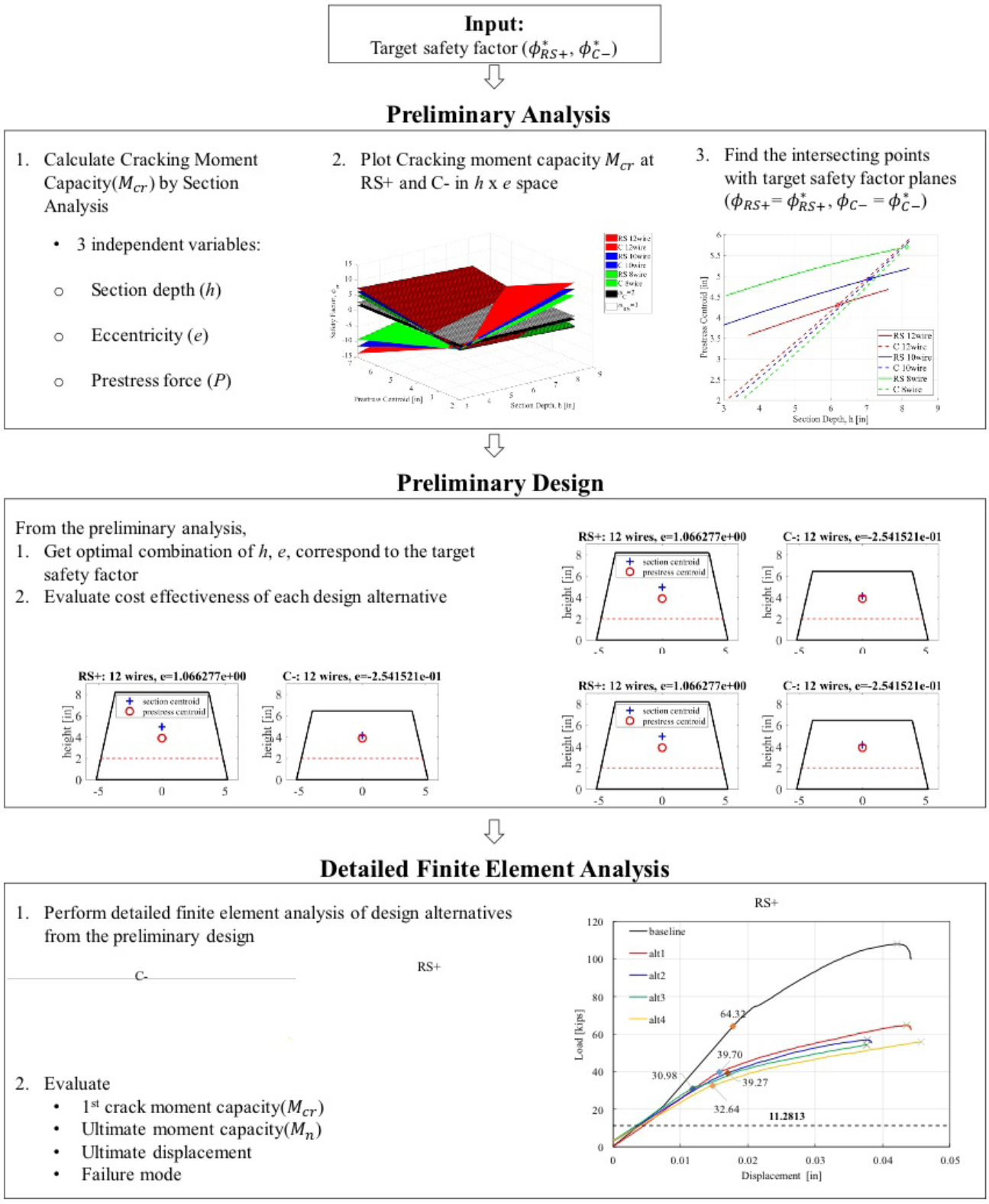

Figure 4-13

Flow chart of proposed design optimization process

Preliminary Analysis Phase

In the preliminary analysis phase, the optimal section designs having target safety factors are determined by section analysis. The purpose of the section analysis is to find the cracking moment capacity (M_{cr}) of the section. In the section analysis, the crosstie is assumed to be prismatic within the range of rail seat region and the center region, respectively. As noted, the cracking moment capacity (M_{cr}) is the function of three independent variables: section depth (h), eccentricity (e) between the prestressing tendons and the centroid of the section, and prestressing force applied to the section (P). Considering geometric relations of the section, M_{cr} can be written in terms of section depth (h), eccentricity (e), and prestressing force (P).

$$M_{cr}=f(h,e,P) \tag{4-2}$$

Once the M_{cr} is written in function for both rail seat positive and center negative, Φ_{cr} can be calculated with Eq. 4-1. As shown in Figure 4-14, the Φ_{cr} surface for rail seat positive and center negative can be plotted in 3D with respect to section depth (h) as the x-axis and eccentricity (e) as the y-axis. The optimal combination of the three variables having target safety factor values can be found by drawing a target plane parallel to the x-y plane. The target safety factor can be set differently for the rail seat positive and the center negative.

Figure 4-14

Safety surface for rail seat positive and center negative with different numbers of prestressing tendons

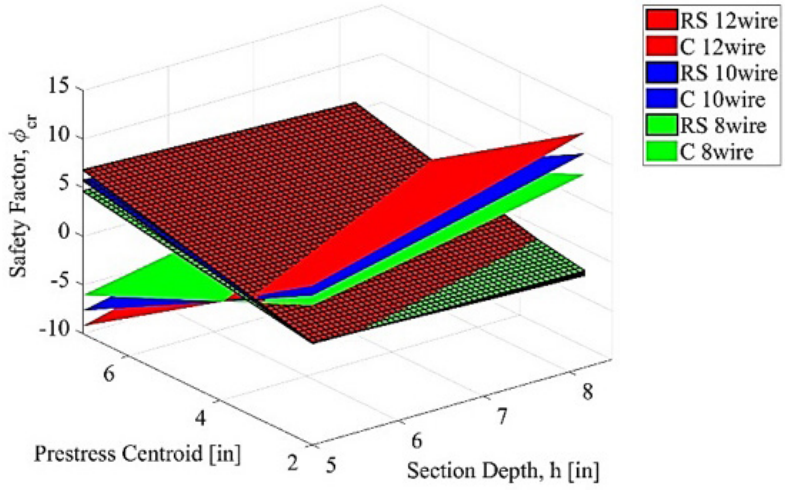

The optimal combination of section depth (h) and eccentricity (e) can be found by the procedure as follows: 1) draw a target plane for rail seat positive and center negative, 2) obtain intersecting lines from safety surface and the target plane individually, and 3) find an intersecting point where lines obtained meets. Figure 4-15 shows the three intersecting points of target safety factor of 3 and 2 for the rail seat positive and the center negative, respectively. Each intersecting point represents an optimized design alternative. In the following FE Analysis phase, these design alternatives will be evaluated in detail.

Figure 4-15

Intersection lines of target safety factor and safety surfaces

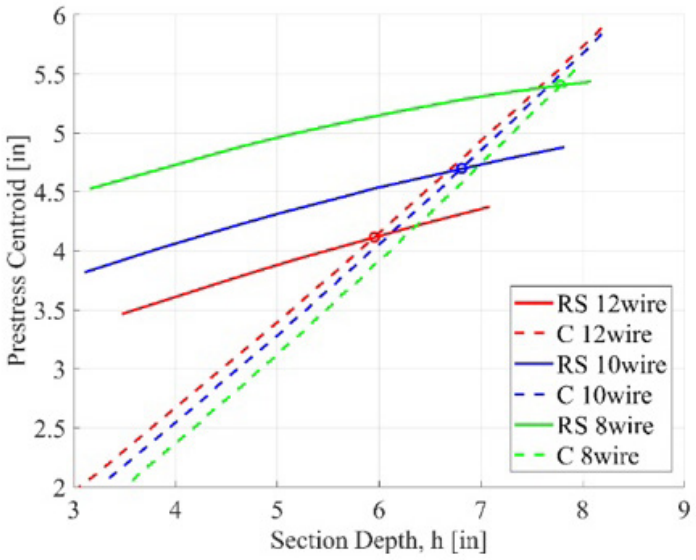

Detailed FE Analysis Phase

In this phase, design alternatives obtained from the preliminary analysis were evaluated using FEM. Since the calculations conducted in the preliminary phase were simplified and more conservative, detailed analysis considering the geometric and material nonlinearity was required. In the detailed analysis phase, ultimate capacity and failure mechanism were determined. For the ultimate stage, deflection of the crosstie at the rail seat and the center also was an important parameter to check, since it relates to derailment potential.

From the preliminary analysis, the design alternatives for the target safety of 2 and 3 for rail seat positive and the center negative is shown in Figure 4-16. Table 4-3 and Figure 4-17 show the service and the ultimate capacity of the crosstie and the corresponding deflection. The service level safety factor derived from the FEM was greater than the target safety factor, as expected.

Figure 4-16

Design alternatives obtained from preliminary analysis phase

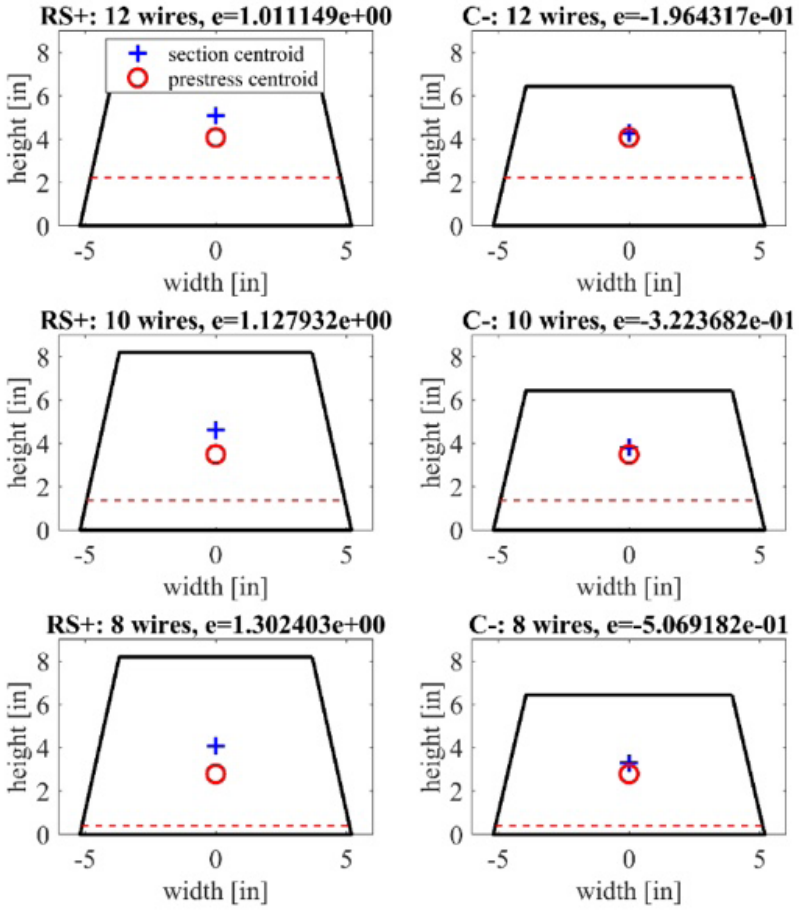

Table 4-3

Detailed Analysis Results for Design Alternatives 1 and 2

	Alt1		Alt2	
	Rail Seat	Center	Rail Seat	Center
Safety factor	2.5	2.5	3	2
Section depth (in.)	7.304293711		7.781749236	
Prestress centroid (in.)	4.750536582		5.403378277	
Reduction depth (in.)	0.883206		0.405751	
1st crack load (kips)	33.58061	8.861816	38.03529	6.646926
1st crack disp (in.)	0.031006	0.085426	0.04117	0.047102
Service safety factor	2.977005	4.790171	3.371923	3.592933
Ultimate load (kips)	61.19659	11.0195	67.60814	11.124
Ultimate disp (in.)	0.054467	0.15207	0.062106	0.201109
Ultimate safety factor	5.42523	5.956489	5.99363	6.012971

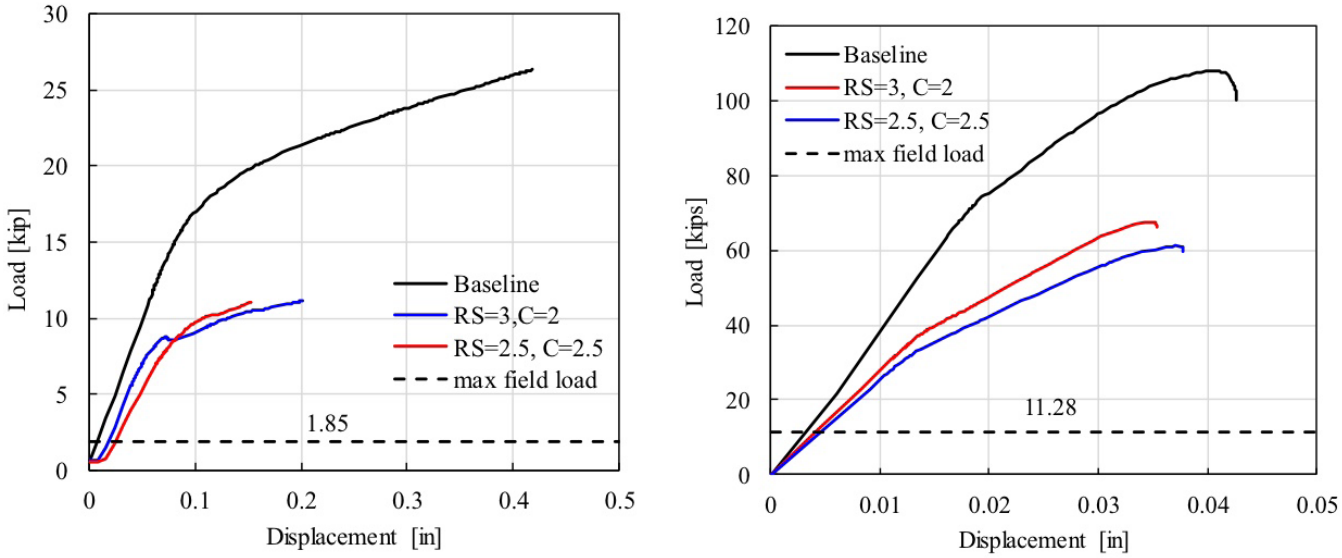

Figure 4-17

Load-displacement curve for design alternative 1 and 2—center negative test and rail seat positive test

SECTION

5

Conclusion and Future Work

This report describes the development and application of a method to quantify flexural demands on prestressed, monoblock concrete crossties for use in generating designs that are optimized for rail transit field loading conditions. Field testing and evaluation of a broad range of rail transit infrastructure has proven useful in identifying variables that influence crosstie flexural demand. Collection of extensive data for more than one year at each rail transit field site provided a robust dataset that allowed the UIUC research team to develop a multivariate model for center and rail seat moment prediction. The data then were used to develop and implement a probabilistic design methodology using structural reliability analysis (SRA), leading to a number of conclusions, as summarized below.

Conclusions

Summary of Rail Transit Static and AW Loading Conditions

A thorough study of current rail transit wheel loads was conducted and is summarized in Section 1. Significant volumes of concrete crossties and elastic fastening systems were used on rail transit infrastructure, and the inventory is summarized in Section 1.

Non-Destructive Bending Moment Instrumentation Methodology

A non-intrusive and non-destructive instrumentation method using concrete surface strain gauges was successfully developed and deployed to measure bending strains and resulting moments experienced by concrete crossties under a variety of types of rail infrastructure in the US. This method was robust and yielded reliable and repeatable results over long time durations (up to three years), with very few in-service failures. Additionally, data collected using this method were generally clean and required minimal filtering in order to obtain peak bending responses.

Input Loading Environment at Wheel-Rail Interface

UIUC investigated the aggregate effect of speed and other vehicle and track irregularities to generate accurate load factors that represent the total rail transit wheel load environment, including dynamic and impact loads. The following conclusions were drawn:

- Total load factor distributions for the three rail transit systems studied were statistically different, demonstrating that unique load factors are needed to adequately represent the existing wheel loads and improve the design of critical components that make up the track structure. Distributions indicate that the current AREMA impact factor of 3 could be reduced by as much as 50%.
- Dynamic load factors were analyzed, and it was found that the Talbot approach to estimating dynamic loading due to speed and wheel diameter was a poor predictor for rail transit modes. This method overestimates light rail transit wheel loading environment by a factor of 3. Conversely, heavy rail transit wheel loading factors are underestimated by approximately 50%. The Talbot method was, however, a good predictor for commuter rail transit wheel load factors.
- Focused wheel-rail interface instrumentation can be deployed in the field to answer loading questions within a given rail transit mode. The modest effort required to install instrumentation and process data from such an installation can provide substantial returns on investment (ROI) by helping develop more economically mechanistically designed track components.

Non-Destructive Field Quantification of Bending Moments

The concrete surface strain gauge instrumentation developed as a part of this effort was successful in measuring the bending strains and resulting moments experienced by concrete crossties under a variety of types of rail traffic. The data were used to answer questions related to crosstie-to-crosstie variability and the occurrence and magnitude of temperature-induced curl. The following conclusions were drawn:

- Bending moments vary widely from crosstie-to-crosstie. This was demonstrated on a HAL freight railroad application, showing bending moments at the crosstie center that ranged from 0 kNm (0 kip-in.) to 22.8 kNm (202 kip-in.). This is consistent with prior research [54, 64, 58].
- Temperature-induced curl (e.g., warping of the crosstie due to different temperatures on the top and bottom) has a quantifiable impact on concrete crosstie flexural demand. Curl in concrete crossties was found to change over the course of the day as the temperature gradient changed, which affected the bending moments induced in the concrete crossties [53, 54], a behavior similar to that which has been noted in rigid pavement applications [61].

Factors that Influence Rail Transit Bending Moments

Field deployments on MetroLink (light rail) and NYCTA (heavy rail) allowed UIUC researchers to address questions specific to rail transit concrete crosstie performance including quantification of bending moment magnitudes, calculation of reserve structural capacity, and measurement of crosstie-to-crosstie variability. The following conclusions were drawn:

- Maximum center negative bending moments ranged from 25 kip-in. (2.8 kNm) on MetroLink (light rail) to 120 kip-in. (13.5 kNm) on NYCTA (heavy rail).
- Significant residual flexural capacity was also found; 99th percentile bending moments resulted in residual load factors of 6 and 2 for LRT and HRT systems, respectively.
- Bending moments experienced by concrete crossties on rail transit systems varied from crosstie-to-crosstie, ranging from as little as 10% for center negative (C-) bending on MetroLink to as much as 100% on NYCTA. The latter is similar to that previously demonstrated in the HAL freight environment. Crosstie-to-crosstie variability between the two transit modes was also quite different, with the greatest variability associated with HRT center negative bending moments.

Probabilistic Crosstie Design

In addition to the methods described in Section 4, UIUC developed and demonstrated a probabilistic design process based on structural reliability analysis concepts. Using first-order reliability methods, values for reliability indices (ß) for new designs were obtained and compared with existing designs. New, optimized designs had the following characteristics:

- New heavy rail transit designs had a reduced center negative moment capacity of 50%.
- In most cases, compared to current designs, the proposed designs for both rail modes had fewer prestressing wires and a higher centroid of prestressing steel.
- In all cases, the flexural capacities at the crosstie center and rail seat are better balanced from a structural reliability standpoint when compared to current designs.

Impact on Mechanistic-Empirical Design of Railway Track Components

More broadly, this research focused on advancement of the mechanistic component of mechanistic-empirical design. This is important because the response of components must be well understood before inferences can be made as to how they should be designed. Specific advancements were made to better understand the effects of various rail transport loading conditions on bending moment magnitudes, reserve structural capacity, thermal gradient effects, and crosstie-to-crosstie variability.

A design process incorporating many of the elements proposed was used to develop a new crosstie for Amtrak's Northeast Corridor. This was the first instance in which a US concrete crosstie design was based on mechanistic elements in a process that has traditionally relied on an iterative approach and

assumptions based on empirical data. This design example was an initial step toward closing the gap between the current best practices and an ideal solution that incorporates an appropriate amount of both mechanistic and empirical design content (Figure 5-1).

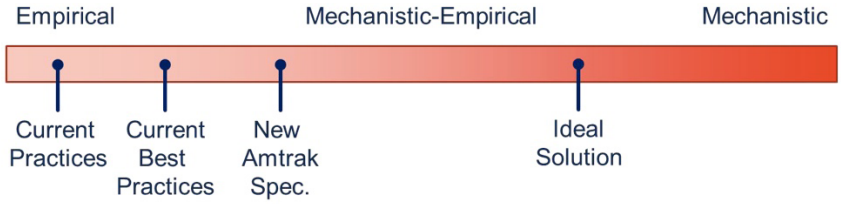

Figure 5-1

Flow chart representation of contribution to application of mechanistic design to rail engineering in context of concrete crossties

The probabilistic design method using structural reliability analysis fundamentals demonstrated is a critical step in the development of mechanistic-empirical practices for the design of concrete crossties. The next steps for advancing the development of mechanistic design for railway track components are shown in Figure 5-2. Establishing failure criteria will be the most challenging, especially for concrete crossties given new findings that have called into question the importance of cracking [65, 67].

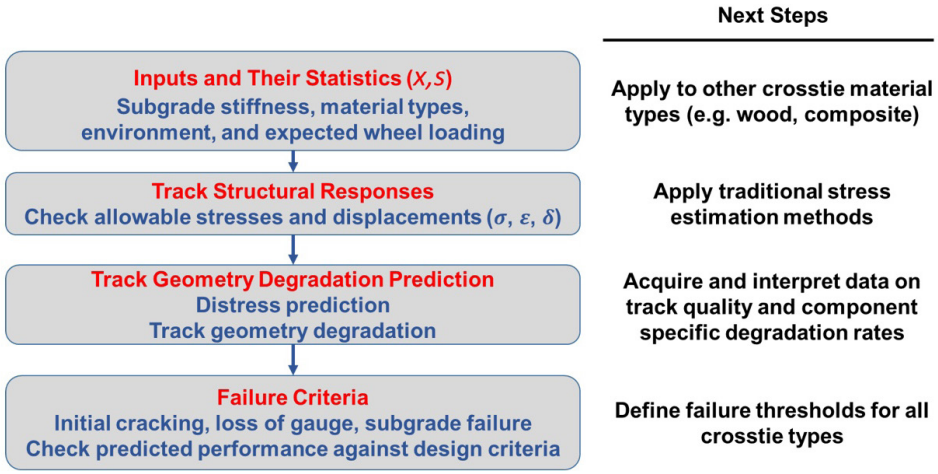

Figure 5-2

Next steps for advancement of proposed framework for mechanistic-empirical design of railroad track infrastructure components

Beyond crossties, the proposed framework will enable future application of mechanistic-empirical design practices to other railway track components. Track components and materials adjacent to the crosstie (e.g., ballast and fastening systems) are the most reasonable candidates for near-term adoption. The fastening system has received comparatively little research, but emerging mechanistic work on premium fastening systems for timber crossties lends itself to the mechanistic design process. Additionally, prior work on lateral load transfer and magnitude within the fastening system is relevant and can be applied to the design process [49, 68]. The application of the mechanistic component of mechanistic design to a variety of track superstructure components was also preliminary documented by Edwards et al. [49].

Work Products

The results from this project benefit the transit industry in a variety of ways. Products produced include the following:

- **Prototype crosstie designs** developed with applicability to multiple rail transit modes
- **Prototype crossties** manufactured and installed
- **Field sites** established for monitoring over long (multi-year) time durations
- **Improved communication and cohesiveness** through transit agency infrastructure management meeting at the UIUC-organized international Crosstie and Fastening System Symposia and other conference interactions
- **Workforce development gains** (students trained in rail transit and pursuing careers in the rail transit sector)

Future Research

The results presented herein will facilitate the optimization of future concrete crosstie bending moment requirements based on flexural demands recorded during revenue service field tests. Given the accuracy and repeatability of data from surface strain gauging of concrete crossties, broader deployment is warranted to investigate scenarios that were not previously considered. Specific track conditions and manufacturing processes that warrant additional study are described in the following sub-sections.

Direct Fixation Track Systems

Beyond concrete crossties, there is significant direct fixation track that is reaching the end of its useful life. These systems need to be replaced, and improvements can be made to extend the life beyond what was experienced with the first-generation systems. Preliminary work was conducted by UIUC at WMATA, but additional research needs exist that relate to quantification of loading and displacements in the field and determining the best qualification tests and parameters for new systems that are developed.

Variations in Track Quality

Given that much of the work conducted to date pertains to collection of data on track that is well- maintained, future work focusing on the deployment of this method in more demanding or partially-degraded field conditions would be of value, such as track transition zones and areas with fouled ballast. These areas have received considerable attention for track substructure reasons but are also of interest in the area of superstructure performance.

Concrete Crosstie Design

Alternative methods of prestressing concrete crossties have begun to emerge in the North American market, including end-plated systems that eliminate many of the challenges associated with the transfer of prestressing forces to the concrete. These, along with post-tensioned concrete crosstie designs that are beginning to appear, should be the subject of research aimed at understanding their long-term performance. Such a study should also ensure that the methods by which their initial structural capacity and load vs. deflection behavior are accurate. Additionally, as alternative crosstie types emerge, it is important to understand whether the analysis and design methods and procedures proposed are robust to changes in crosstie manufacturing method (e.g., pre-tensioned vs. post-tensioned designs) and design geometries (e.g., length, depth, etc.).

Finally, further study of concrete crosstie life-cycle cost (LCC) is proposed. There has been little focus on this topic within the realm of track superstructure components, and it is of particular importance if capital and maintenance dollars are scarce. It also provides a logical method to include the quantification of other environmental impacts to ensure concrete crossties are being designed, manufactured, maintained, and disposed of in a sustainable manner.

Concrete Crosstie Performance

The transient behavior of concrete crossties should be considered. This is a subject whose importance has been illustrated recently by a study of the track support structure and its transient performance [69–71]. Initial data on the flexural response of the crosstie to a passing wheel load indicates that the response can vary widely depending on load magnitude and duration, something noted decades ago on Amtrak's NEC in its study of rail pad effectiveness. Understanding the relative importance and trade-offs between flexural demand magnitude and moment duration could influence the design of other resilient track components such as under tie pads (UTPs) and ballast mats.

Other Crosstie Materials

Beyond concrete crossties, there is ongoing interest in performing similar instrumentation on composite crossties. If surface strain gauging similar to that described herein is indeed feasible on composite materials, this would provide an opportunity to understand the behavior of a crosstie material that is inherently different than concrete and allow for an analysis of how the flexural rigidity of the composite crosstie and its interaction with the ballast impact overall track performance. Both short- and long-term impacts of composite crosstie use should be investigated.

APPENDIX

A

Transit Survey Results

1. How many track miles does your organization operate and maintain in total?							
96	659	108	100	75	242	86	700
2. How many track miles is ballasted concrete crosstie track?							
52	13.2	51	95	70	none	54	
3. How many track miles of ballasted concrete crosstie track is equipped with continuous welded rail (CWR)?							
52	8	51	95	70	none	54	
4. What is the typical concrete crosstie spacing for your track?							
30”	24”	30"	30"	30"	30"	24	24"

5. What types of concrete crossties are currently installed? (brand and model, e.g., CXT 100S-09)
CXT Transit ties for 115 RE Rail
CXT conforming to MTA-NYCT Standard Track Drawing T-2057B
CXT 429-20
Rocla T9837, T9825,T9808,T9804
Rocla and CXT
None
CXT
KSA and Rocla

6. What types of fastening systems are currently installed? (brand and model, e.g., Pandrol e-Clip)
Pandrol Fast Clip
Pandrol e-Clip
Pandrol e-Clip, Fast Clip
Pandrol e-Clip
Pandrol e-Clip
None
Pandrol Fast Clip, E-Clip
Fast Clip

7. What are the most common rail sections on your system?
115 RE; 132 RE
115 RE;100-8
115 RE
115 RE
115 RE
100 ARA-A; 115 RE; 90 AS
115 RE
115 RE;136 RE

8. What is the maximum gross static wheel load of passenger railcars?
Research required
16,500 lbf
149,200 lb/car
14,916lbs
18,000 lbs
11 K +/-
7500
197000

9. What is the maximum gross static wheel load of work equipment (e.g., ballast car)?
Research required
12,700 lbf
Not defined
N/A
4,000
15 K +/- (railbound crane)
6,250
100 tn
10. What is the maximum gross static wheel load of commuter rail locomotives? (if applicable)
Research required
14,000 lbf
N/A
N/A
N/A
N/A
300,000#
11. Is there any ballasted concrete crosstie track shared with freight train operations?

No	No	Yes, but maintained by freight operator	n/a	No	No	Yes	Yes

12. What is the typical dynamic load impact factor used in design? (%) (e.g., 300% = 3 ace • static loading)
Research required
1.333
4
29,833 lbs
Varies
Max load 286,000 pd on track
AREMA
13. What is the maximum operating speed of passenger trains?

55 mph	55 mph	55 mph	55 mph	55 mph	70 mph	65 mph	80 mph

14. What is the annual tonnage on your heaviest used ballasted concrete crosstie track? (million gross ton)
Research required
30 MGT
Do not measure this way
12.25MGT
NA
10 million
16 MGT
15. Does your organization have any passenger car procurement and/or rehabilitation plans within the next 5 years? If so, what is the maximum gross static wheel load of the new passenger cars?
Research required
Yes, goal is to limit wheel load to 15,000 lbf if possible
No
No
Yes, same
Unknown
No
Yes, same as above

16. Does your organization have any future concrete crosstie renewal or replacement plans? If so, how many track miles of track renewal and/or replacement are anticipated?
Warranty work currently ongoing for defective concrete ties
Yes, approximately 2.2 trk-mi per year
No
No
No
No
No
Yes
17. Does your organization have any future track expansion plans? If so, what type of track superstructure will be installed? How many track miles are anticipated?
Research required
Yes, Second Avenue Subway Phase II - Low-Vibration Track (LVT) will be used
Potentially, but type of structure and mileage TBD
Additional 10 mi, ballast and concrete ties
Yes, ballasted concrete tie, 25 track mi
Yes, varies 10+/-
No
Yes, concrete tie

18. From your point of view, how relevant is each of the following track structure conditions in terms of contributing to the occurrence of railway accidents on concrete crosstie track?							
Derailment damage	5	4	2	2	3	1	4
Cracking from strong support under rail seat (rail seat positive bending)	4	4	1	1	3	1	3
Cracking from center binding (center negative bending)	4	3	1	1	3	1	3
Cracking from environmental or chemical degradation	5	3	5	1	5	1	3
Cracking from dynamic loads	5	3	4	1	3	1	4
Tamping damage	3	3	3	1	3	1	2
Shoulder/fastener wear or fatigue	3	4	3	1	3	4	3
Rail seat deterioration (RSD) and other forms of rail cant deficiency	5	4	4	1	3	4	3
Concrete crosstie with deteriorated bottom	4	3	2	1	3	4	3
Missing rail pad	5	3	3	1	3	4	3
Worn or missing insulator	5	3	3	1	3		3
Broken or worn shoulder	5	4	3	1	3	3	4
Missing clip	3	2	3	1	3	4	4
Fouled ballast	3	3	4	1	3	3	5
Insufficient depth of ballast	3	3	3	1	3	1	5
Weak subgrade	4	3	3	1	3	1	5

19. From your point of view, how relevant is each of the following deficiencies of concrete crosstie and fastening systems in terms of contributing to the occurrence of railway accidents on concrete crosstie track?							
Deficient concrete strength	5	4	2	1	3	1	5
Improper prestress force	5	3	2	1	3	1	5
Poor material quality or behavior (of clamp, insulator, rail pad, or crosstie)	5	3	2	1	3	1	5
Poor environmental conditions (e.g., moisture or fines intrusion)	5	3	3	1	3	1	5
Manufacturing flaws	5	4	2	1	3	1	5

Improper component design (of clamp, insulator, rail pad, or crosstie)	5	3	2	1	3	1	4
Fastening system damage	5	4	3	1	3	1	5
Concrete deterioration beneath the rail	5	4	4	1	3	1	4
Poor bonding of concrete to prestress	5	4	2	1	5	1	5
Alkali-silica reaction (ASR)	5	5	3	1	5	1	5

20. What specific steps do you take to repair distressed, worn, or damaged concrete crossties?
Replace tie
No failures of concrete ties; if tie defective, replaced with new one
Never had to repair a concrete crosstie; would remove and replace
None
With relatively light loads our equipment imposes on track structure, have not experienced concrete tie deterioration; have replaced a few ties as a result of derailment/accident damage
N/A
Replace tie
Replace tie
21. What specific steps do you take to repair distressed, worn, or damaged fastening systems?
Replace pad, insulators and clips
No failures of fastening systems on concrete ties; if tie defective, replaced with new one
Remove and replace. Believe broken clips were a manufacturing flaw.
replace missing e-clips
Has not been a problem
NA
Replace tie
Replace ties
22. What set of standards or industry-recommended practices do you follow for the design, manufacture, testing, and installation of concrete crossties and fastening systems?
Pre-existing tie design, manufacturers recommendations
AREMA
AREMA, ASTM, PCI, ACI referenced in documents; TriMet has own design criteria
AREMA
AREMA
AREMA
Amtrak and LIRR
23. Would your organization be willing to provide UIUC research team with data on concrete crosstie and fastening system use and performance? (Information of interest includes amount of required maintenance, actual service life, and reasons for maintenance or replacement with the track location, curvature, grade, tonnage, and train speed.)

Yes	Yes	No	Yes	No	No		

24. Do you have any additional general comments do you have on concrete crosstie and fastening system design, manufacture, testing, and installation that you would like to provide to UIUC researchers?
Several projects with concrete ties, oldest (installed in 1999) are rock solid, no issues. For projects in 2003 and 2007, manufacturing defect led to failed ties in field; ongoing warranty work will replace bad ties
Not at this time
No problems
No
Contact rail, guard rail, and restraining rail installation details
Ballast compatibility
Rai- to-rail electrical isolation
Pandrol fast clip with concrete tie

25. Would your organization be willing to provide the UIUC research team with concrete crosstie and fastening system design specifications and standards, including those that apply to the fastening assembly and standards on the maintenance and inspection of concrete crossties?							
Yes	Yes	Yes	No	No	No	Yes	Yes
26. If your organization has conducted its own research on concrete crossties and fastening systems, would you be willing to share relevant information with the University of Illinois research team? If research has been conducted, what were the primary topics?							
Yes, ASR and manufacturing process							
N/A							
Have not conducted our own research							
None							
No							
Not aware of any current effort							
N/A							
27. In your opinion, how could the resiliency of concrete crosstie and fastening systems be improved in the face of natural disasters (e.g., hurricane, flood, and snow/ice) or other events that place increased stress on infrastructure and its components?							
Research required							
Make sure that rail-holding elements (shoulders, clips, insulators, pads, etc.) are resistant to corrosion and damage under all conditions							
Not sure							
Given our exposure to natural disasters, current systems suffice							
No such experience							
Have not experienced any issues							
28. Please rank the following areas of concrete crosstie and fastening system research in terms of their potential benefit.							
Fastener design—clips, insulators, inserts, tie pads	5	5	4	4	1	5	5	5
Material design: concrete mix, pre-stress strand arrangement	5	4	4	4	1	3	5	5
Optimize crosstie design: spacing, cross-section, body shape, specific uses (curves, grades, etc.)	5	5	5	4	2	5	5	2
Prevention of rail seat deterioration (RSD) or repair of abraded crossties	5	5	1	4	1	5	5	4
Track system design: determining track service environment and required crosstie characteristics	5	5	5	4	2	5	5	3

APPENDIX

B

Concrete Crosstie Manufacturer Survey Results

1. What is the name of your typical concrete crosstie that is used by the transit agencies you supply components to ballasted concrete crosstie track?			
G13T	101L for Class I	CXT 100S	
2. What is the concrete design mix of your typical concrete crosstie that is used by the transit agencies you supply components to?			
600 kg cement, 25 kg silica fume, 800 kg coarse agg, 650 kg fine agg, 200 kg water, 7.1 kg HRWR, 1.5 kg AEA			
Same mix as supplied to others, containing about 15% fly ash			
600 lb min cement			
3. What is the design air content of the concrete mix? (% or range of %)			
4–7%	3.5–7%	3.5% min in hardened concrete	
4. What type of cement is used? (e.g., Type III cement)			
CPO 40 R (Mexican classification)	Type III low alkali	Type III	
5. What type of coarse aggregate is used?			
Limestone		Yes	
Dolomite	Yes		
Granite		Yes	Yes
Basalt			
Other			
6. What is the origin of the coarse aggregate used?			
Sedimentary rocks	Yes		
Metamorphic rocks			
Glacial deposits			Yes
Alluvial fans			
Stream channel and terrace deposits			
Marine deposits			
Other			
7. What is the shape of the aggregate?			
Crushed/ angular	Crushed/angular	Round	
8. What is the average slump of your concrete at placement?			
9"	3-6”	4”	
10. What consolidation method is used?			
Vibration mechanism	Yes	Yes	Yes
Self-consolidating concrete			
Physical compaction of concrete			Yes
Alluvial fans			
Other	Automated curing chamber		
11. Curing membrane (e.g., wet burlap)—what methods are used to control concrete curing? Please select all that apply.			
Curing membrane (e.g., wet burlap)			
12. What methods are used to control concrete curing? Please select all that apply.			
Curing membrane (e.g., wet burlap)		Yes	
Liquid curing compound			
Steam	Yes	Yes	

Oil		Yes	Yes
Radiant Heat			
None			
Other	Automated curing chamber		
13. Maximum allowable internal temperature:What is the maximum allowable internal temperature of the typical concrete crosstie during curing? What is the rate of temperature increase during curing?			
65 deg C	158	140 deg F	
14. Rate of temperature increase:What is the maximum allowable internal temperature of the typical concrete crosstie during curing? What is the rate of temperature increase during curing?			
20 deg C per hour		max 36 deg F per hour	
15. What is the minimum allowable concrete strength at prestress transfer?			
5000 psi	4000	4500 psi	
16. What is the average time that elapses between concrete placement and transfer of prestress forces to the concrete? (hours)			
14	4	10 hrs	
17. Is the surface of the rail seat treated in any way?			
No	No	No	
If so, how is it treated?			
Epoxy coated per client's request/spec only			
18. What is the design 28-day compressive strength of your concrete mix?			
7.5–9 kpsi (50–60 megapascals)	6–7.5 kpsi (40–50 megapascals)	6–7.5 kpsi (40–50 megapascals)	
19. Are the crossties pre-tensioned or post-tensioned?			
Pre-tensioned	Pre-tensioned	Pre-tensioned	
20. What form of steel is used?			
Wires	Yes	Yes	Yes
Strands			
Bars			
Other	automated curing chamber		
Steel Information			
Number of steel/how many	8	18	16
Diameter	7 mm	5.25	5.32mm
Yield strength	242 ksi (min)	260,000	267,000 psi
Jacking force	48 kN per wire	7,000	7,000 lb
21. How are the concrete crossties manufactured?			
Carousel	Yes		
Long line		Yes	Yes
Other			
22. Is your typical concrete crosstie manufactured to incorporate a specific fastening system?			
No	Yes	Yes	
If so, what is the fastening system?			
SKL	Pandrol Fast clip		
23. Which light rail transit systems and lines use your concrete crossties?			
MBTA light rail (Boston)		Yes	
Metro Rail light rail (Los Angeles)		Yes	Yes
Muni Metro (San Franscisco)			
San Diego Trolley (San Diego)			

MAX Light Rail (Portland)			Yes
SEPTA light rail (Philadelphia)		Yes	
DART (Dallas)		Yes	
Denver RTD (Denver)		Yes	
TRAX (UTA) (Salt Lake City)		Yes	Yes
MetroLink (St. Louis)			Yes
Hudson-Bergen Light Rail (Jersey City)		Yes	
METRO Light Rail (Minneapolis)			Yes
Other	Mexico City Light Rail		Phoenix VMR, Santa Clara VTA
24. Which heavy rail transit systems and lines use your concrete crossties?			
New York City Subway			
Washington Metro			
Chicago 'L'			
MBTA Subway ("The T")		Yes	
Bay Area Rapid Transit (BART)		Yes	Yes
SEPTA		Yes	
Port Authority Trans-Hudson (PATH)			
MARTA rail system			
Metro Rail (Los Angeles)		Yes	Yes
Other			
25. Which commuter rail transit systems and lines use your concrete crossties?			
MTA Long Island Rail Road		Yes	
New Jersey Transit Rail		Yes	
MTA Metro-North Railroad		Yes	
Metra		Yes	Yes
SEPTA Commuter Rail		Yes	
MBTA Commuter Rail		Yes	
Caltrain		Yes	Yes
Metrolink		Yes	Yes
MARC Train			
Other			San Diego NCTD
26. What is the design life of your concrete crosstie? (years)			
Not a quotable parameter	30	50	
27.. What is the design axle load for your concrete crosstie? (kips)			
19 tons	82	35 kips	
28. What is the maximum design bending moment? (in.-kips)			
RS + 300	340	250 in.-kips	
29. What is the typical concrete crosstie spacing for transit systems?			
24”	30”	28”	
30. What is the typical impact factor used in design? (%) (e.g., 200% = 2 × static load)			
300%	200	200%	
31. What is the typical design speed?			
70 mph	80 mph	79 mph	
32. How relevant is each of the following track structure conditions in terms of contributing to the risk for failure of concrete crosstie?			
Cracking from center binding (center negative bending)	4	1	3
Cracking from rail seat positive bending	1	4	1

Cracking from environmental or chemical degradation	3	1	1
Cracking from dynamic loads	3	2	3
Tamping damage	4	3	3
Shoulder/fastener wear or fatigue	2	4	3
Rail seat deterioration (RSD) and other forms of rail cant deficiency	2	5	3
Missing rail pad	3	2	4
Worn or missing insulator	3	4	4
Broken or worn fastener shoulder	3	3	4
Missing clip	3	4	4
Fouled ballast	4	5	4
Insufficient depth of ballast	3	2	4
Weak subgrade	4	2	4
Damage during installation	4		
Insufficient concrete strength	3	1	4
Improper prestress force	4	1	5
Poor material quality or behavior (of clamp, insulator, rail pad, or crosstie)	4	3	3
Poor environmental conditions (e.g., moisture or fines intrusion)	3	3	4
Manufacturing flaws	3	2	5
Improper component design (of clamp, insulator, rail pad, or crosstie)	2	2	4
Fastening system damage	3	3	4
Concrete deterioration beneath the rail	2	3	4
Poor bonding of concrete to prestress	4	1	4
Chemical reaction (ASR)	4	3	5
Concrete crosstie shrinkage	4	1	2
Freeze-thaw cycle			2

33. In your opinion, how could the resiliency of concrete crossties be improved in the face of natural disasters (e.g., floods, and snow/ice, etc.) or other events that place increased stress on infrastructure and its components?			
Material design: concrete mix	5	2	2
Pre-stress strand arrangement	3	1	1
Optimize crosstie: spacing	2	2	5
Optimize crosstie: cross-section	4	1	4
Optimize crosstie: body shape	4	3	4
Optimize crossties for specific uses (curves, grades, etc.)	2	2	4
Prevention of rail seat deterioration (RSD) or repair of abraded ties	2	4	3
Track system design: determining the track service environment and required tie characteristics	4	2	4
Prestress design	5		
Verifying real stresses on tie under true in-track conditions		5	
Lateral track stability			4

APPENDIX

C

Fastening System

1. What is the name of your typical concrete crosstie that is used by the transit agencies you supply components to ballasted concrete crosstie track?		
Light rail	e-Clip	W 21 / W 42
Heavy rail	ME system (skl)	W 21 / W 42
Commuter rail	e-Clip	W 21 / W 30
2. What type of fastening system does your organization manufacture for rail transit systems? (e.g., e-Clip, Fastclip)		
Light rail	e-Clip, Safelok, ME (skl), direct fixation, embedded track	Skl 21 / 42
Heavy rail	e-Clip, Safelok, ME (skl), direct fixation, embedded track	Skl 21 / 42
Commuter rail	e-Clip, Safelok, embedded track, direct fixation	Skl 42 / 30
3. What is the rail pad geometry? (e.g., dimpled, grooved, studded, flat)		
Light rail	Many	Flat
Heavy rail	Many	Flat
Commuter rail	Many	Dimpled/studded
4. What is the rail pad material? (e.g., polyurethane, rubber)		
light rail	NBR, SBR, EVA,	EPDM
heavy rail	Polyurethane	EPDM
commuter rail	NBR SBR EVA	EPDM/TPU
5. What is the material of the component in the fastening system that provides electrical insulation? (e.g., polyurethane, nylon)		
light rail	Polyurethane rubber nylon	Polyamid 6 with 30% glass fibers
heavy rail	Polyurethane rubber nylon eva hdpe	PA 6, GF 30
commuter rail	Rubber eva elastomertric compounds	PA 6, GF 30
6. What is the rated resistance of insulating materials in the fastening system? (ohms, Ω)		
Light rail	10^12 ohms	Volume resistivity (ohm-cm): > 1*10^9
Heavy rail	10^12 ohms	Volume resistivity (ohm-cm): > 1*10^9
Commuter rail	10^12 ohms	Volume resistivity (ohm-cm): > 1*10^9
7. What is the design life of the fastening system? (years)		
Light rail	Customer specific or 20 yrs min	30+
Heavy rail	Life of rail minimum	30+
Commuter rail	Customer specific or 20 yrs min.	30+
8. What is the clamping force (toe load) of your typical fastening system? (lbs)		
Light rail	5,000 lb-f / assembly	4500+
Heavy rail	5600 lb-f / assembly	4500+
Commuter rail	5,000 lb-f / assembly	4500-5600
9. What are the most important properties that transit agencies look for in a fastening system?		

Vibration mitigation performance	2	2
Mechanical fatigue strength	4	4
Low maintenance	5	5
Long life-cycle	5	5
Low cost	3	5
Corrosion resistance		3
Electrical resistance		5
Acoustical performance	2	
10. Which transit systems and lines use your fastening systems? (e.g., CTA Red Line)		
MBTA light rail (Boston)	Yes	
Metro Rail light rail (Los Angeles)	Yes	
Muni Metro (San Francisco)		
San Diego Trolley (San Diego)	Yes	
MAX Light Rail (Portland)	Yes	
SEPTA light rail (Philadelphia)	Yes	
DART (Dallas)	Yes	
Denver RTD (Denver)	Yes	
TRAX (UTA) (Salt Lake City)	Yes	
MetroLink (St. Louis)		
Hudson-Bergen Light Rail (Jersey City)		
METRO Light Rail (Minneapolis)		
Other		Buffalo (NFTA)
Other		Calgary, Edmonton (DFF slab track)
11. Which heavy rail transit systems and lines use your fastening systems?		
New York City Subway	Yes	
Washington Metro	Yes	
Chicago 'L'		
MBTA Subway ("The T")	Yes	
Bay Area Rapid Transit (BART)		
SEPTA	Yes	Yes
Port Authority Trans- Hudson (PATH)		
MARTA rail system	Yes	
Metro Rail (Los Angeles)	Yes	
Other		Metrorrey (Monterrey, Mexico) (Slab track)
Other		Calgary, Edmonton (DFF slab track)
12. Which commuter rail transit systems and lines use your fastening systems?		
MTA Long Island Rail Road	Yes	
New Jersey Transit Rail	Yes	
MTA Metro-North Railroad		
Metra	Yes	
SEPTA Regional Rail		
MBTA Commuter Rail	Yes	
Caltrain	Yes	
Metrolink	Yes	
MARC Train		
Other		All Aboard Florida / Brightline

13. Do you see any forms of deterioration with your fastening systems that require maintenance activities? If so, what is this deterioration? (e.g., fastener fatigue failure)		
Light rail	Corrosion over prolonged use	N/A
Heavy rail	Gauge widening due to insulator wear	N/A
Commuter rail	None	N/A
14. If deterioration has been observed, what remedial protocols have been put in place to mitigate fastening system deterioration?		
Light rail	Change in specs & reinstall with new and improved	N/A
Heavy rail	Maintenance at intervals and change in fastener	N/A
Commuter rail	N/A	N/A
15. Which areas of transit infrastructure typically see are most fastening system deterioration?		
Light rail	Tangent	
	Curve	
	Special trackwork	Special trackwork
	Bridges	Bridges
	Tunnels	Tunnels
	Grade crossings	Grade crossings
Heavy rail	Tangent	
	Curve	Curve
	Special trackwork	Special trackwork
	Bridges	Bridges
	Tunnels	
	Grade crossings	Grade crossings
Commuter rail	Tangent	
	Curve	
	Special trackwork	Special trackwork
	Bridges	
	Tunnels	
	Grade crossings	Grade crossings
16. Has rail rotation been identified as a major concern at any transit providers your serve? If yes, are there any particular situations where fastening systems have not performed satisfactorily in limiting rail rotation? Please describe.		
None	No, elastic pad geometry and middle bend of tension clamp prevent rail rotation	
17. What is the required range of lateral rail head displacement that is specified by your customers? (mm)		
Light rail	Varies greatly but 8mm	
Heavy rail	5	
Commuter rail	varies	
18. How relevant is each of the following fastening system conditions in terms of contributing to the risk for of failure of fastening system?		
Shoulder/fastener wear or fatigue	1	1
Rail seat deterioration (RSD) and other forms of rail cant deficiency	2	1
Missing rail pad	4	1
Worn or missing insulator or	4	1

insulating material		
Missing clip of fastener clamp	2	1
Special trackwork	3	2
Poor material quality or behavior (of clamp, insulator, or rail pad)	2	1
Manufacturing flaws	2	1
Improper component design (of clamp, insulator, or rail pad)	2	1
Fastening system damage	4	1
Low toe load	4	1
High lateral forces	3	1
Insufficient lateral restraint	3	1
19. Do you have any general comments on fastening system design, manufacture, testing, and installation that you would like to provide to UIUC researchers?		
Test 6 AREMA offers most up-to-date, toughest test for HH	See accompanying presentation	
20. In your opinion, how could the resiliency of fastening systems be improved in the face of natural disasters (e.g., floods, snow/ice, saltwater intrusion, etc.) or other events that place increased stress on infrastructure and its components?		
Coatings for longer life in corrosive environments.	Geometry of clamp must provide fail-safe resiliency; corrosion resistance (and use of non-corrosive materials) a must in face of floods, snow/ice, and saltwater	
21. Please rank the following areas of concrete crosstie and fastening system research in terms of their potential benefit.		
Fastener design: clips	5	5
Fastener design: insulators	4	1
Fastener design: inserts	2	5
Fastener design: rail pads	3	5
Track system design	5	5
Corrosion of metal components	3	4

REFERENCES

1. A. Harvey, *In re Lone Star Industries, Inc., concrete railroad cross ties litigation*, United States District Court, D. Maryland, Baltimore, MD, , 1991.
2. Railway Tie Association (RTA), Tie Report #12, Railway Tie Association, Fayetteville, GA, 2012.
3. S. Kaufman, C. Qing, N. Levenson, and M. Hanson, Transportation during and after Hurricane Study, Rudin Center for Transportation, NYU Wagner Graduate School of Public Service, New York, NY, 2012.
4. J. Sneider, Hurricane Sandy: Four years later, New York City Transit is still fixing, fortifying the rail system, 2016.
5. J. Sneider, Hurricane Sandy: LIRR, Metro-North railroads' recovery, resiliency projects continue, 2016.
6. U.S. Department of Transportation, Transportation for a new generation: Strategic plan for fiscal years 2014–18, 2015.
7. Federal Transit Administration, Revenue Vehicle Inventory, National Transit Database (NTD), 2013.
8. J. M. Tuten, D. B. Mesnick, L. E. Daniels, J. A. Hadden, and D. R. Ahlbeck, Performance of direct-fixation track structure, Transit Cooperative Research Program, Project D-5, 1999.
9. V. R. Vuchic, *Urban Transit Systems and Technology*. New York, NY, USA: John Wiley & Sons, 2007.
10. Parsons Brinckerhoff, Inc., *Track Design Handbook for Light Rail Transit,* 2nd Ed., Transportation Research Board, Washington, DC, 155, 2012.
11. J. Keating, V. Tokar, and M. McInnis, A concrete decision selection of cross ties for new track construction, AREMA 2001 Annual Conference & Exposition, Illinois, 2001.
12. H. Nassif, K. Ozbay, P. Lou, and D. Su, Fatigue evaluation of the increased weight on transit railway bridge, Mineta National Transit Research Consortium, San Jose, CA, 12-24, 2-14.
13. Federal Transit Administration, 2013 Revenue Vehicle Inventory, National Transit Database (NTD), 2013.
14. Virginia Railway Express (VRE), Scope of work, request for proposals, new gallery-style passenger rail cars, VA, 08-014, 2008.
15. S. Smith and M. Schroeder, Changes in rider anthropometrics and the effect on rail car design, America Public Transportation Association, Washington, DC, 2013.
16. Flight Standards Service, *Aircraft Weight and Balance Control.* Washington, DC: Federal Aviation Administration, 2005.
17. G. Fleming, Guide specifications for structural design of rapid transit and light rail structures, Massachusetts Bay Transportation Authority, Boston, MA, 2005.
18. B. J. Van Dyk, Characterization of loading environment for shared-use railway superstructure in North America, Master's thesis, University of Illinois at Urbana-Champaign, Department of Civil and Environmental Engineering, 2013.
19. American Railway Engineering and Maintenance-of-Way Association (AREMA), Chapter 30, Part 4: Concrete Ties, in *Manual for Railway Engineering*, Landover, MD, American Railway Engineering and Maintenance of Way Association, 2015.
20. J. G. Allen, J. P. Aurelius, and J. Black, Electric power supply for commuter rail, *Transportation Research Record*, 2219, 88-96, 2011.
21. W. W. Hay, *Railroad Engineering, 2nd Ed.*, Vol. 1. New York, NY, USA: John Wiley & Sons, 1982.
22. B. J. Van Dyk, A. J. Scheppe, J. R. Edwards, M. S. Dersch, and C. P. L. Barkan, Methods for quantifying rail seat loads and a review of previous experimentation, *Proc. Inst. Mech. Eng. Part F J. Rail Rapid Transit*, 230(3), 935–945, March 2016.

23. A. D. Kerr, *Fundamentals of Railway Track Engineering*. Omaha, NE: Simmons Boardman, 2003.
24. American Railway Engineering and Maintenance-of-Way Association (AREMA), Manual for Railway Engineering. Landover, MD: American Railway Engineering and Maintenance of Way Association, 2017.
25. W. W. Hay, *Railroad Engineering, 1st Ed.*, Vol. 1. New York, NY: John Wiley & Sons, 1953.
26. H. D. Harrison, L. R. Cheng, and W. GeMeiner, Tracking the performance of heavy axle load vehicles in revenue service, in *Proceedings of the 2006 ASME International Mechanical Engineering Congress and Exposition*, Chicago, IL, 2006.
27. B. Stratman, Y. Liu, and S. Mahadevan, Structural health monitoring of railroad wheels using wheel impact load detectors, *J. Fail. Anal. Prev.*, 7(3), 218-225, July 2007.
28. B. J. Van Dyk, Characterization of the loading environment for shared-use railway superstructure in North America, Master's thesis, University of Illinois at Urbana-Champaign, Department of Civil and Environmental Engineering, Urbana, IL, 2014.
29. B. J. Van Dyk, J. R. Edwards, M. S. Dersch, C. J. Ruppert, and C. P. Barkan, Evaluation of dynamic and impact wheel load factors and their application in design processes, *Proc. Inst. Mech. Eng. Part F J. Rail Rapid Transit*, 231(10), 33-43, January 2017.
30. X. Lin, J. R. Edwards, M. S. Dersch, T. A. Roadcap, and C. Ruppert, Load quantification of the wheel–rail interface of rail vehicles for the infrastructure of light, heavy, and commuter rail transit, *Proc. Inst. Mech. Eng. Part F J. Rail Rapid Transit*, 232(2), 596-605, February 2018.
31. N. F. Doyle, *Railway Track Design: A Review of Current Practice*. Melbourne, Australia: Canberra: Australian Government Publishing Service, 1980.
32. J. Sadeghi and P. Barati, Comparisons of the mechanical properties of timber, steel and concrete sleepers, *Struct. Infrastruct. Eng.*, 8(12), 1151-1159, August 2010.
33. B. Van Dyk, M. Dersch, J. Edwards, C. Ruppert Jr., and C. Barkan, Load characterization techniques and overview of loading environment in North America, *Transportation Research Record,* 2448, 80-86, December 2014.
34. J. Leong and M. H. Murray, Probabilistic analysis of train–track vertical impact forces, in *Proceedings of the Institution of Civil Engineers Transport 2008*, 161, 15-21, 2008.
35. Standards Australia, Railway Track Material, Part 14: Prestressed Concrete Sleepers, Standards Australia Committee CE-002, Sydney, NSW, Australia, Draft AS 1085.14:2019, 2003.
36. K. Knothe and S. Stichel, *Rail Vehicle Dynamics*. New York, NY: Springer, 2013.
37. J. R. Edwards, A. Cook, M. S. Dersch, and Y. Qian, Quantification of rail transit wheel loads and development of improved dynamic and impact loading factors for design, *Proc. Inst. Mech. Eng. Part F J. Rail Rapid Transit*, 232(10), 2406-2417, November 2018.
38. B. J. Van Dyk, J. R. Edwards, C. J. Ruppert Jr, and C. P. Barkan, Considerations for mechanistic design of concrete sleepers and elastic fastening systems in North America, in *Proceedings of the 10th International Heavy Haul Association Conference*, New Delhi, India, 2013.
39. Canadian National (CN), Wheel impact load detectors: The early history on CN, in *Proceedings of the 31st Annual North American Rail Mechanical Operations Seminar,* St. Louis, MO, 2011.
40. R. Wiley and A. Elsaleiby, A review of wheel impact measurement variation, *Technology Digest,* TD-11-007, Transportation Technology Center, Inc., Pueblo, CO, 2007.
41. A. A. S. Elsaleiby, Wheel imbalance effect on the output of wheel impact load detector system (WILD), Master's thesis, Department of Industrial and Systems Engineering, Colorado State University, Pueblo, CO, 2014.

42. R. J. Quirós-Orozco, Prestressed concrete railway crosstie support variability and its effect on flexural demand, Master's thesis, University of Illinois at Urbana-Champaign, Department of Civil and Environmental Engineering, Urbana, IL, 2018.
43. W. H. Press, S. A. Teukolsky, W. T. Vetterling, and B. P. Flannery, *Numerical Recipes in C++: The Art of Scientific Computing, 2nd ed*. Cambridge, UK: Cambridge University Press, 2002.
44. D. A. Darling, The Kolmogorov-Smirnov, Cramer-Von Mises tests, *Ann. Math. Stat*., 28(4), 823-838, December 1957.
45. A. N. Talbot, Stresses in railroad track: Bulletins of the Special Committee on Stresses in Railroad Track, American Railway Engineering Association (AREA), Washington, DC, 1980.
46. J. R. Edwards, Z. Gao, H. E. Wolf, M. S. Dersch, and Y. Qian, Quantification of concrete railway sleeper bending moments using surface strain gauges, *J. Int. Meas. Confed.*, 111, 197-207, December 2017.
47. J. C. Zeman, Hydraulic mechanisms of concrete-tie rail seat deterioration, MS thesis, University of Illinois at Urbana-Champaign, Department of Civil and Environmental Engineering, Urbana, IL, 2010.
48. M. McHenry and J. LoPresti, Field evaluation of sleeper and fastener designs for freight operations, in *Proceedings of the 11th World Congress on Railway Research,* Milan, Italy, 2016.
49. J. R. Edwards, M. S. Dersch, and R. G. Kernes, Improved concrete crosstie and fastening systems for US high speed passenger rail and joint corridors (Volume 2), US Department of Transportation, Federal Railroad Administration, Washington, DC, Technical Report DOT/FRA/ORD-17/23, November 2017.
50. A. Windisch, Safety to brittle failure in prestressed concrete structures with bond, *Period. Polytech. Civ. Eng.*, 14(4), 341-359, 1970.
51. R. Gettu, Z. P. Bazant, and M. E. Karr, Fracture properties and brittleness of high-strength concrete, *Am. Concr. Inst. Mater.* J., 87(6), 608-618, 1990.
52. R. A. Mayville, L. Jiang, and M. Sherman, Performance evaluation of concrete railroad ties on the northeast corridor, US Department of Transportation, Federal Railroad Administration, Washington, DC, Final Report DOT/FRA/RPD-14/03, March 2014.
53. H. E. Wolf, Y. Qian, J. R. Edwards, M. S. Dersch, and D. A. Lange, Temperature-induced curl behavior of prestressed concrete and its effect on railroad crossties, *Constr. Build. Mater.*, 115, 319-326, July 2016.
54. H. E. Wolf, Flexural behavior of prestressed concrete monoblock crossties, Master's thesis, University of Illinois at Urbana-Champaign, Department of Civil and Environmental Engineering, Urbana, IL, 2015.
55. W. Venuti, Field investigation of the Gerwick RT-7 prestress concrete tie, Department of Civil and Environmental Engineering, San Jose State University, San Jose, CA, February 1970.
56. W. J. Venuti, Structural response of the BART concrete ties, Bay Area Rapid Transit District, Oakland, CA, September 1990.
57. O. Kerokoski, T. Rantala, and A. Nurmikolu, Deterioration mechanisms and life-cycle of concrete monoblock railway sleepers in Finnish conditions, in *Proceedings of the 11th World Congress on Railway Research*, Milan, Italy, 2016.
58. Z. Gao, H. E. Wolf, M. S. Dersch, Y. Qian, and J. R. Edwards, Field measurements and proposed analysis of concrete crosstie bending moments, in *Proceedings of the American Railway Engineering and Maintenance-of-Way Association Annual Conference*, Orlando, FL 2016.
59. H. Askarinejad, M. Dhanasekar, and C. Cole, Assessing the effects of track input on the response of insulated rail joints using field experiments, *Proc. Inst. Mech. Eng. Part F J. Rail Rapid Transit*, 227(2), 176-187, March 2013.

60. N. Zong, H. Askarinejad, T. B. Heva, and M. Dhanasekar, Service condition of railroad corridors around the insulated rail joints, *Am. Soc. Civ. Eng. J. Transp. Eng.*, 139(6), 643-650, June 2013.

61. C. Beckemeyer, L. Khazanovich, and H. Thomas Yu, Determining amount of built-in curling in jointed plain concrete pavement: Case study of Pennsylvania 1-80, Transportation Research Record, 1809, 85-92, January 2002.

62. Z. Cai, G. P. Raymond, and R. J. Bathurst, Estimate of static track modulus using elastic foundation models, Transportation Research Record, 1470, 65-72, 1994.

63. Á. E. Canga Ruiz, Analysis of the design of railroad track superstructure components for rail transit applications, Master's thesis, University of Illinois at Urbana- Champaign, Department of Civil and Environmental Engineering, Urbana, IL, 2018.

64. H. E. Wolf, S. Mattson, J. R. Edwards, M. S. Dersch, and C. P. L. Barkan, Flexural analysis of prestressed concrete monoblock crossties: Comparison of current methodologies and sensitivity to support conditions, in *Proceedings of the 94th Annual Meeting of the Transportation Research Board of the National Academies*, Washington, DC, 2015.

65. J. C. Bastos, Analysis of the performance and failure of railroad concrete crossties with various track support conditions, Master's thesis, University of Illinois at Urbana-Champaign, Department of Civil and Environmental Engineering, Urbana, IL, 2016.

66. American Concrete Institute (ACI), *ACI 318-14 Building Code Requirements for Structural Concrete and Commentary*. Farmington Hills, MI: American Concrete Institute, 2014.

67. J. C. Bastos, M. S. Dersch, J. R. Edwards, and B. O. Andrawes, Flexural behavior of concrete crossties under different support conditions, *Am. Soc. Civ. Eng. J. Transp. Eng.*, 143(12), 04017064, December 2017.

68. D. E. Holder, M. V. Csenge, Y. Qian, M. S. Dersch, J. R. Edwards, and B. J. Van Dyk, Laboratory investigation of the Skl-style fastening system's lateral load performance under heavy haul freight railroad loads, *Eng. Struct.*, 139(2017), 71-80, May 2017.

69. W. Hou, B. Feng, W. Li, and E. Tutumluer, Evaluation of ballast behavior under different tie support conditions using discrete element modeling, Transportation Research Record, 2672(10), 106-115, 2018.

70. T. D. Stark and S. T. Wilk, Root cause of differential movement at bridge transition zones, *Proc. Inst. Mech. Eng. Part F J. Rail Rapid Transit*, 230(4,) 1257-1269, May 2016.

71. S. T. Wilk, Mitigation of differential movements at railroad bridge transition zones, Doctoral dissertation, University of Illinois at Urbana-Champaign, Department of Civil and Environmental Engineering, Urbana, IL, 2017.

U.S. Department of Transportation

Federal Transit Administration

U.S. Department of Transportation
Federal Transit Administration
East Building
1200 New Jersey Avenue, SE
Washington, DC 20590
https://www.transit.dot.gov/about/research-innovation